N73-26983
NASA TM X-2747

NASA TECHNICAL MEMORANDUM

NASA TM X-2747

SUPERSONIC AERODYNAMIC CHARACTERISTICS OF HYPERSONIC LOW-WAVE-DRAG ELLIPTICAL-BODY—TAIL COMBINATIONS AS AFFECTED BY CHANGES IN STABILIZER CONFIGURATION

by Bernard Spencer, Jr., and Roger H. Fournier

Langley Research Center
Hampton, Va. 23665

NATIONAL AERONAUTICS AND SPACE ADMINISTRATION • WASHINGTON, D. C. • JULY 1973

1. Report No.	2. Government Accession No.	3. Recipient's Catalog No.
NASA TM X-2747		

4. Title and Subtitle	5. Report Date
SUPERSONIC AERODYNAMIC CHARACTERISTICS OF HYPERSONIC LOW-WAVE-DRAG ELLIPTICAL-BODY—TAIL COMBINATIONS AS AFFECTED BY CHANGES IN STABILIZER CONFIGURATION	July 1973
	6. Performing Organization Code
7. Author(s)	8. Performing Organization Report No.
Bernard Spencer, Jr., and Roger H. Fournier	L-8640
	10. Work Unit No.
9. Performing Organization Name and Address	502-37-01-01
NASA Langley Research Center Hampton, Va. 23665	11. Contract or Grant No.
	13. Type of Report and Period Covered
12. Sponsoring Agency Name and Address	Technical Memorandum
National Aeronautics and Space Administration Washington, D.C. 20546	14. Sponsoring Agency Code

15. Supplementary Notes

16. Abstract

An investigation has been made at Mach numbers from 1.50 to 4.63 to determine systematically the effects of the addition and position of outboard stabilizers and vertical- and vee-tail configurations on the performance and stability characteristics of a low-wave-drag elliptical body. The basic body shape was a zero-lift hypersonic minimum-wave-drag body as determined for the geometric constraints of length and volume. The elliptical cross section had an axis ratio of 2 (major axis horizontal) and an equivalent fineness ratio of 6.14. Base-mounted outboard stabilizers were tested at various dihedral angles from 90° to -90° with and without a single center-line vertical tail or a vee-tail. The angle of attack was varied from about -6° to 27° at sideslip angles of 0° and 5° and a constant Reynolds number of 4.58×10^{6} (based on body length).

17. Key Words (Suggested by Author(s))	18. Distribution Statement
Supersonic aerodynamic characteristics Outboard stabilizers Elliptical body Tail configurations	Unclassified – Unlimited

19. Security Classif. (of this report)	20. Security Classif. (of this page)	21. No. of Pages	22. Price*
Unclassified	Unclassified	93	$3.00

*For sale by the National Technical Information Service, Springfield, Virginia 22151

SUPERSONIC AERODYNAMIC CHARACTERISTICS OF HYPERSONIC LOW-WAVE-DRAG ELLIPTICAL-BODY—TAIL COMBINATIONS AS AFFECTED BY CHANGES IN STABILIZER CONFIGURATION

By Bernard Spencer, Jr., and Roger H. Fournier
Langley Research Center

SUMMARY

An investigation has been made in the Langley Unitary Plan wind tunnel through a Mach number range from 1.50 to 4.63 to determine systematically the effects of the addition and position of outboard stabilizers and vertical- and vee-tail configurations on the performance and stability characteristics of a low-wave-drag elliptical body. The body had a longitudinal area distribution conforming to the theoretical shape required to minimize the zero-lift hypersonic wave drag under the geometric constraints of given length and volume. The elliptical cross section had an axis ratio of 2 (major axis horizontal) and an equivalent fineness ratio of 6.14. Base-mounted outboard stabilizers were tested at various dihedral angles from 90° to -90° with and without a single center-line vertical tail or a vee-tail. The angle of attack was varied from about -6° to 27° at sideslip angles of 0° and 5° and a constant Reynolds number of 4.58×10^6 (based on body length).

The addition of the outboard stabilizers at 0° dihedral to the basic body resulted in increases in untrimmed maximum lift-drag ratio at the lower Mach numbers. Untrimmed performance increments due to the addition of the outboard stabilizers decreased as Mach number increased to 4.63. Increasing the stabilizer dihedral angle from 0° (positively or negatively) resulted in losses in maximum lift-drag ratio.

An examination of the out-of-trim moment occurring at maximum lift-drag ratio indicated considerably less out-of-trim moment for the stabilizers at positive dihedral than at negative dihedral of equal magnitude.

Addition of the outboard stabilizers at 0° dihedral angle had a favorable effect on the center of pressure, especially at the higher Mach numbers. Positive effective dihedral was noted for all positive-dihedral outboard-stabilizer configurations at positive angles of attack at all Mach numbers. A region of negative effective dihedral occurred at low angles of attack for the stabilizers at negative dihedral, especially at the lower test Mach numbers.

The addition of a center-line vertical tail to the configuration having outboard stabilizers at positive or negative dihedral caused large adverse yaw at angles of attack above about 12° to 16° at Mach numbers up to 2.86. This effect disappeared at Mach numbers of 3.96 to 4.63, as the vertical tail became shadowed and the local flow approached hypersonic conditions (i.e., reduced vortex strength). These results at high supersonic Mach numbers correspond approximately to those obtained at Mach 10 in a previous investigation.

INTRODUCTION

Numerous studies have been directed toward increasing the aerodynamic performance attainable from a class of volumetrically efficient lifting bodies at hypersonic speeds. Some of this effort has been in the form of wind-tunnel tests at hypersonic speeds on bodies having various longitudinal contours and cross-sectional shapes (refs. 1 to 6). Results of these studies have indicated that improvements in hypersonic performance can be attained by selection of proper longitudinal and transverse contours that satisfy particular design considerations such as length and volume, rather than using an equivalent cone. In addition, experimental results have indicated that, for a given cross-sectional shape, minimum-wave-drag bodies which are designed in accordance with the methods of references 7 and 8 have supersonic as well as hypersonic aerodynamic performance equal to or better than that for similarly constrained power-law bodies previously investigated. (See refs. 1 and 3.) Performance is often of prime concern, depending on the cruise or cross range desired. However, the configuration and location of stabilizing surfaces to reduce trim penalties are of equal importance for realistic operational vehicles.

Accordingly, a low-wave-drag body designed from volume and length constraints (ref. 8) has been used as the basic shape, and a systematic study has been initiated to determine the effects of the location of various horizontal and vertical stabilizer combinations on both the stability and performance characteristics of the body. Previous results obtained at hypersonic and transonic speeds have been reported in references 9 and 10, respectively. It is the purpose of this paper to present results for the same configuration at Mach numbers from 1.50 to 4.63. The tests were made at angles of attack from about -6° to 27° for angles of sideslip of 0° and 5° and a constant Reynolds number of 4.58×10^{6} (based on body length).

SYMBOLS

Longitudinal data are referred to the stability-axis system and lateral-directional data are referred to the body-axis system. All coefficients are normalized with respect

to the projected planform area, length, and span of the body alone. The moment reference point was on the body center line at 55 percent of the body length.

a semimajor axis of ellipse at base of body (semispan of body), m (ft)

A body aspect ratio, $\frac{(2a)^2}{S}$

A_b base area of body, m^2 (ft^2)

b semiminor axis of ellipse (one-half the base height of body), m (ft)

C_D drag coefficient, $\frac{\text{Drag}}{qS}$

$C_{D,min}$ minimum drag coefficient

C_L lift coefficient, $\frac{\text{Lift}}{qS}$

C_{L_α} lift-curve slope, $\frac{\partial C_L}{\partial \alpha}$ at $\alpha \approx 0^o$, per deg

C_l rolling-moment coefficient, $\frac{\text{Rolling moment}}{2aqS}$

C_{l_β} effective-dihedral parameter, $\frac{\Delta C_l}{\Delta \beta}$, from values of C_l for $\beta \approx 0^o$ and 5^o, per deg

C_m pitching-moment coefficient, $\frac{\text{Pitching moment}}{qSl}$

C_N normal-force coefficient, $\frac{\text{Normal force}}{qS}$

C_n yawing-moment coefficient, $\frac{\text{Yawing moment}}{2aqS}$

C_{n_β} directional-stability parameter, $\frac{\Delta C_n}{\Delta \beta}$, from values of C_n for $\beta \approx 0^o$ and 5^o, per deg

$C_{p,b}$ base-pressure coefficient, $\frac{p_b - p_\infty}{q}$

C_Y side-force coefficient, $\frac{\text{Side force}}{qS}$

C_{Y_β}	side-force parameter, $\frac{\Delta C_Y}{\Delta \beta}$, from values of C_Y for $\beta \approx 0^o$ and 5^o, per deg
f	equivalent fineness ratio, $\frac{l}{2\sqrt{ab}}$
l	length of body, 0.508 m (1.667 ft)
L/D	lift-drag ratio
$(L/D)_{max}$	maximum lift-drag ratio
M	Mach number
p_∞	free-stream static pressure, N/m^2 (lb/ft^2)
p_b	base pressure, N/m^2 (lb/ft^2)
q	dynamic pressure, N/m^2 (lb/ft^2)
r	radius
S	projected planform area of body, m^2 (ft^2)
S_t	exposed planform area of outboard stabilizers, m^2 (ft^2)
S_v	exposed planform area of vertical tail $\left(0.5S_t\right)$
x_{cp}/l	center-of-pressure location in percent body length ($\alpha \approx 0^o$), $0.55 - \frac{\partial C_m}{\partial C_N}$
α	angle of attack, deg
β	angle of sideslip, deg
Γ_s	outboard-stabilizer dihedral angle (fig. 1), deg
θ_v	tail dihedral angle, deg; the axis of rotation is the body longitudinal axis (fig. 1)

MODEL

The model was an elliptical low-wave-drag body designed under the geometric constraints of volume and length (ref. 7) with an equivalent fineness ratio of 6.14. The axis ratio of the cross section was 2 with the major axis horizontal. Details of the model are presented in figure 1 and photographs of the model are presented in figure 2.

The outboard horizontal stabilizers were mounted with trailing edge coincident with the base of the model, had a leading-edge sweep of 65°, a delta planform, and a constant leading-edge radius of 0.165 cm (0.065 in.) as measured normal to the leading edge. (See fig. 1.) The total exposed area of each outboard stabilizer was 7.15 percent of the projected body planform area. The stabilizing surfaces were wedge shaped in cross section and had an included angle of 3° which resulted in a blunt trailing edge.

The vee-tail ($\theta_V = 30^{\circ}$) and the single center-line vertical tail ($\theta_V = 90^{\circ}$) were identical in planform and cross section to the horizontal stabilizers. (See fig. 1.)

APPARATUS AND METHODS

Tunnel

The investigation was performed in both the low and high Mach number test sections of the Langley Unitary Plan wind tunnel. The tunnel is a variable-pressure, return-flow type with both test sections approximately 1.22 m (4 ft) square and 2.13 m (7 ft) long. The nozzles leading to each test section have asymmetric sliding blocks which permit variations of Mach number from approximately 1.50 to 2.90 in the low Mach number test section and from 2.30 to 4.63 in the high Mach number test section.

Tests and Corrections

Forces and moments were measured by means of a six-component electrical strain-gage balance. The model was sting supported and attached to a remotely operated angle-of-attack mechanism. The tests were made through a range of angles of attack from about -6° to 27° at sideslip angles of 0° and 5° and a constant Reynolds number of 4.58×10^6 (based on body length). All angles of attack and sideslip have been corrected for deflection of the balance and sting due to aerodynamic loads. The angles of attack were also corrected for tunnel flow misalinement. Static-pressure measurements were taken at the base of the model and the data are presented in the form of pressure coefficients in figure 3. The drag results presented herein represent gross drag, that is, drag uncorrected for base pressure effects.

Test Conditions

The Mach numbers, stagnation pressures, and stagnation temperatures were as follows:

M	Stagnation pressure		Stagnation temperature	
	kN/m^2	lb/ft^2, abs	K	^oF
1.50	73.26	1530	338	150
1.90	83.55	1745	338	150
2.36	103.66	2165	338	150
2.86	134.88	2817	338	150
3.96	253.48	5294	352	175
4.63	345.98	7226	352	175

The stagnation dewpoint was maintained sufficiently low (238 K (-30^o F)) to insure that no appreciable condensation effects would be encountered in the test sections.

Transition strips 0.16 cm (1/16 in.) wide composed of No. 60 sand were located, in accordance with the methods prescribed in reference 11, 3.05 cm (1.2 in.) aft of the apex of the model nose and 0.43 cm (0.17 in.) aft of the leading edge of the horizontal and vertical tails (measured normal to the leading edge).

PRESENTATION OF RESULTS

Basic longitudinal aerodynamic characteristics and summary lateral-directional and longitudinal characteristics are presented in the following figures for the various configurations tested.

DISCUSSION

Longitudinal Aerodynamic Characteristics

Addition of stabilizing surfaces.- The addition of the outboard stabilizers ($\Gamma_S = 0^o$) to the body resulted in large increases in C_{L_α} and $C_{D,min}$, especially at the lower Mach numbers (see fig. 4 and summary of data in fig. 16). Resultant increases in untrimmed $(L/D)_{max}$ from about 2.1 to 2.45 occurred at $M = 1.5$ and from about 3.05 to 3.30 at $M = 4.63$, or about 16.6 and 8.2 percent, respectively. The larger increases in $(L/D)_{max}$ noted at the lower Mach numbers result from the improvement in drag due to lift caused by addition of the lifting surfaces to the body, since the local flow over the stabilizer is subsonic and some efficiency (leading-edge suction) is retained. Similar results were noted in reference 10 at transonic speeds. At the highest Mach numbers, however, as flow approaches near-hypersonic conditions less improvement in $(L/D)_{max}$ results. This effect is further illustrated in figure 20. For hypersonic conditions (ref. 9) significant losses (approximately 15 percent) in $(L/D)_{max}$ resulted from addition of the stabilizing surfaces to the body.

The addition of either the single center-line vertical tail or the vee-tail results in a slight reduction in $(L/D)_{max}$ (fig. 16) at all Mach numbers. Increasing the Mach number results in increased $(L/D)_{max}$ for any given configuration because of the reduction in base drag (fig. 3) which accompanies increasing Mach number.

As shown in figures 17 to 19 the addition of the outboard stabilizers ($\Gamma_s = 0^o$) on the longitudinal stability characteristics of the body causes large rearward shifts in x_{cp}/l from about 0.55 (body alone) to 0.76 at $M = 1.50$ and from about 0.56 to 0.67 at the highest test Mach number.

Effects of dihedral angle.- The basic longitudinal aerodynamic characteristics, showing the effect of changing the outboard-stabilizer dihedral angle with or without the center-line vertical tail or vee-tail, are presented in figures 5 to 9, and are summarized in figures 17 to 19 ($\theta_v = 90^o$ or 30^o). Increasing Γ_s (positively or negatively) results in losses in C_{L_α} and $(L/D)_{max}$ (except for $\Gamma_s = -30^o$ at the lower test Mach numbers, fig. 20) and considerably less rearward shift in x_{cp}/l, as would be expected (figs. 17 to 19).

The variation of pitching moment with angle of attack for negative dihedral of the outboard stabilizers (figs. 7 and 8) indicates continually increasing stability with increasing angle of attack at all Mach numbers. Nonlinear variations of C_m with angle of attack occur for the stabilizers at positive dihedral (figs. 5 and 6), especially at $M = 1.50$ to $M = 2.36$. Reduced stability is noted in the angle-of-attack range of approximately 4^o to 12^o and increased stability at the higher angles of attack. These effects disappear as Mach number is increased above $M = 2.36$.

An examination of the out-of-trim moment occurring at $(L/D)_{max}$ (fig. 21) indicates considerably less out-of-trim moment for the stabilizers at positive dihedral than at negative dihedral of equal magnitude. Therefore, less control deflection and resultantly less trim-drag penalty would be incurred by use of the positive-dihedral stabilizers. These effects are shown at all test Mach numbers, with the largest difference noted near transonic speeds.

Lateral-Directional Characteristics

Addition of stabilizing surfaces.- The effects of the addition of outboard stabilizers ($\Gamma_s = 0^o$) on the lateral-directional stability parameters with and without the center-line vertical tail or vee-tail are shown in figure 10. These data indicate that the stabilizers provide a positive increment in C_{n_β} at angles of attack above about 6^o at low Mach numbers and at all test angles of attack at the higher Mach numbers. This favorable effect of the stabilizers on C_{n_β} is probably caused by a slight rearward shift in center of pressure due to windward tail drag with increase in Mach number and angle of attack. This favorable effect of the stabilizers was also noted at $M = 10.03$ in reference 9.

The addition of the center-line vertical tail ($\theta_v = 90^o$) to the body with outboard stabilizers ($\Gamma_s = 0^o$) provides large increases in C_{n_β} at low to moderate angles of attack, but results in adverse yaw contribution at high angles of attack (above about 12^o to 16^o), especially at the lower Mach numbers (up to $M = 2.86$) (fig. 10). The adverse effect of the center-line vertical tail on C_{n_β} was also noted near $M = 1.0$ in reference 10 and is believed to arise from the effect of vortices at high subsonic and low supersonic speeds. At higher Mach numbers, the vortex action diminishes as flow conditions approach those associated with hypersonic characteristics, and the adverse effect of the vertical tail at the higher angles of attack disappears. (See fig. 10(f), $M = 4.63$.) The indication is that the small-span tail is entirely in the region of influence of the body shed vortex sheet with the windward side under an adverse pressure influence, thereby creating adverse yaw. This effect has been noted previously in reference 12. (See tail span effects near $M = 1.0$ in ref. 12.)

The addition of the vee-tail to the body with outboard stabilizers ($\Gamma_s = 0^o$) results in the highest value of C_{n_β} for any of the configurations at all Mach numbers (fig. 10). In addition, the large losses in C_{n_β} at high angles of attack, and particularly at the lower test Mach numbers, for the configurations with the center-line vertical tail are not incurred with the vee-tail, since the rollout of the vee-tail surfaces removes them from the influence of the strong body vortex.

Effects of dihedral angle.- The effects of increases in the positive dihedral angle of the outboard stabilizers on the directional stability characteristics are presented in figures 11 and 12. Increases in C_{n_β} were noted up to $\Gamma_s = 60^o$; losses in C_{n_β} occurred at the higher angles of attack as Γ_s was increased to 90^o with or without the vertical tails. The losses in C_{n_β} occurred at lower angles of attack as Mach number was increased.

The effects of negative dihedral of the outboard stabilizers are presented in figures 13 to 15. Increases in C_{n_β} accompanied increases in Γ_s up to -90^o with or without the center-line vertical tail or vee-tail at all Mach numbers and positive angles of attack.

Positive effective dihedral was noted for all positive-dihedral outboard-stabilizer configurations at positive angles of attack (with or without center-line vertical tail) at all Mach numbers (figs. 11 and 12). For the negative-dihedral outboard stabilizers, a region of negative effective dihedral was noted up to about 6^o angle of attack for configurations without the vertical tail or vee-tail, especially at the lower Mach numbers (fig. 13). The addition of the vee-tail eliminated this adverse roll effect at all positive angles of attack at all Mach numbers (fig. 15). The addition of the center-line vertical tail reduced the region of unfavorable C_{l_β}; however, at the lowest test Mach number a negative effective dihedral occurred up to approximately 4^o angle of attack (fig. 14(a)).

SUMMARY OF RESULTS

An investigation has been made in the Langley Unitary Plan wind tunnel through a Mach number range of 1.50 to 4.63 to determine systematically the effects of the addition of outboard stabilizers and vertical- and vee-tail configurations on the longitudinal and lateral-directional stability characteristics and aerodynamic performance of a low-wave-drag elliptical body. The body had a longitudinal area distribution conforming to the theoretical shape required to minimize the zero-lift hypersonic pressure drag under constraints of given length and volume.

1. The addition of the outboard stabilizers at 0^{o} dihedral angle to the basic body resulted in large increases in untrimmed maximum lift-drag ratio at the lower Mach numbers. At the higher Mach numbers, however, where the flow approached hypersonic conditions, only minor improvements were noted. Increasing the stabilizer dihedral angle from 0^{o} positively or negatively resulted in losses in maximum lift-drag ratio.

2. An examination of the out-of-trim moment occurring at maximum lift-drag ratio indicated considerably less out-of-trim moment for the stabilizers at positive dihedral than at negative dihedral of equal magnitude.

3. Addition of the outboard stabilizers at 0^{o} dihedral angle had a favorable effect on the center of pressure, especially at the higher Mach numbers. Positive effective dihedral was noted for all positive-dihedral outboard-stabilizer configurations at positive angles of attack at all Mach numbers. A region of negative effective dihedral was noted at low angles of attack for the outboard stabilizers at negative dihedral without vertical tail or vee-tail, especially at the lower test Mach numbers.

4. The addition of a center-line vertical tail to the configuration having outboard stabilizers at positive or negative dihedral caused large adverse yaw at high angles of attack at the lower Mach numbers, which is attributable to body shed vortices acting on the small-span tail. This adverse effect disappeared at Mach numbers of 3.96 and 4.63, however, as the vertical tail became shadowed and the flow approached hypersonic conditions.

Langley Research Center,
National Aeronautics and Space Administration,
Hampton, Va., May 23, 1973.

REFERENCES

1. Fournier, Roger H.; Spencer, Bernard, Jr.; and Corlett, William A.: Supersonic Aerodynamic Characteristics of a Series of Related Bodies With Cross-Sectional Ellipticity. NASA TN D-3539, 1966.

2. Spencer, Bernard, Jr.; and Phillips, W. Pelham: Transonic Aerodynamic Characteristics of a Series of Bodies Having Variations in Fineness Ratio and Cross-Sectional Ellipticity. NASA TN D-2622, 1965.

3. Spencer, Bernard, Jr.; and Fox, Charles H., Jr.: Hypersonic Aerodynamic Performance of Minimum-Wave-Drag Bodies. NASA TR R-250, 1966.

4. Spencer, Bernard, Jr.: Hypersonic Aerodynamic Characteristics of Minimum-Wave-Drag Bodies Having Variations in Cross-Sectional Shape. NASA TN D-4079, 1967.

5. Stivers, Louis S., Jr.; and Spencer, Bernard, Jr.: Studies of Optimum Body Shapes at Hypersonic Speeds. NASA TN D-4191, 1967.

6. Love, E. S.; Woods, W. C.; Rainey, R. W.; and Ashby, G. C., Jr.: Some Topics in Hypersonic Body Shaping. AIAA Paper No. 69-181, Jan. 1969.

7. Eggers, A. J., Jr.; Resnikoff, Meyer M.; and Dennis, David H.: Bodies of Revolution Having Minimum Drag at High Supersonic Airspeeds. NACA Rep. 1306, 1957. (Supersedes NACA TN 3666.)

8. Suddath, Jerrold H.; and Oehman, Waldo I.: Minimum Drag Bodies With Cross-Sectional Ellipticity. NASA TN D-2432, 1964.

9. Fox, Charles H., Jr.; and Spencer, Bernard, Jr.: Hypersonic Aerodynamic Characteristics of Low-Wave-Drag Elliptical-Body—Tail Combinations as Affected by Changes in Stabilizer Configuration. NASA TM X-1620, 1968.

10. Fox, Charles H., Jr.; and Spencer, Bernard, Jr.: Transonic Aerodynamic Characteristics of Hypersonic Low-Wave-Drag Elliptical-Body—Tail Combinations as Affected by Changes in Stabilizer Configuration. NASA TM X-1789, 1969.

11. Braslow, Albert L.; Hicks, Raymond M.; and Harris, Roy V., Jr.: Use of Grit-Type Boundary-Layer-Transition Trips on Wind-Tunnel Models. NASA TN D-3579, 1966.

12. Stone, Ralph W., Jr.; and Polhamus, Edward C.: Some Effects of Shed Vortices on the Flow Fields Around Stabilizing Tail Surfaces. AGARD Rep. 108, 1957.

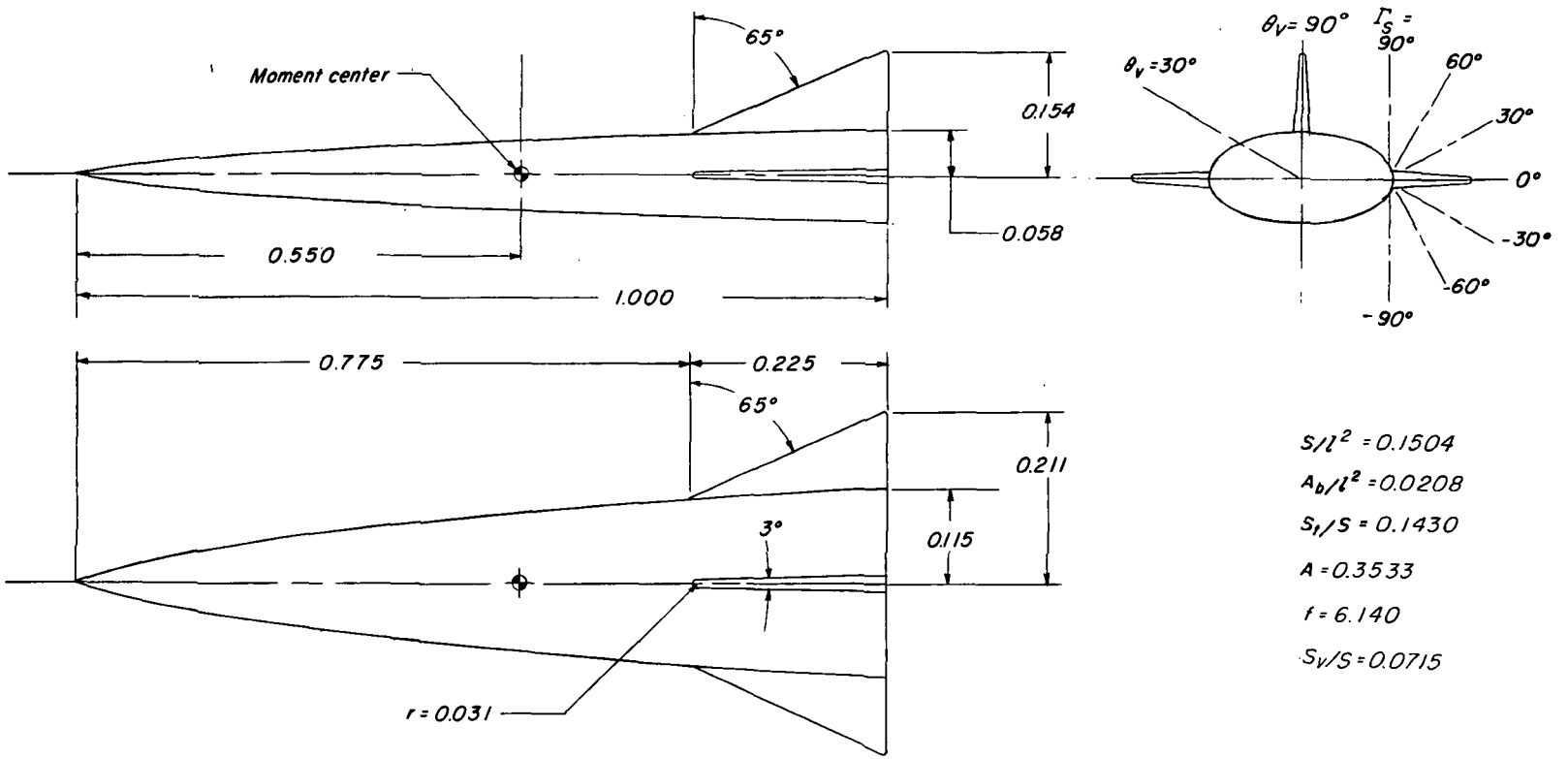

(a) General arrangement.

Figure 1.- Drawing of model investigated. All dimensions are normalized with respect to body length.

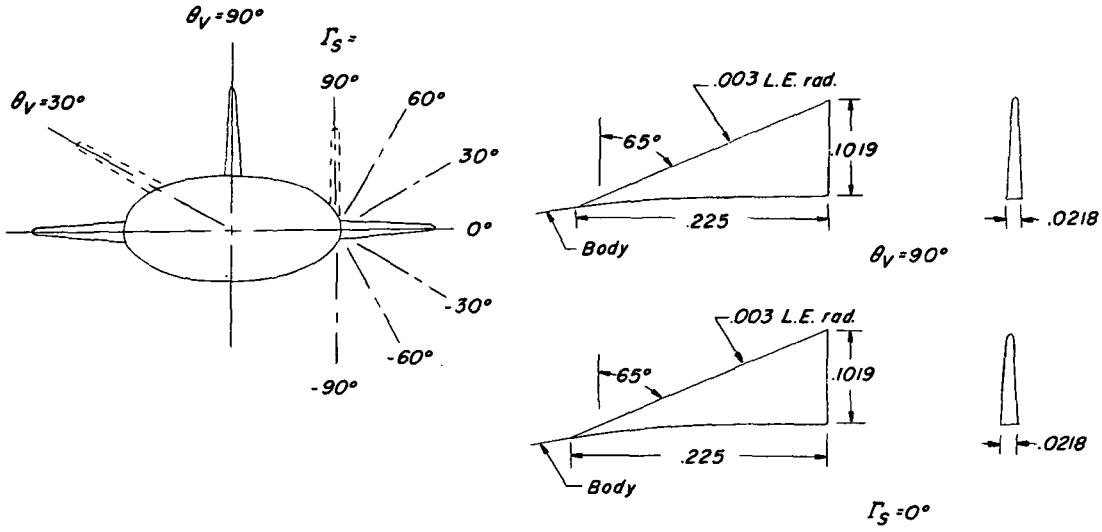

(b) Details of tails and stabilizers.

Figure 1.- Concluded.

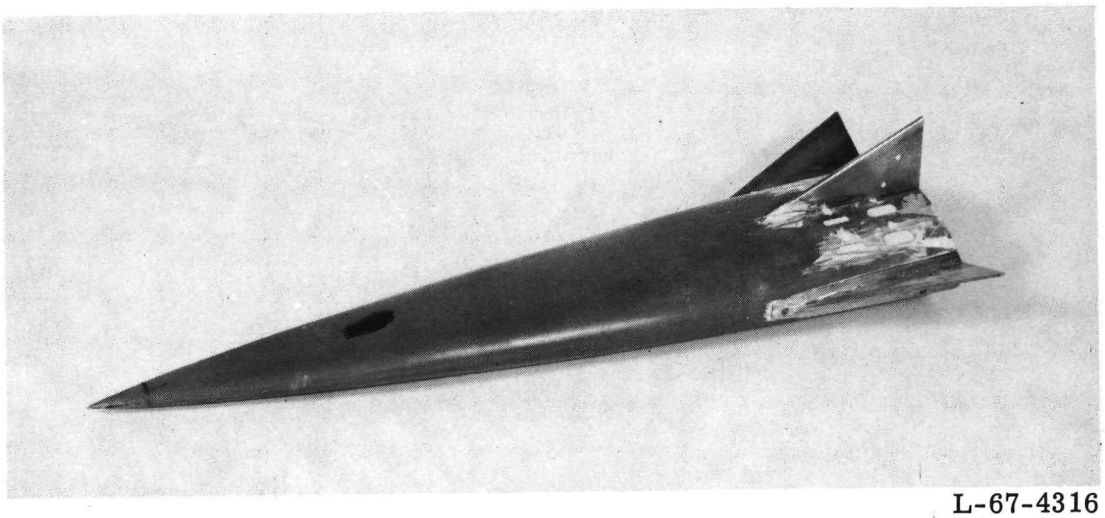

L-67-4316

(a) $\theta_V = 90^o$, $\Gamma_S = 30^o$.

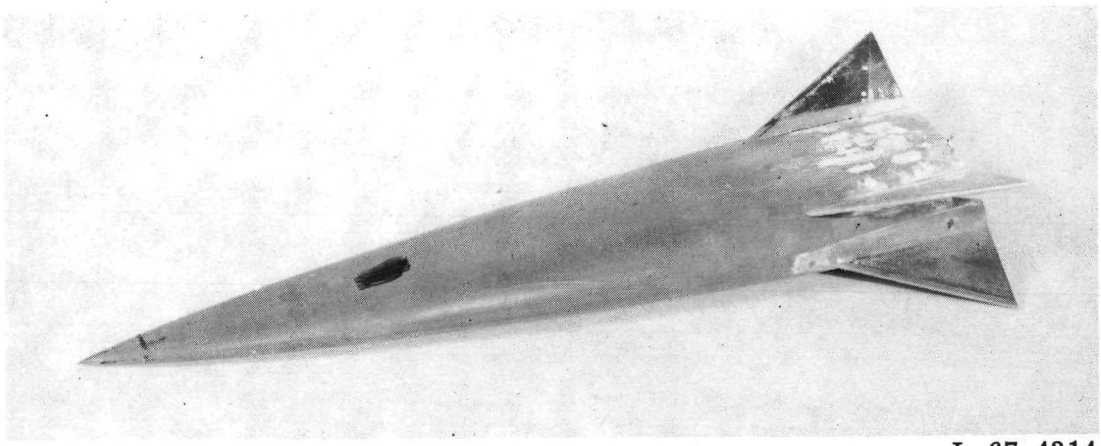

L-67-4314

(b) $\theta_V = 30^o$, $\Gamma_S = -30^o$.

Figure 2.- Typical model photographs.

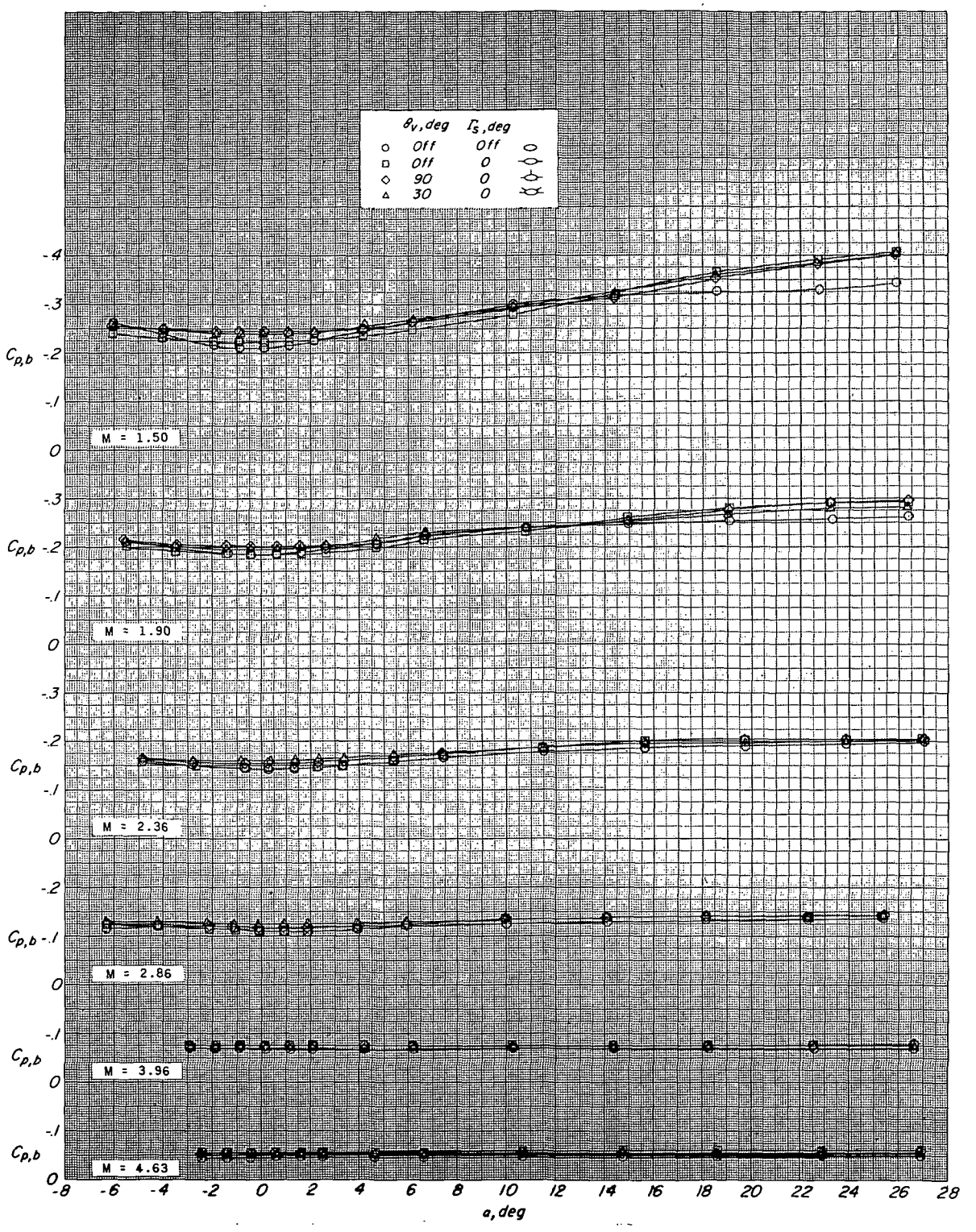

Figure 3.- Variation of base-pressure coefficient with angle of attack and Mach number.

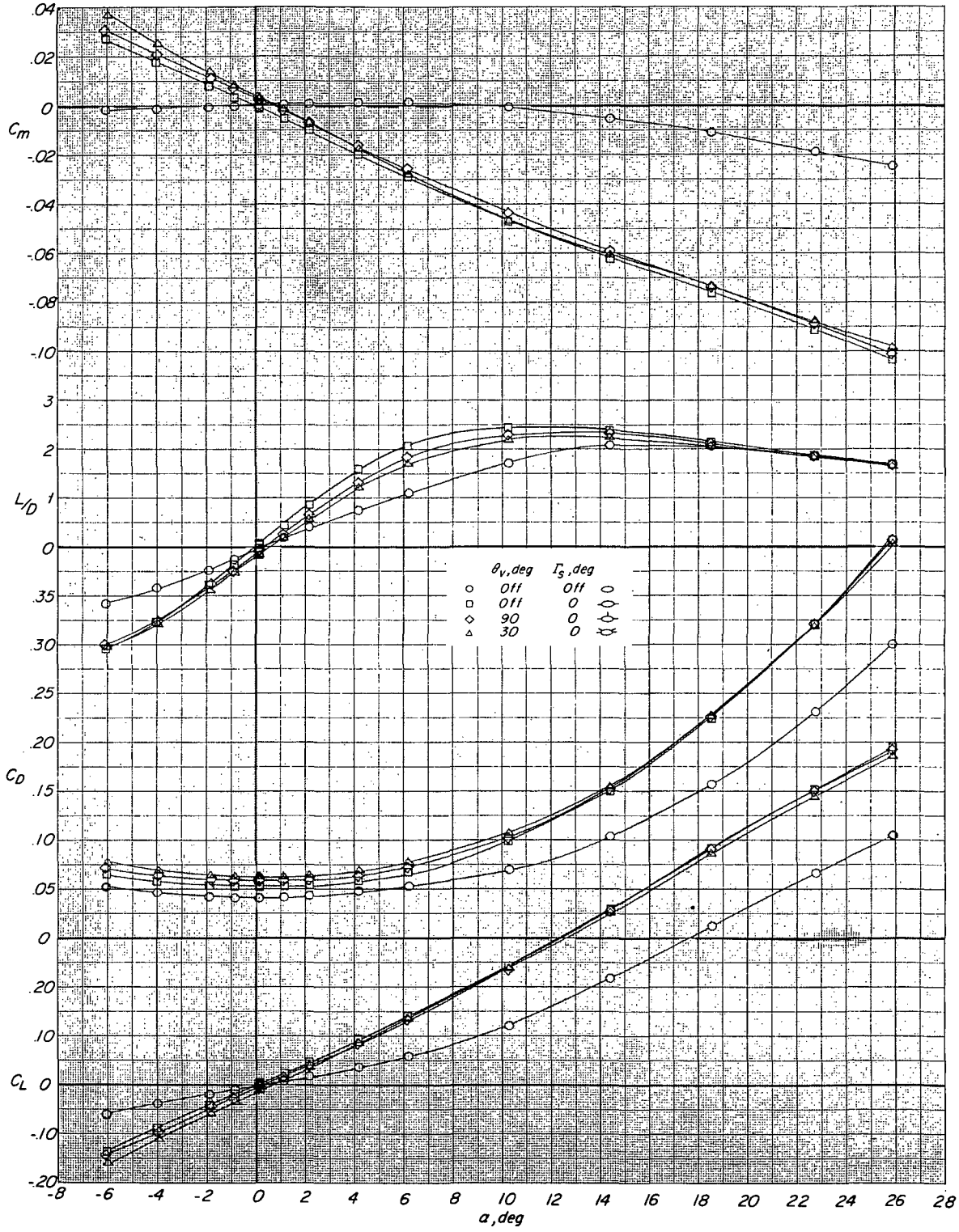

(a) M = 1.50.

Figure 4.- Effect of addition of outboard stabilizers ($\Gamma_S = 0^o$) and vertical tails ($\theta_V = 30^o$ and 90^o) on the longitudinal aerodynamic characteristics of the basic body.

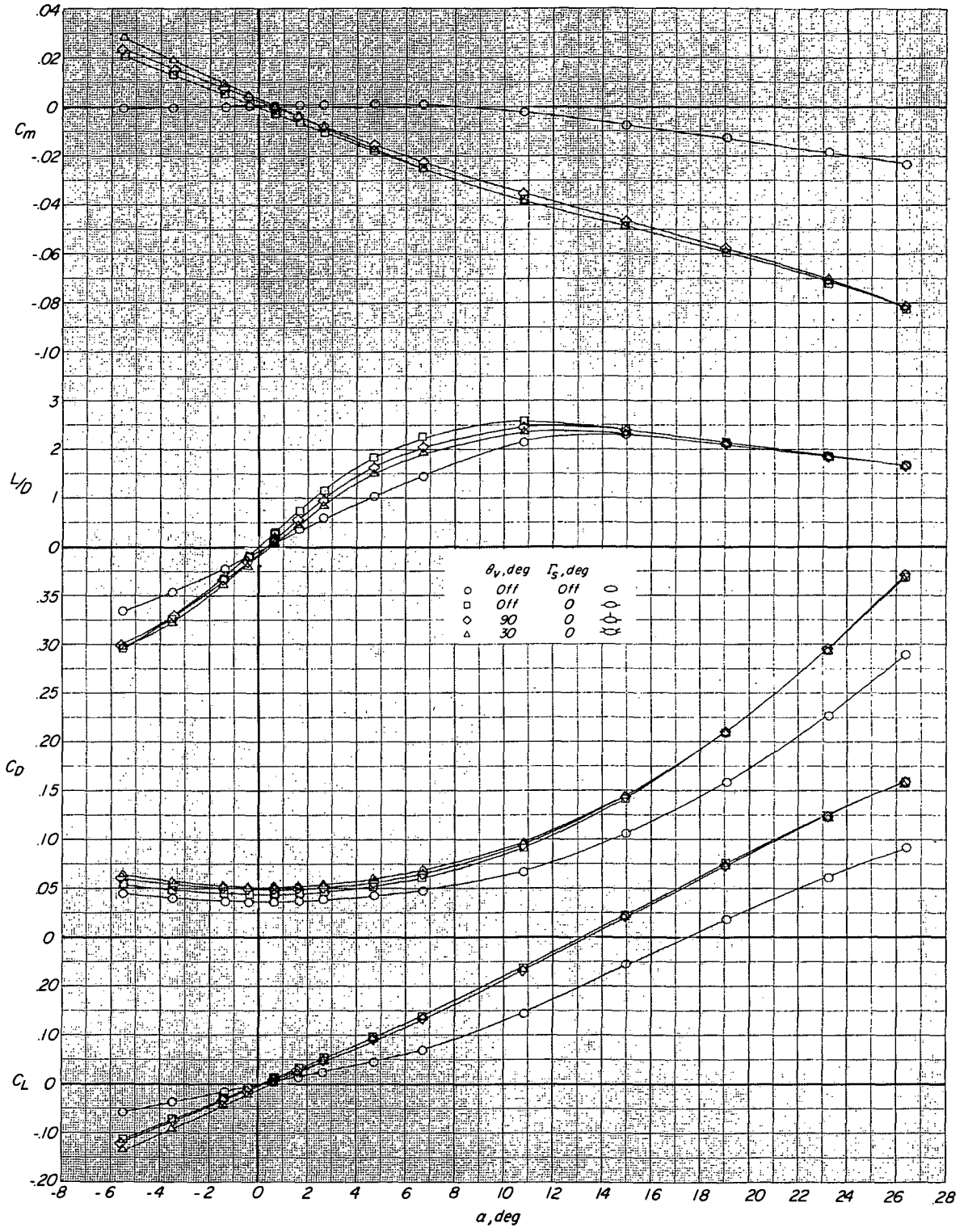

(b) M = 1.90.

Figure 4.- Continued.

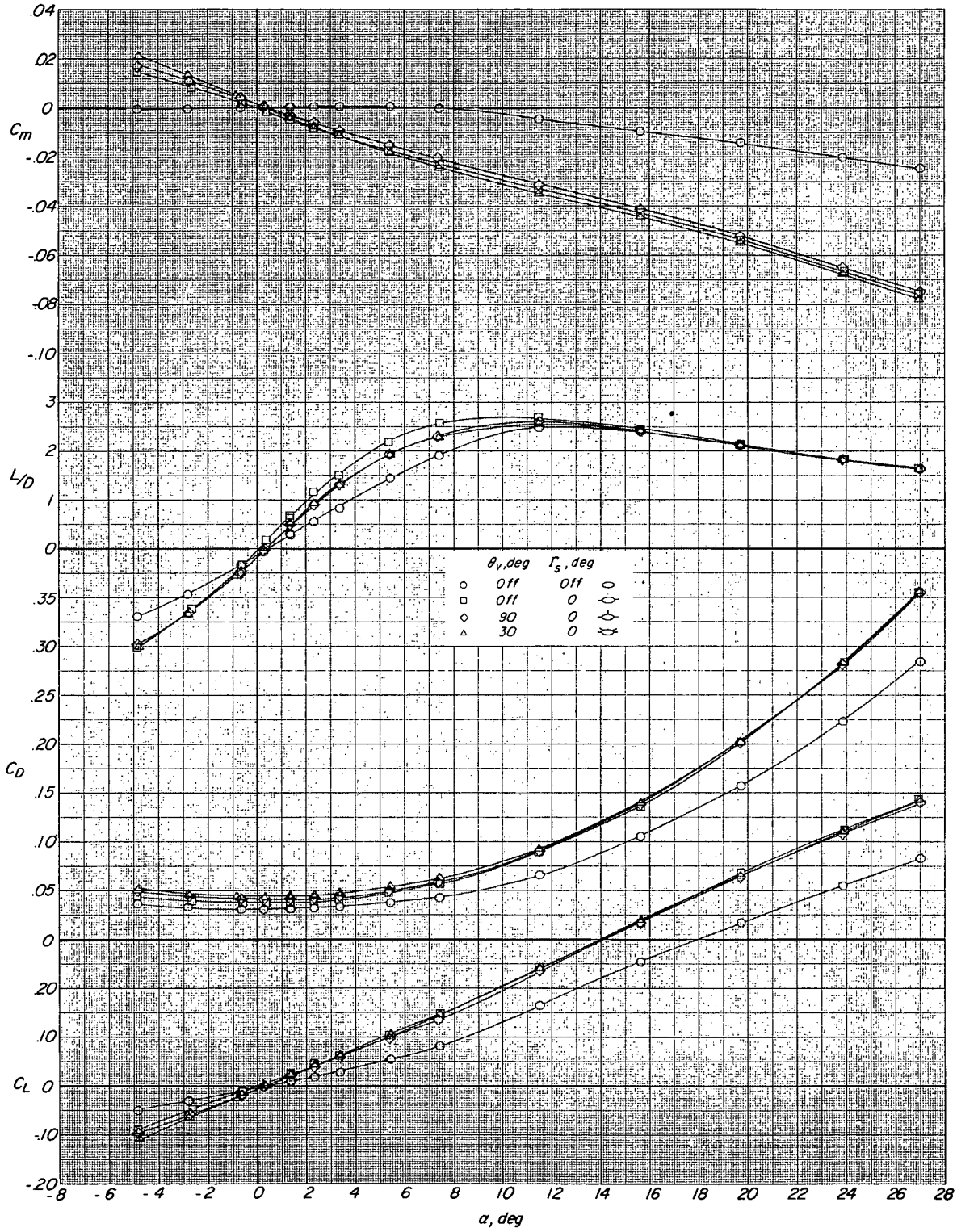

(c) M = 2.36.

Figure 4.- Continued.

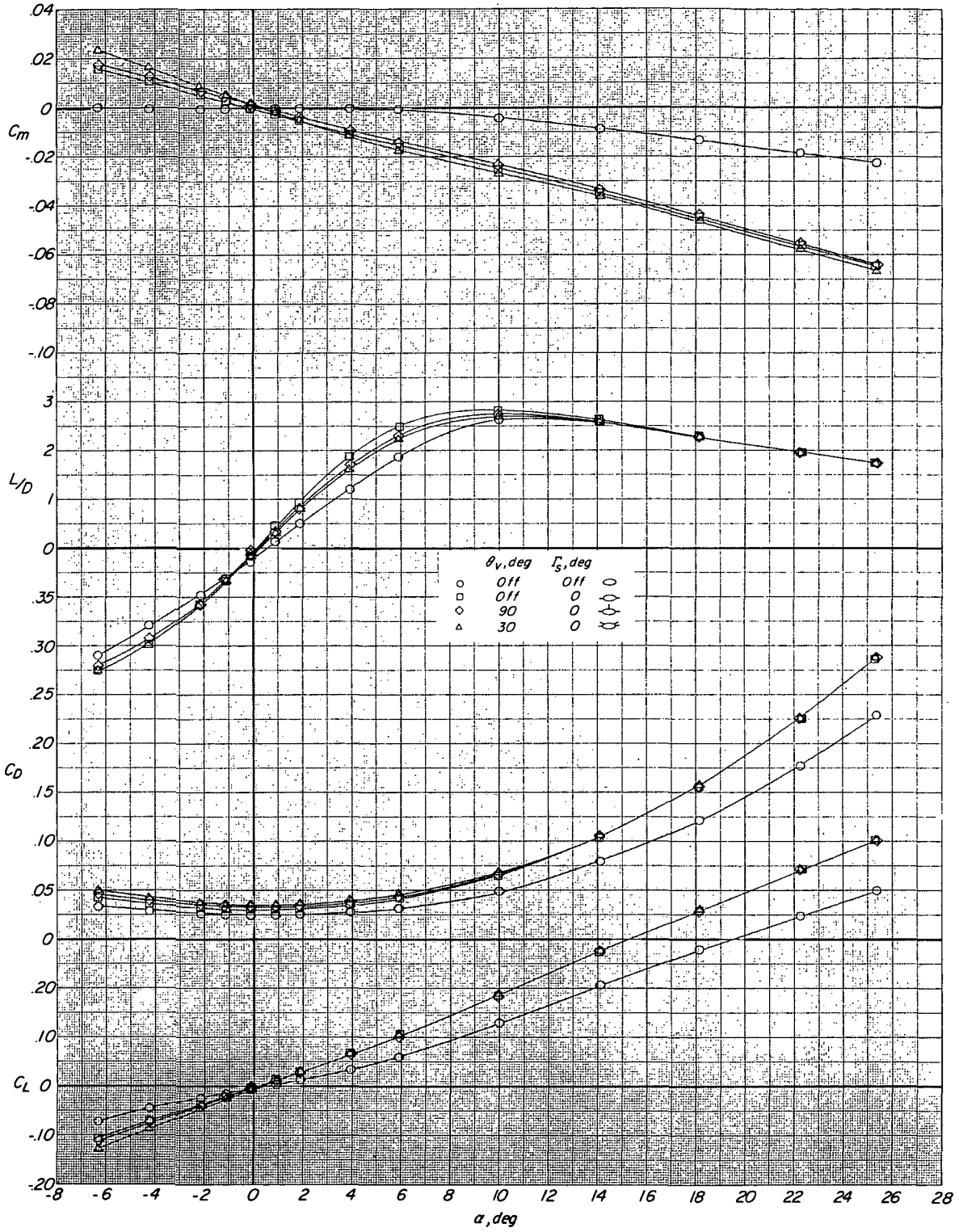

(d) M = 2.86.

Figure 4.- Continued.

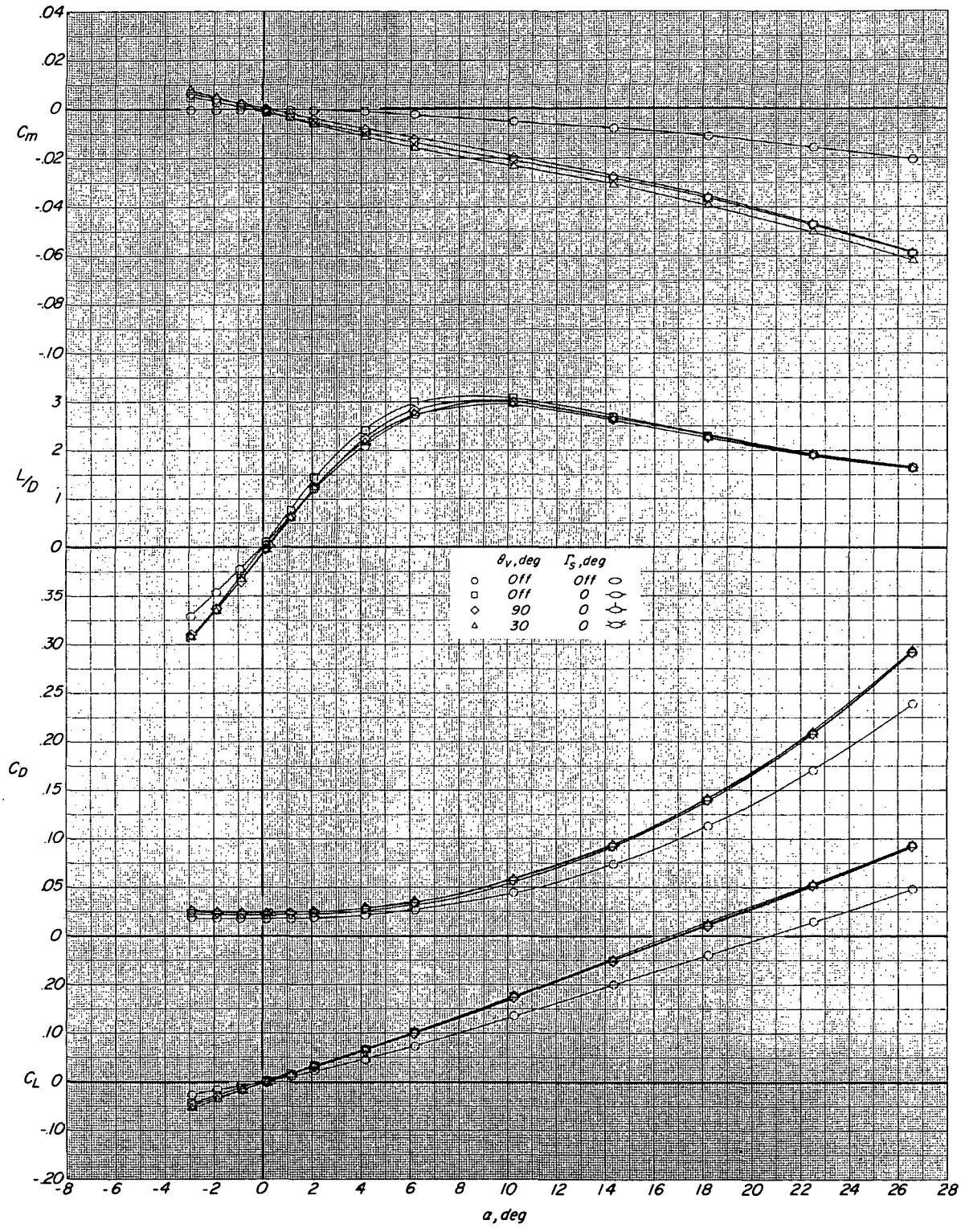

(e) M = 3.96.

Figure 4.- Continued.

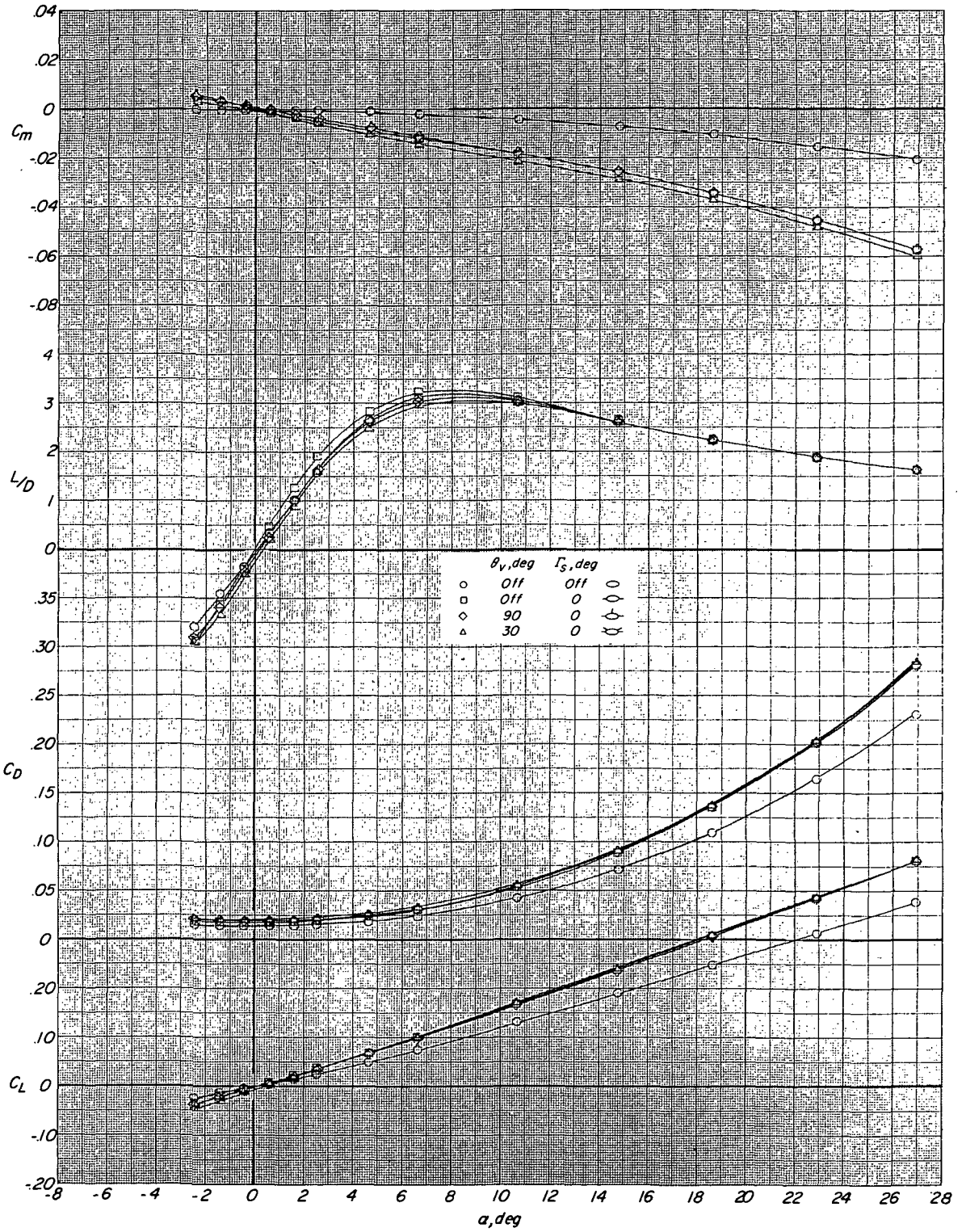

(f) M = 4.63.

Figure 4.- Concluded.

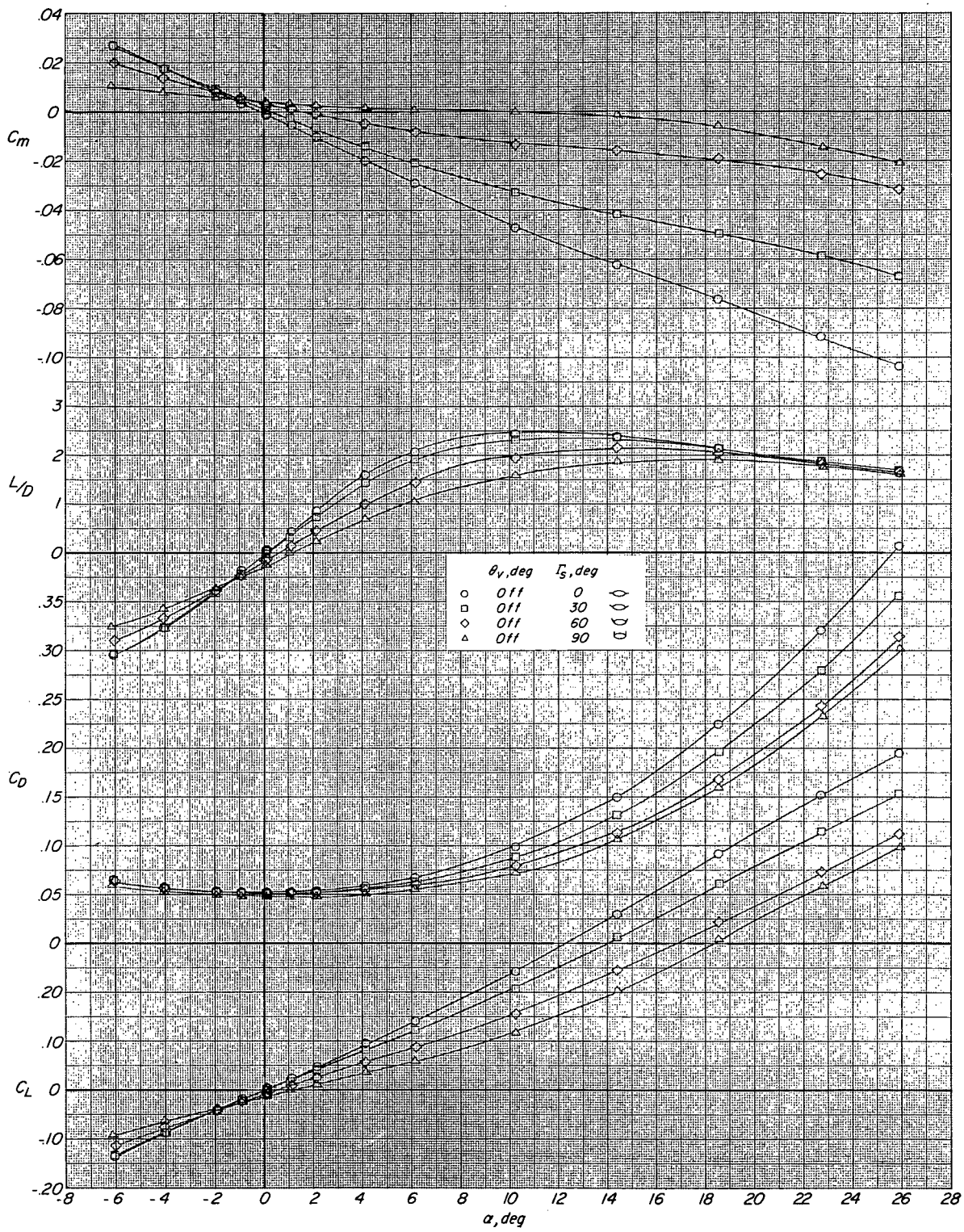

(a) M = 1.50.

Figure 5.- Effect of outboard-stabilizer dihedral on the longitudinal aerodynamic characteristics of the configuration without vertical tail. $\Gamma_s = 0^o$ to 90^o.

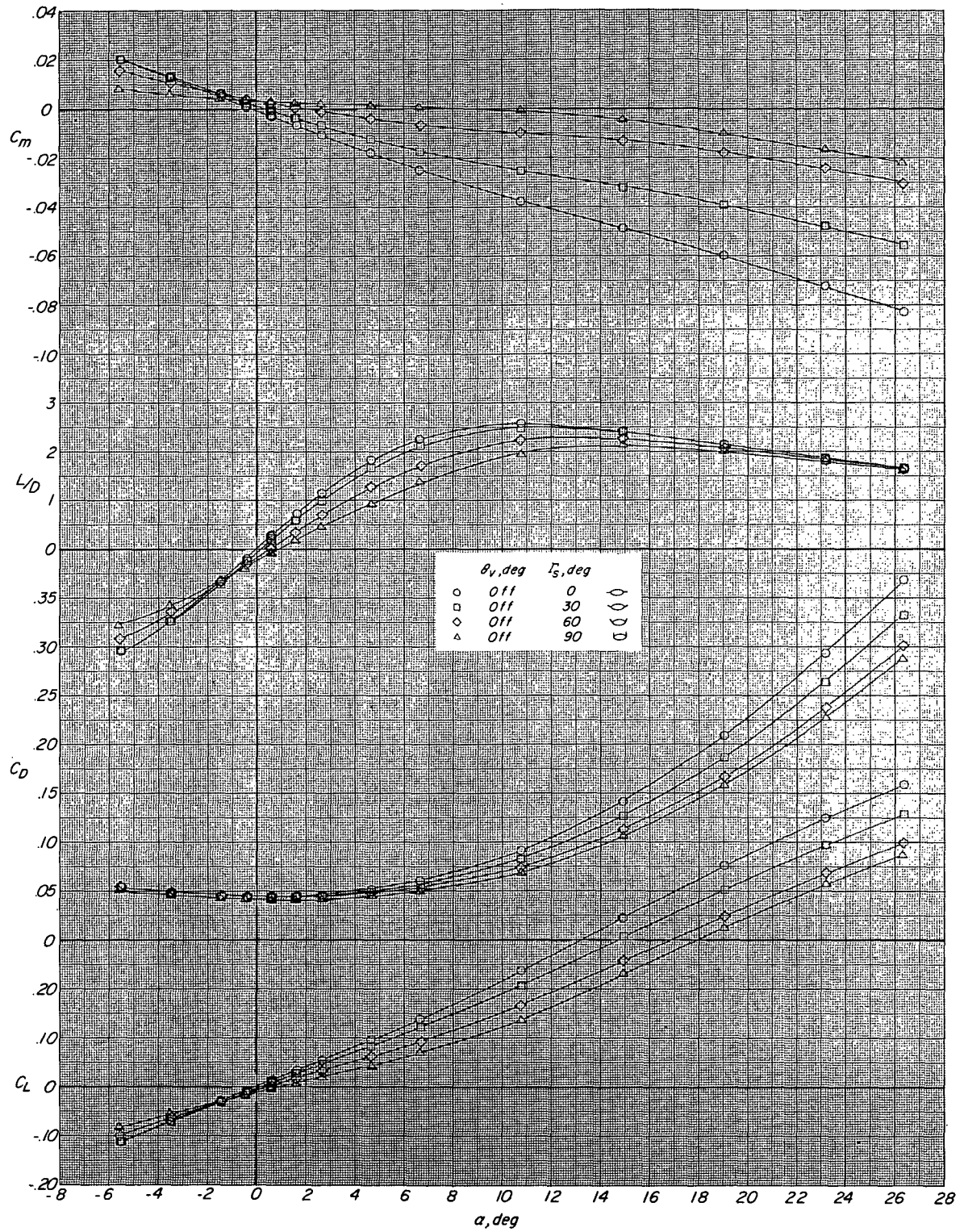

(b) M = 1.90.

Figure 5.- Continued.

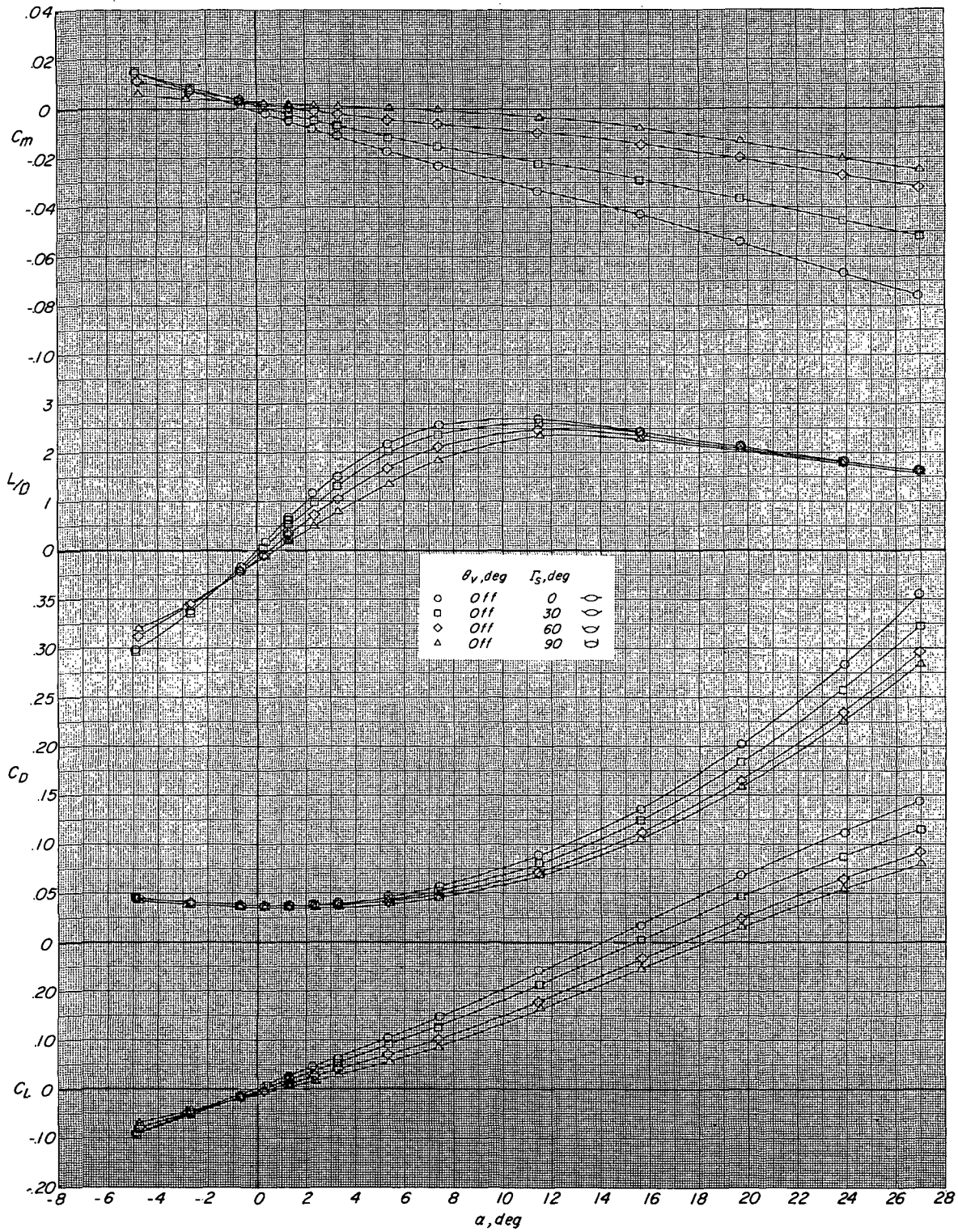

(c) M = 2.36.

Figure 5.- Continued.

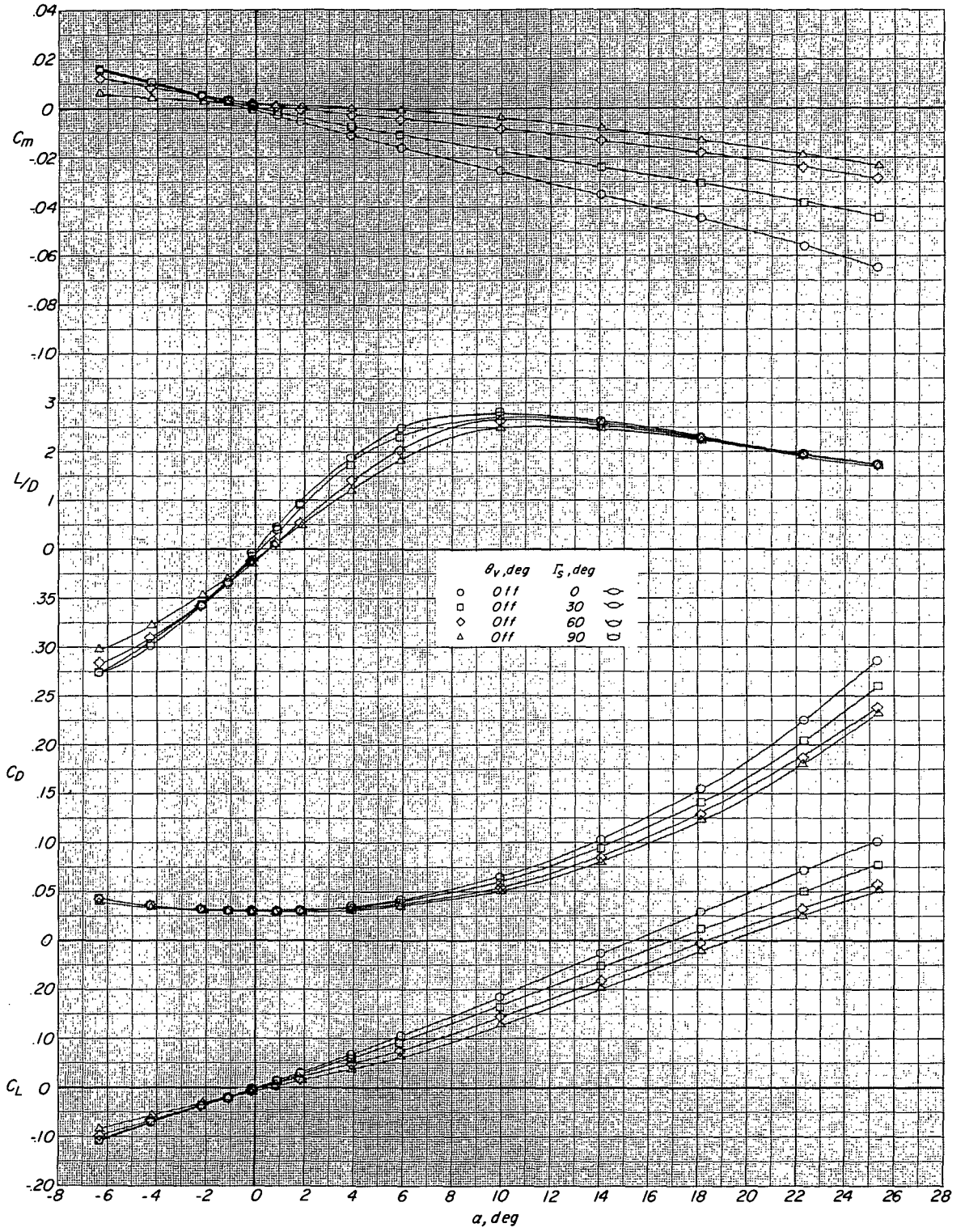

(d) M = 2.86.

Figure 5.- Continued.

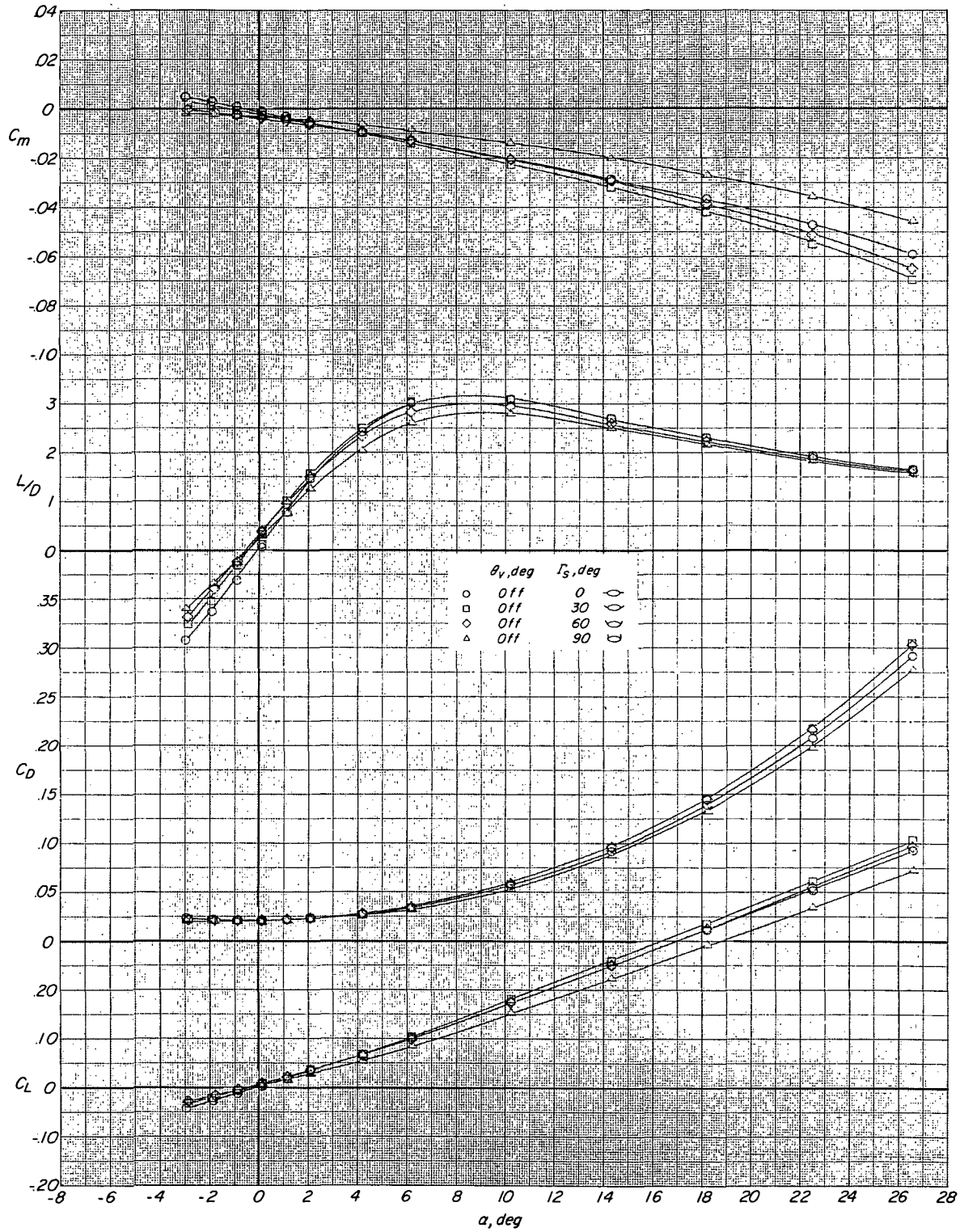

(e) M = 3.96.

Figure 5.- Continued.

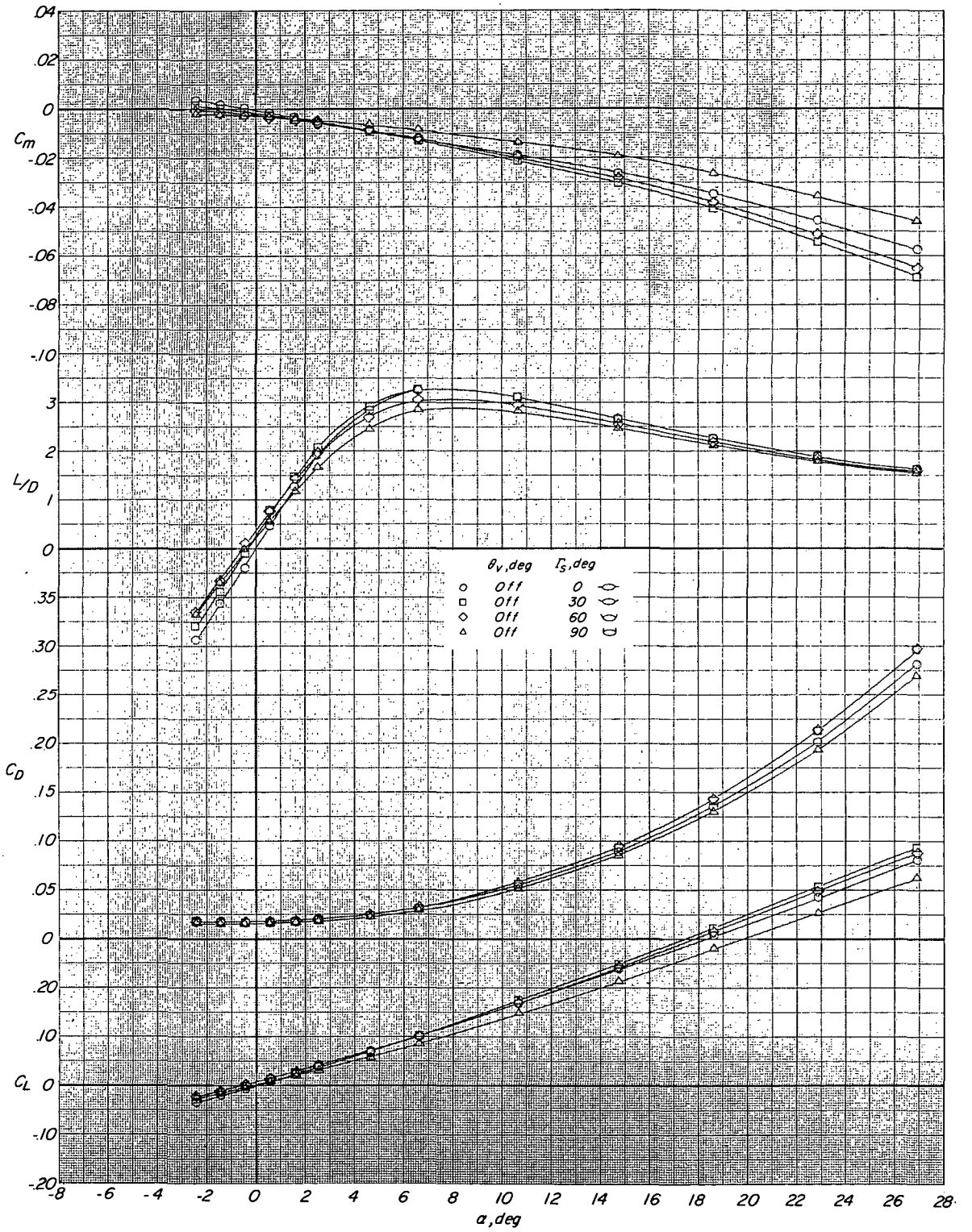

(f) M = 4.63.

Figure 5.- Concluded.

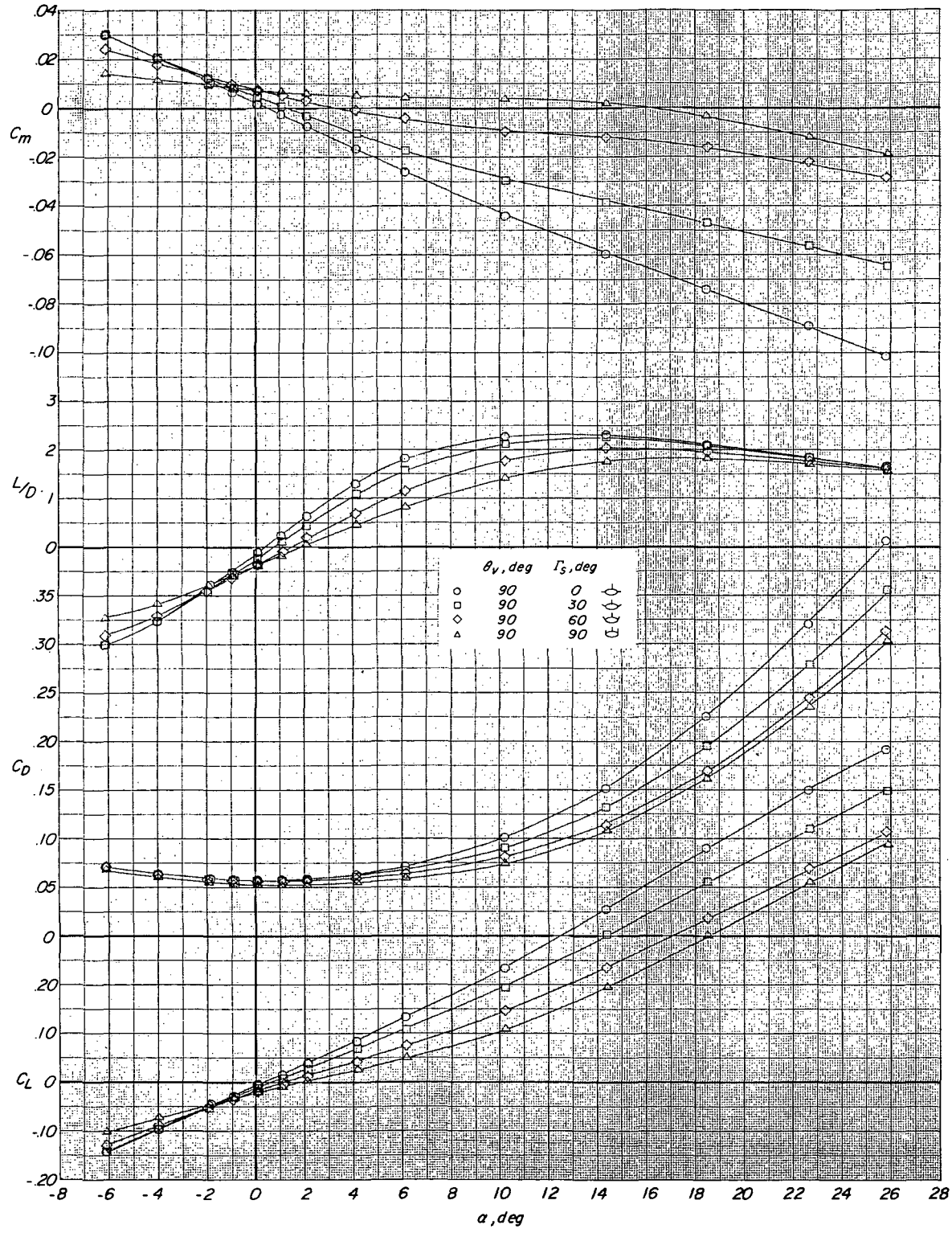

(a) M = 1.50.

Figure 6.- Effect of outboard-stabilizer dihedral on the longitudinal aerodynamic characteristics of the configuration with center vertical tail on. $\Gamma_S = 0^o$ to 90^o.

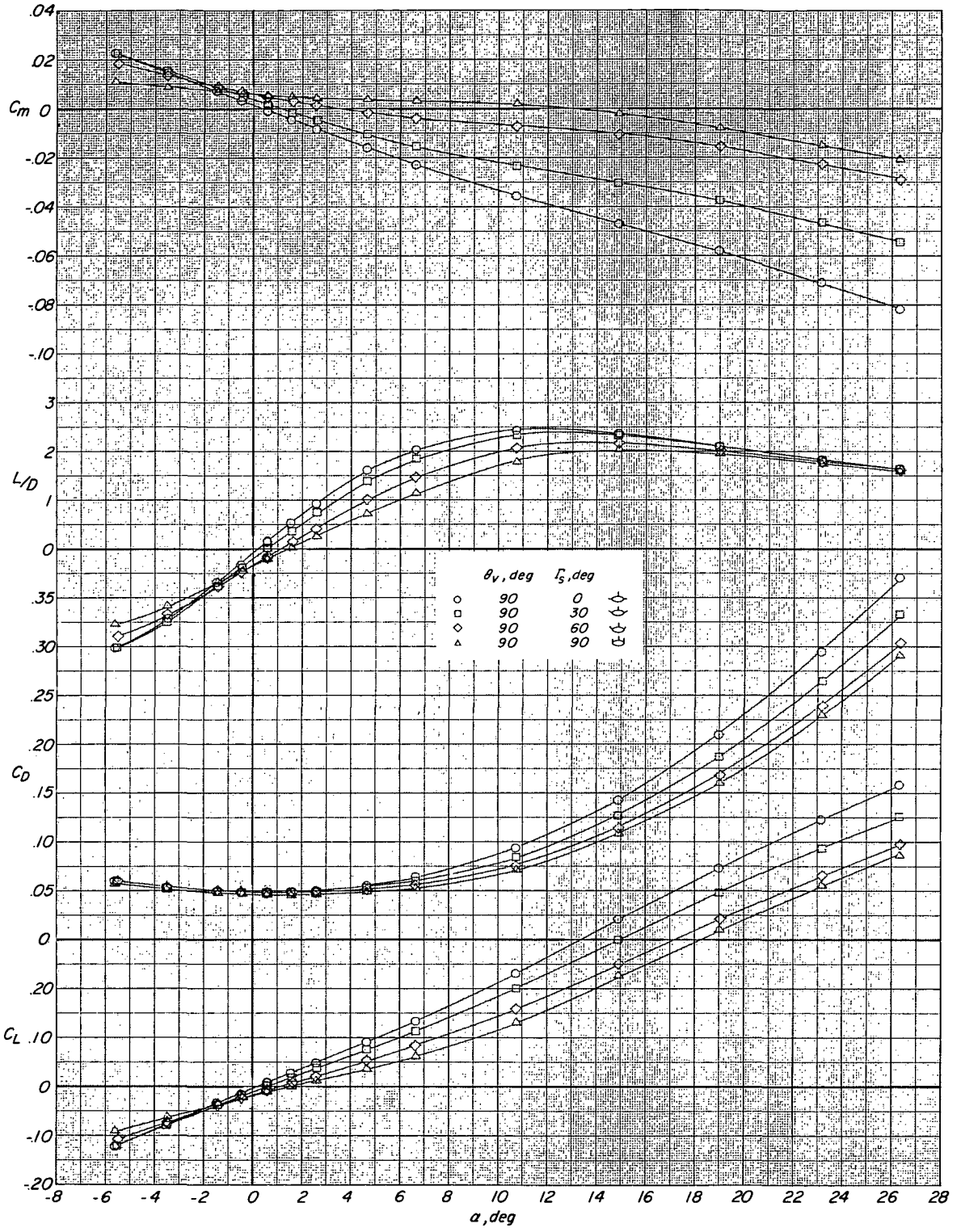

(b) M = 1.90.

Figure 6.- Continued.

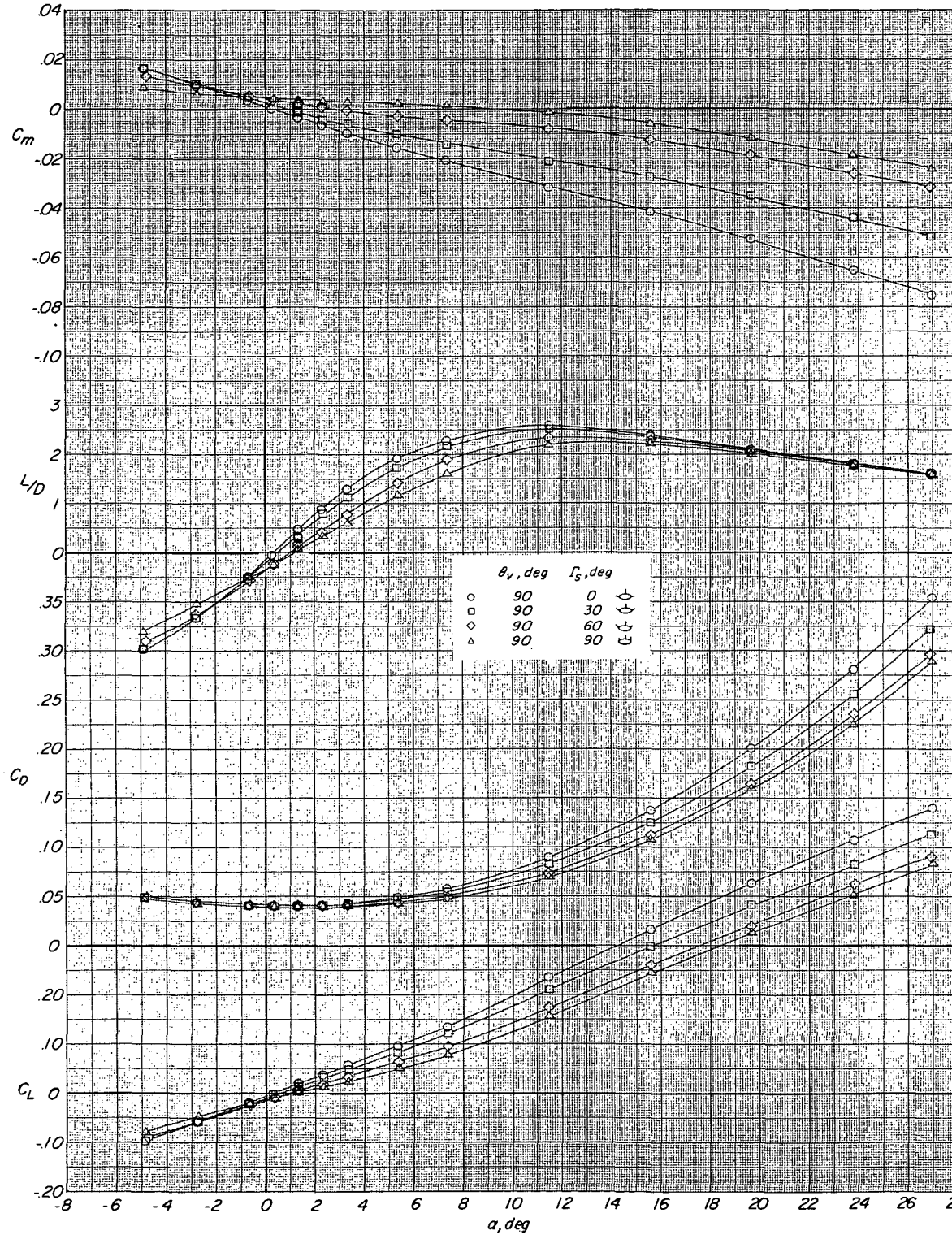

(c) M = 2.36.

Figure 6.- Continued.

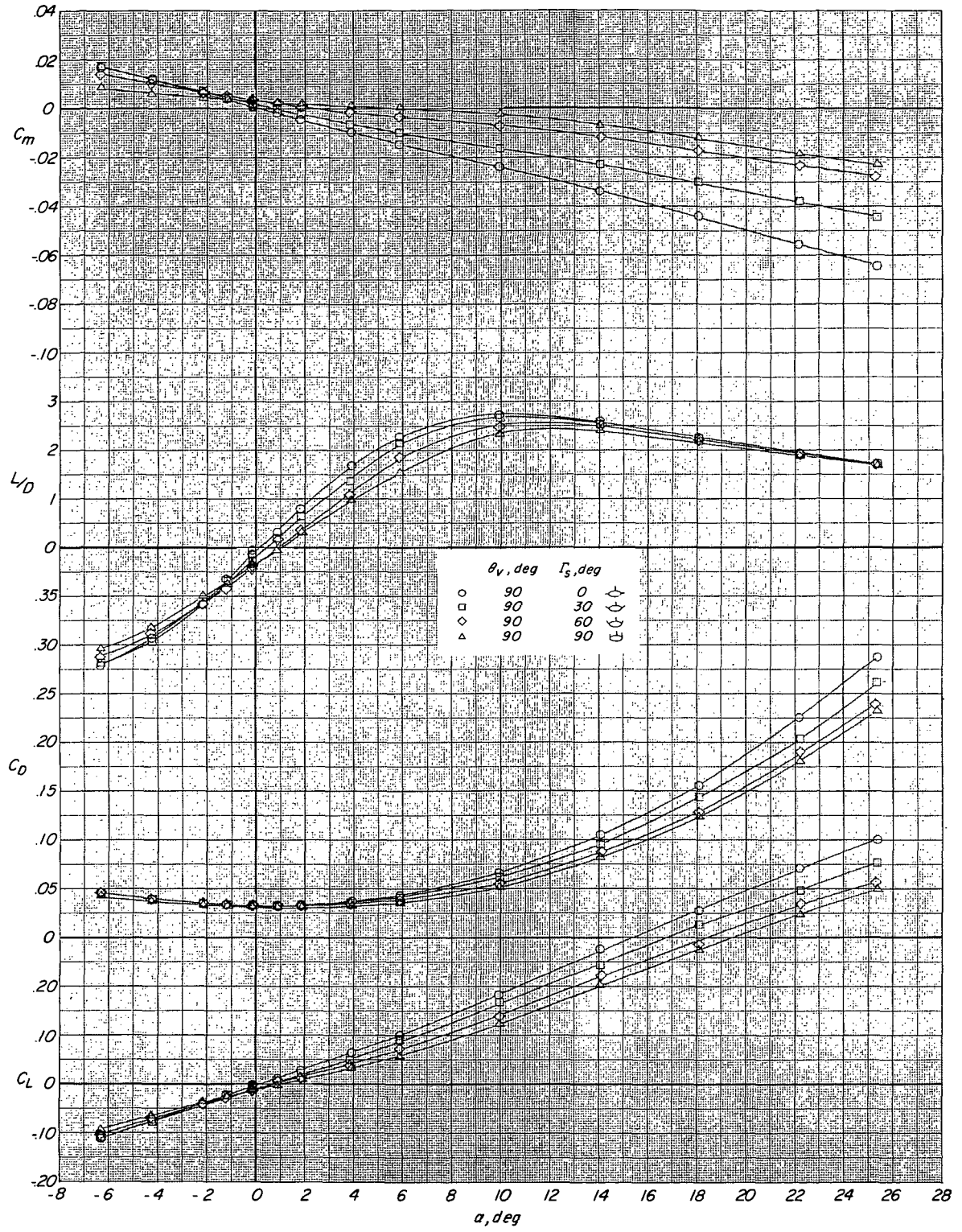

(d) M = 2.86.

Figure 6.- Continued.

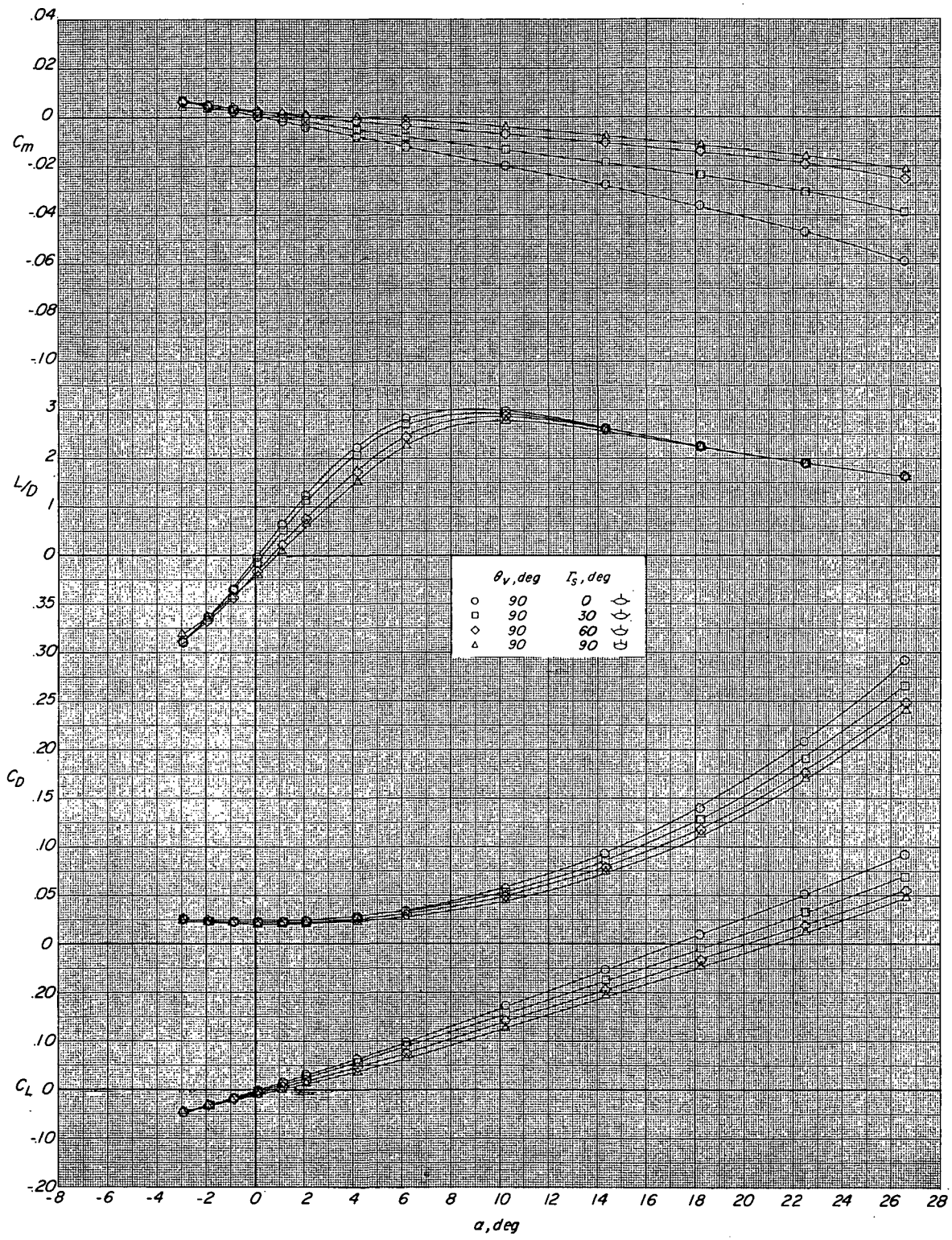

(e) M = 3.96.

Figure 6.- Continued.

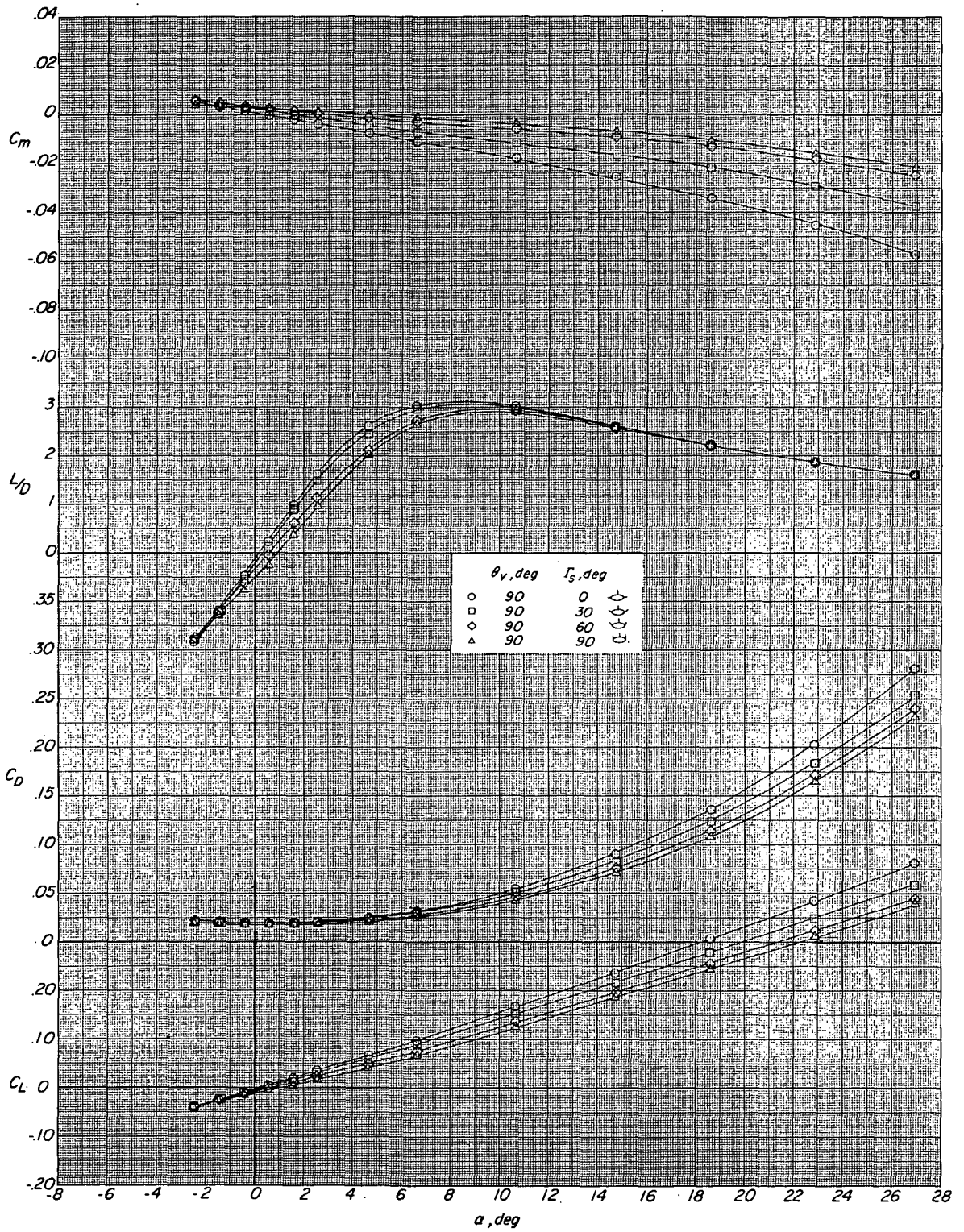

(f) M = 4.63.

Figure 6.- Concluded.

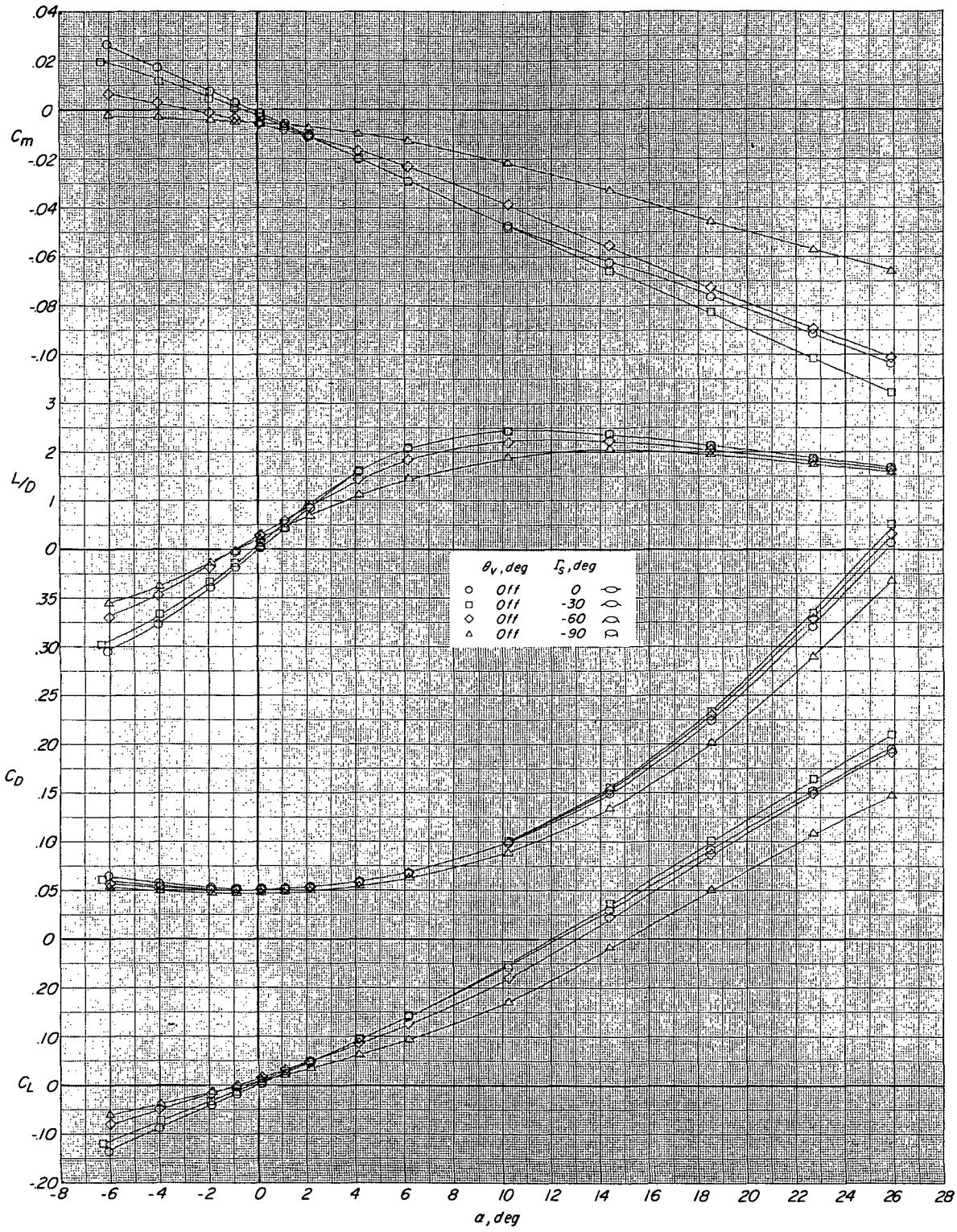

(a) M = 1.50.

Figure 7.- Effect of outboard-stabilizer dihedral on the longitudinal aerodynamic characteristics of the configuration without vertical tail. $\Gamma_S = 0^o$ to -90^o.

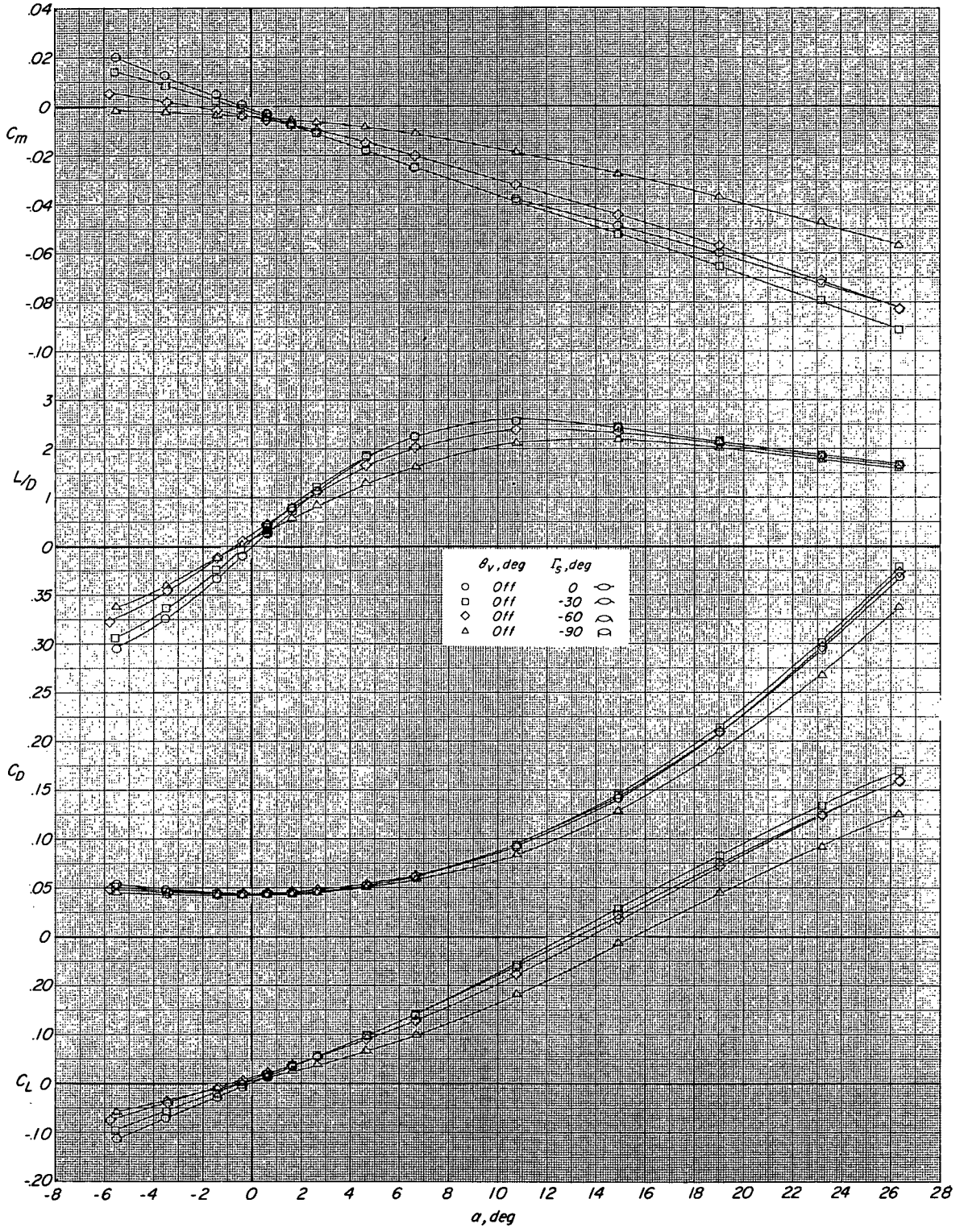

(b) M = 1.90.

Figure 7.- Continued.

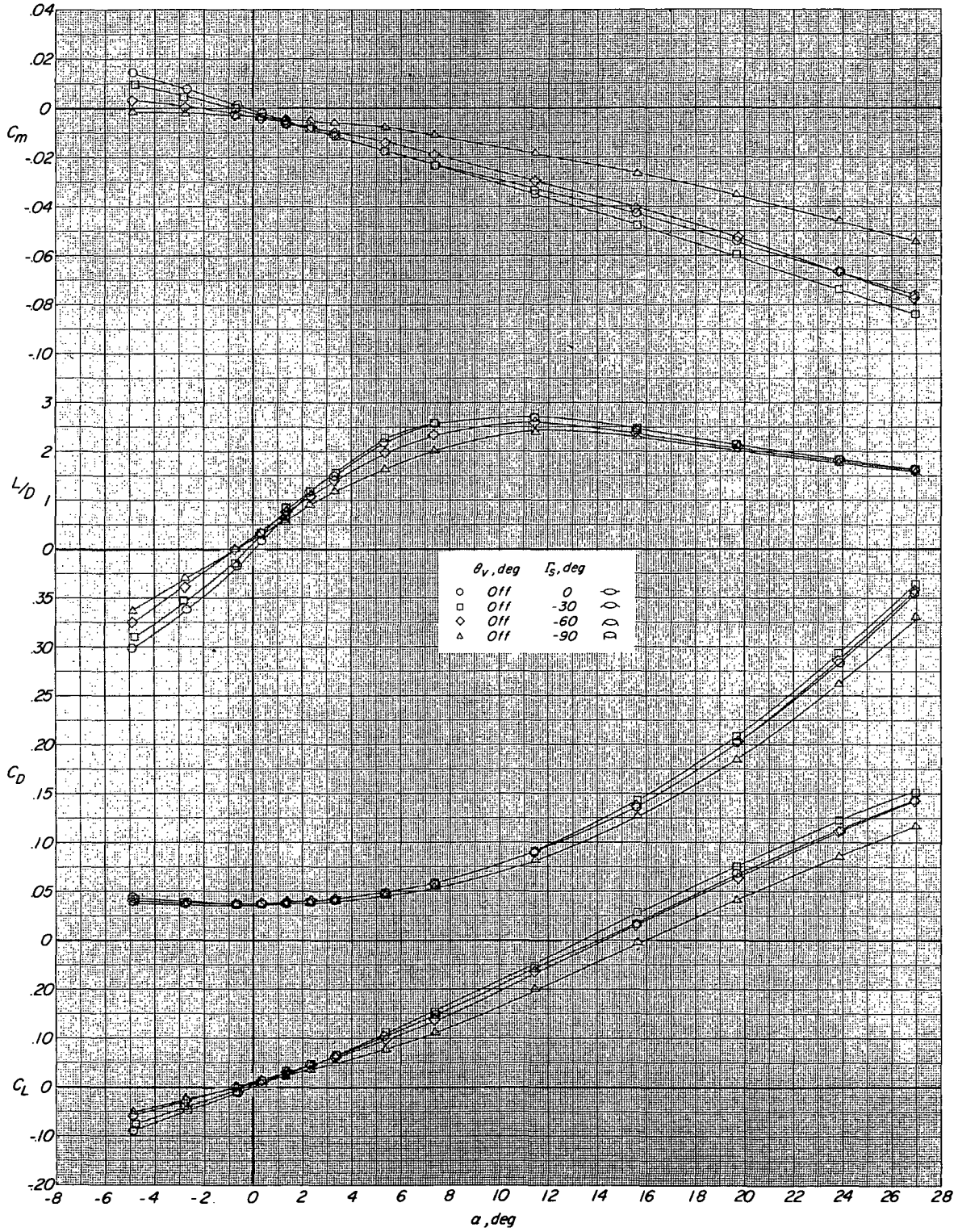

(c) M = 2.36.

Figure 7.- Continued.

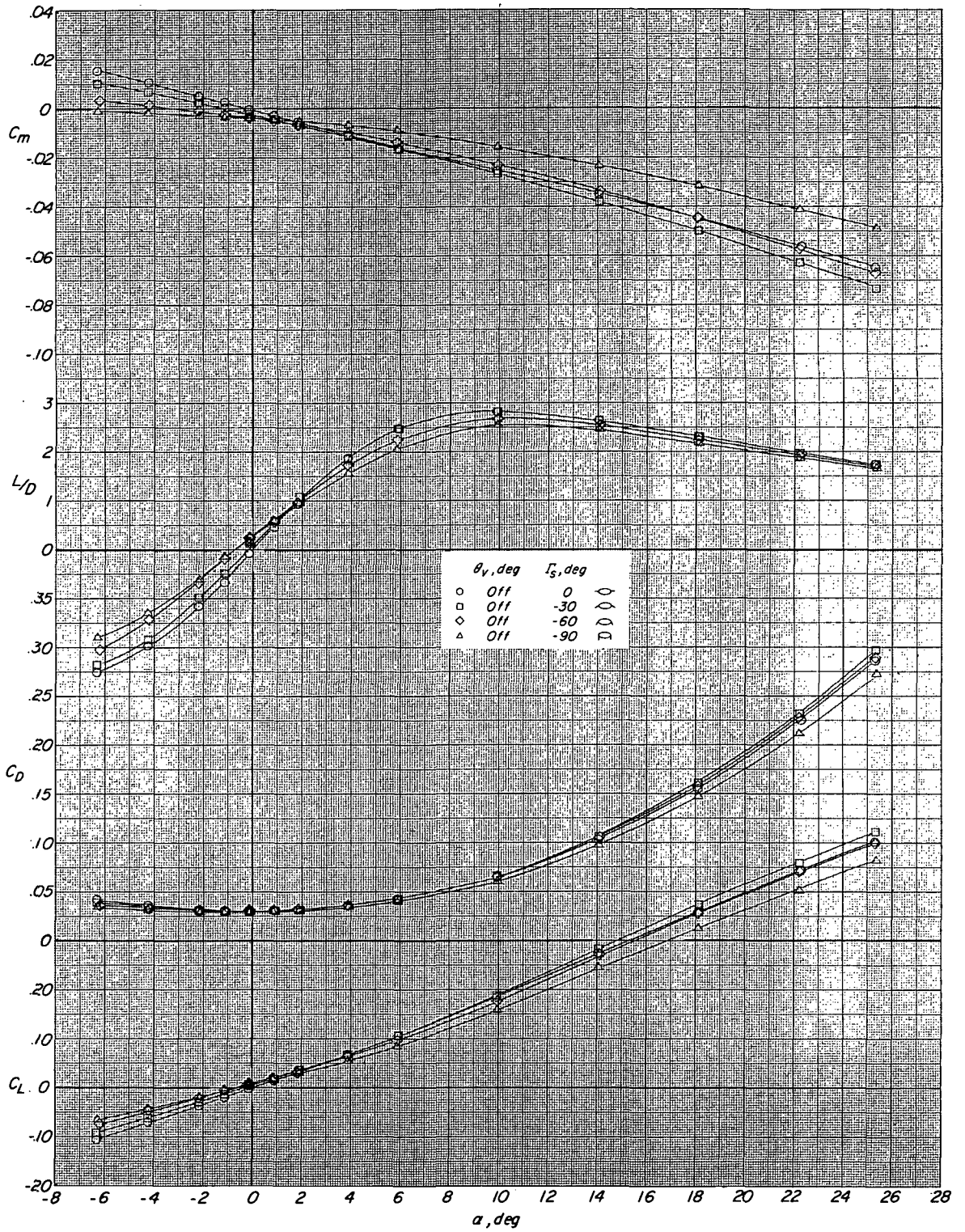

(d) M = 2.86.

Figure 7.- Continued.

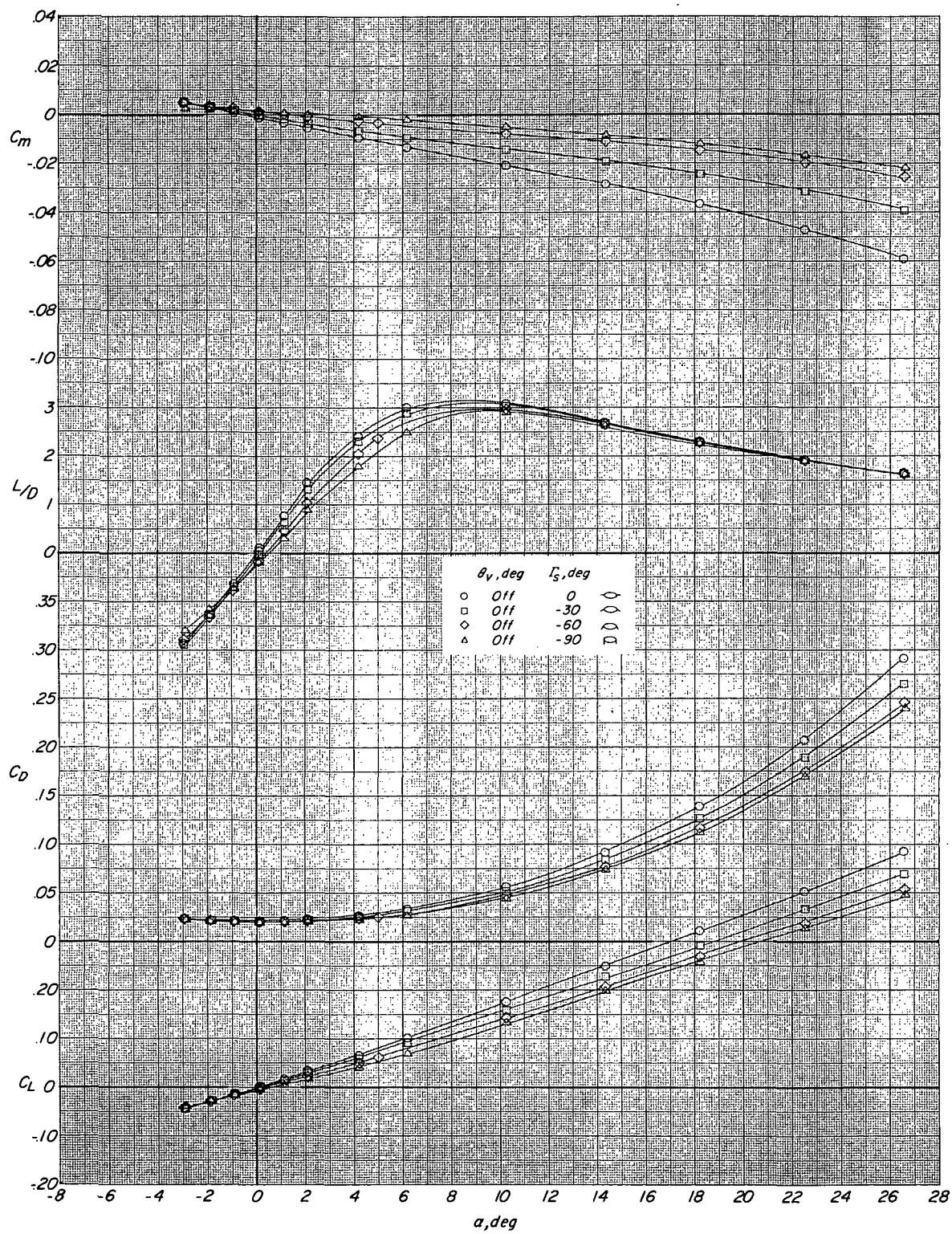

(e) M = 3.96.

Figure 7.- Continued.

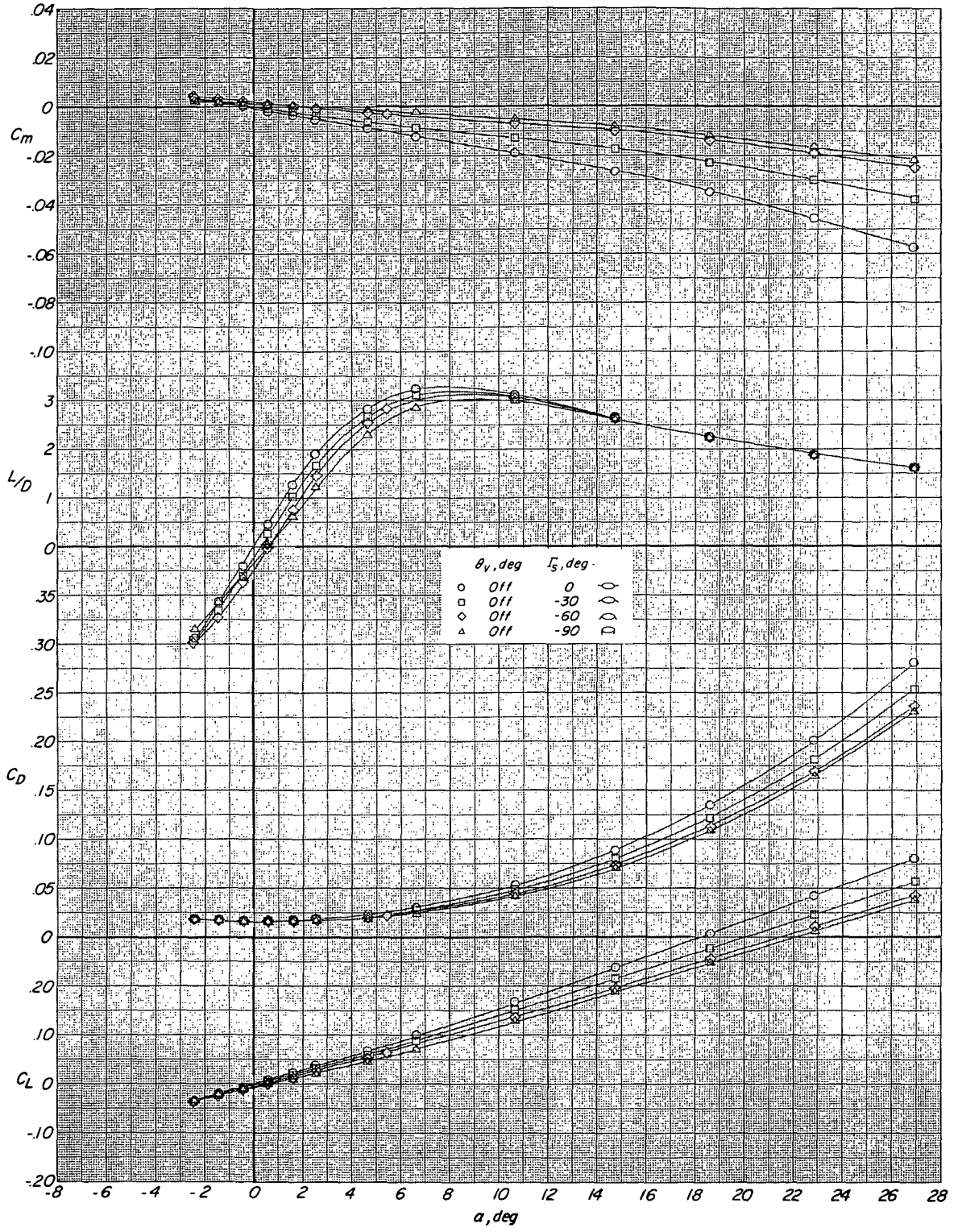

(f) M = 4.63.

Figure 7.- Concluded.

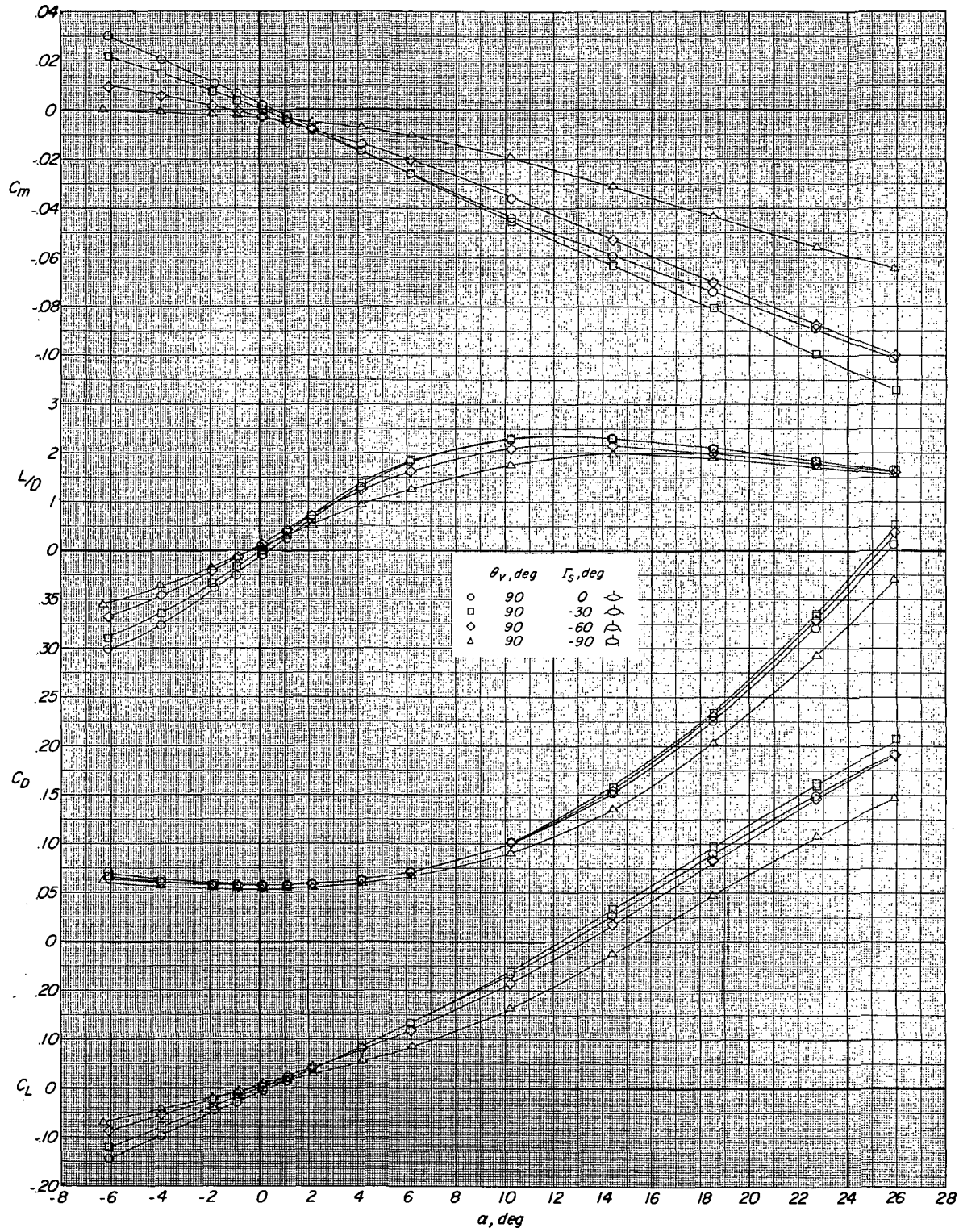

(a) M = 1.50.

Figure 8.- Effect of outboard-stabilizer dihedral on the longitudinal aerodynamic characteristics of the configuration with center vertical tail on. $\Gamma_S = 0^o$ to -90^o.

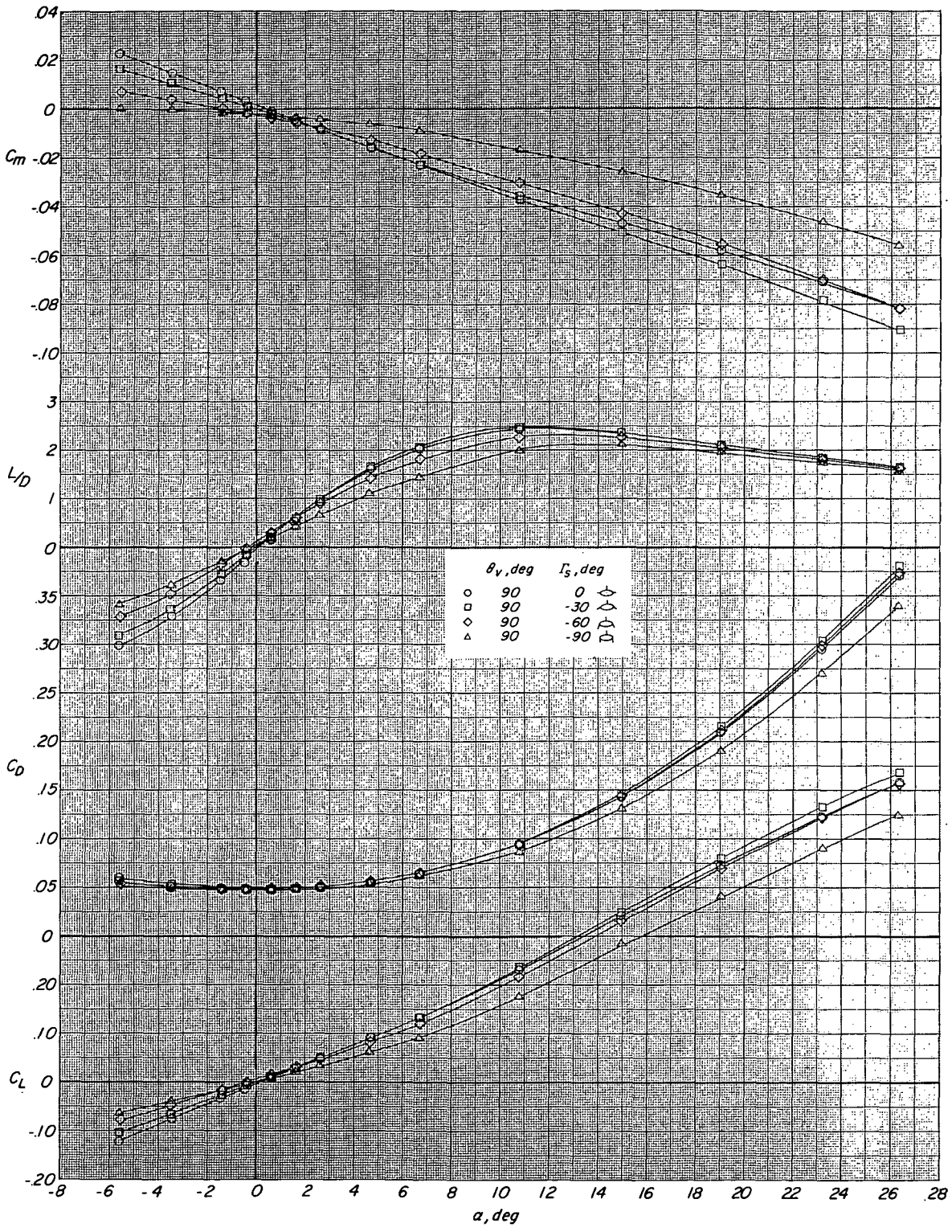

(b) M = 1.90.

Figure 8.- Continued.

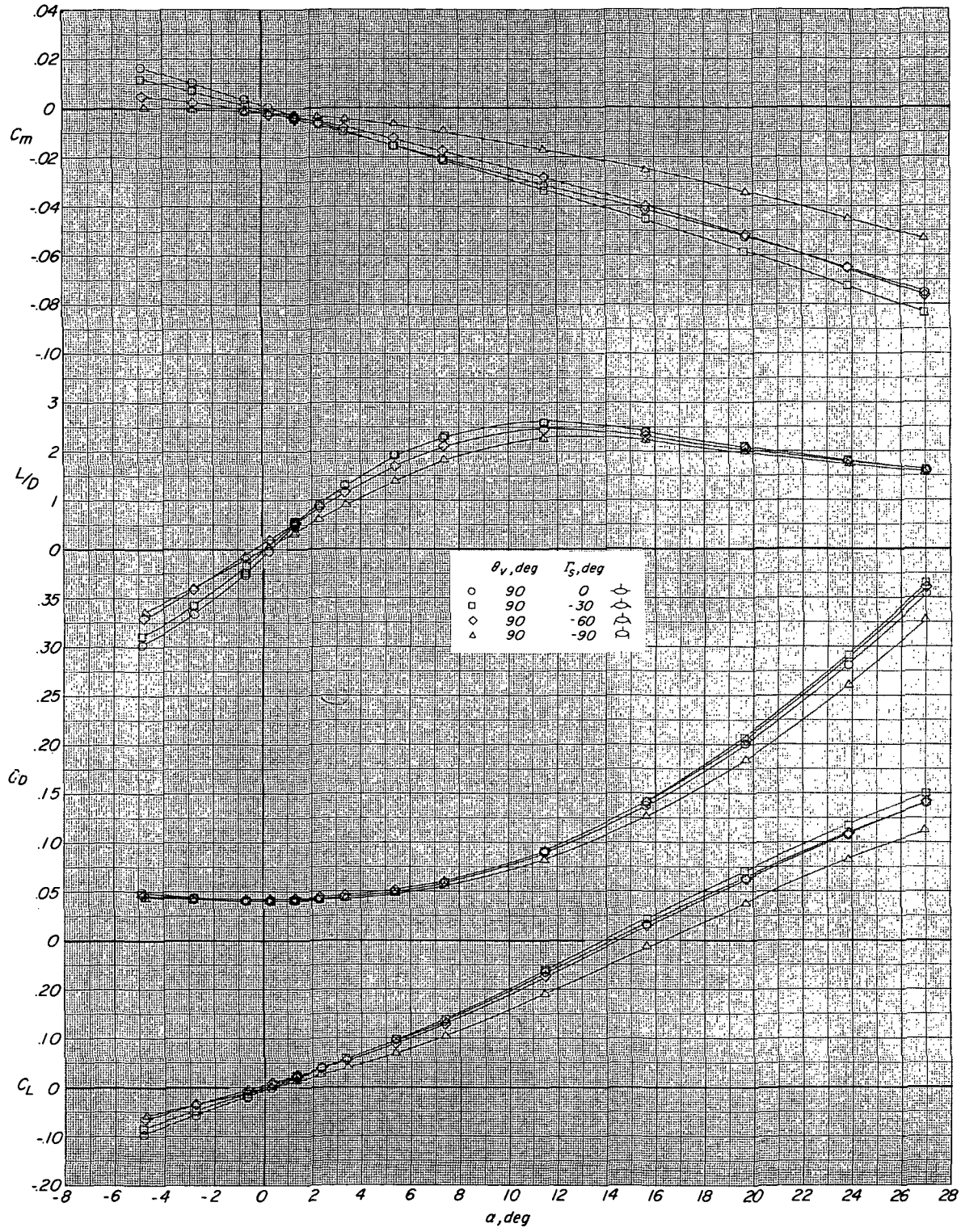

(c) M = 2.36.

Figure 8.- Continued.

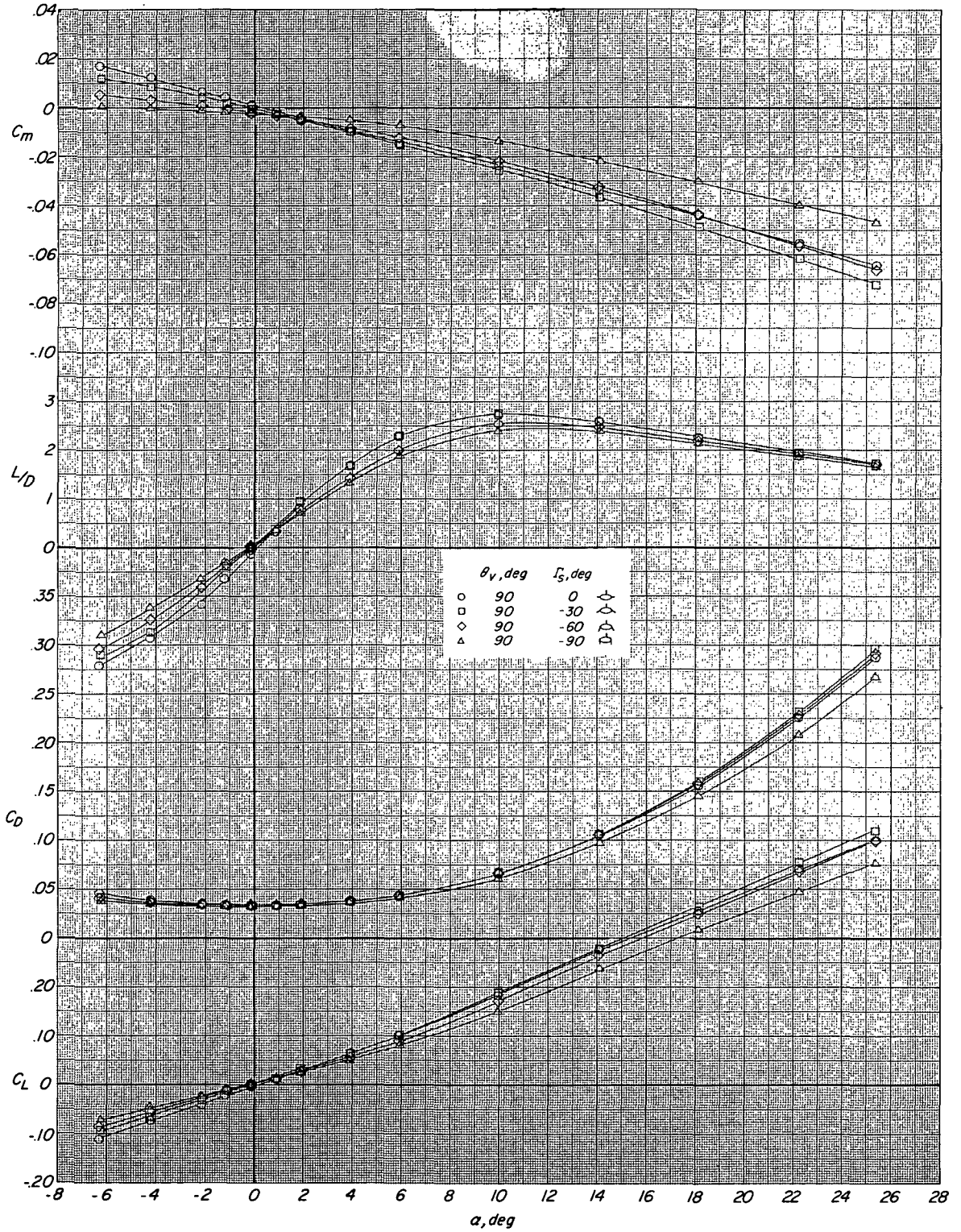

(d) M = 2.86.

Figure 8.- Continued.

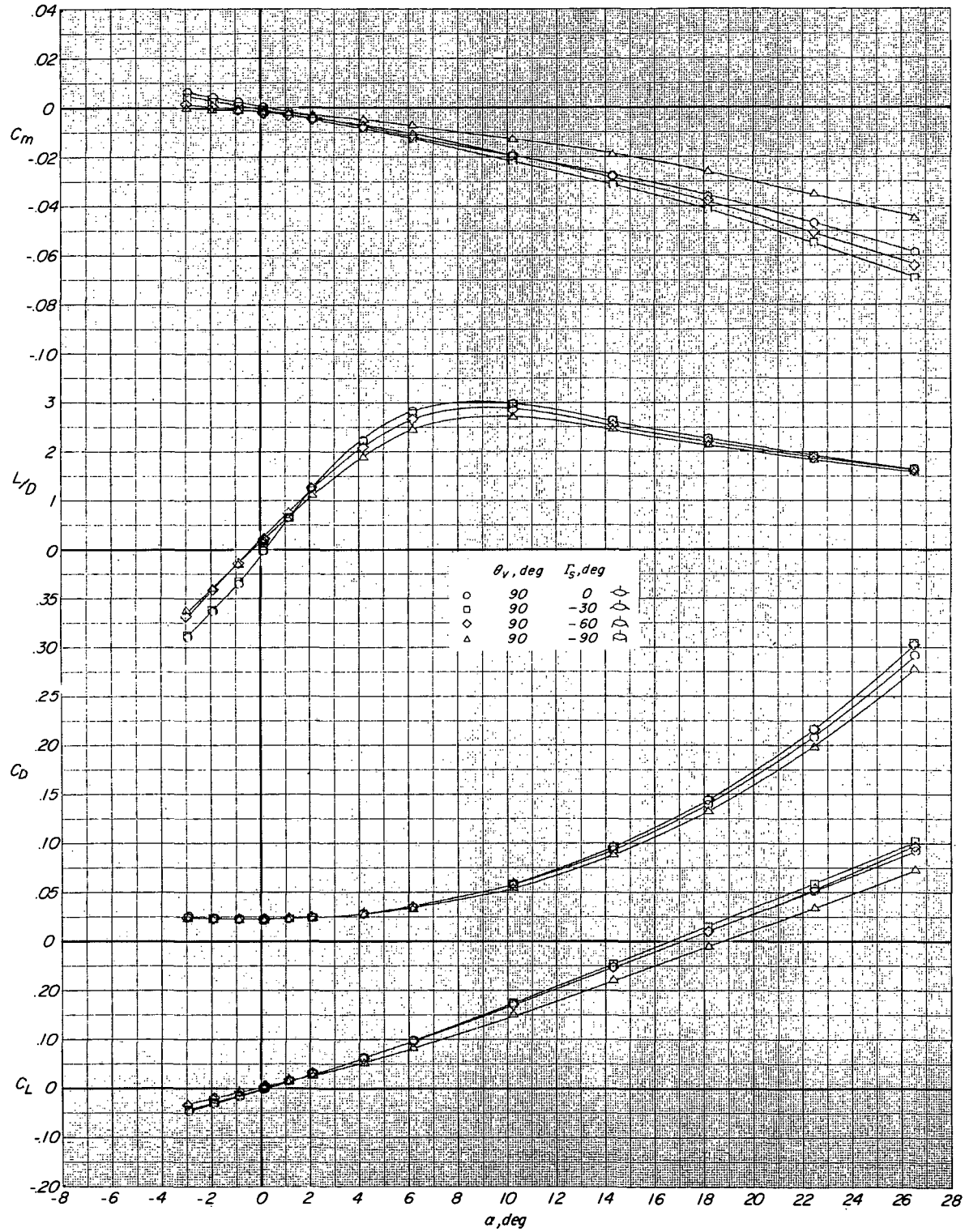

(e) M = 3.96.

Figure 8.- Continued.

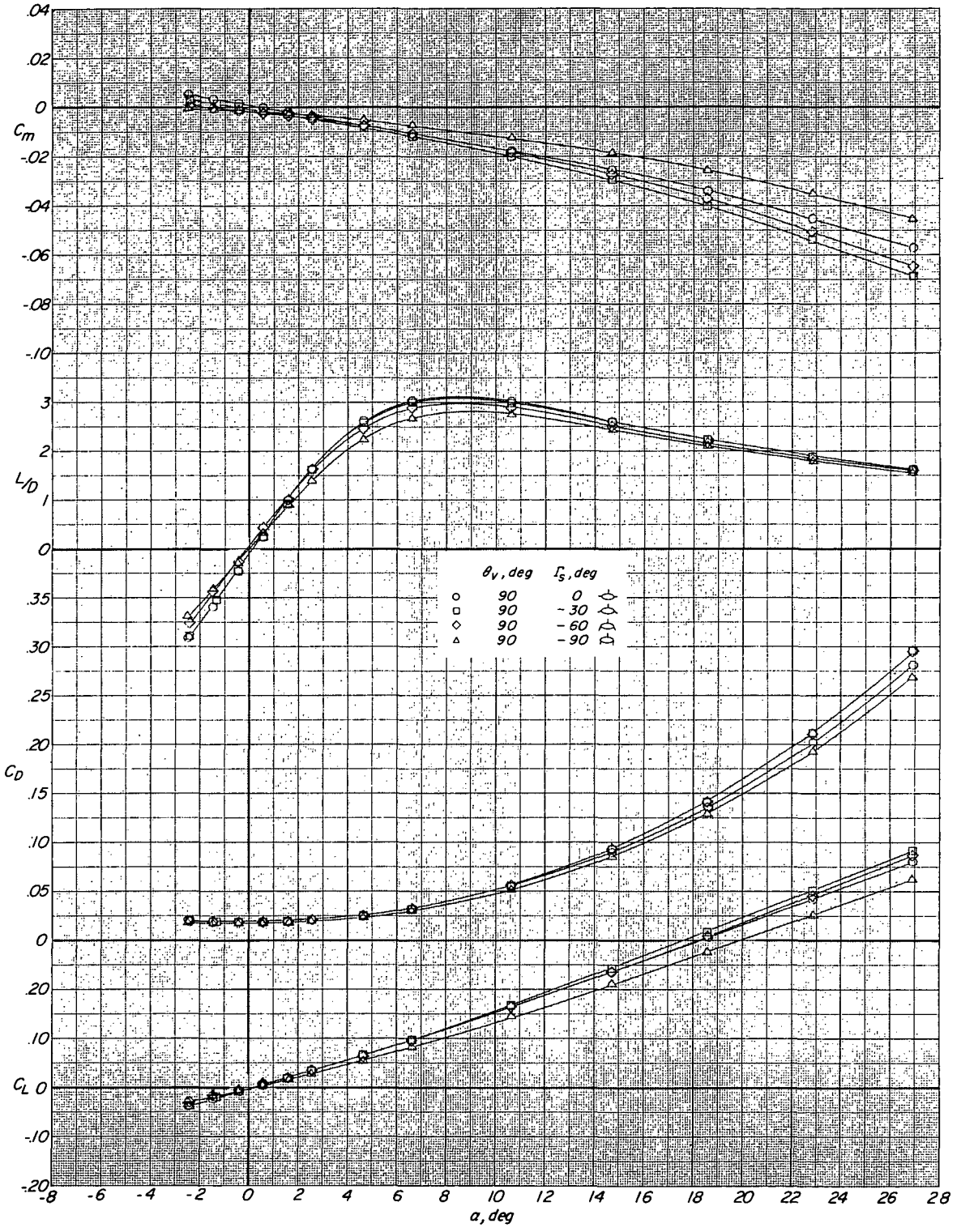

(f) M = 4.63.

Figure 8.- Concluded.

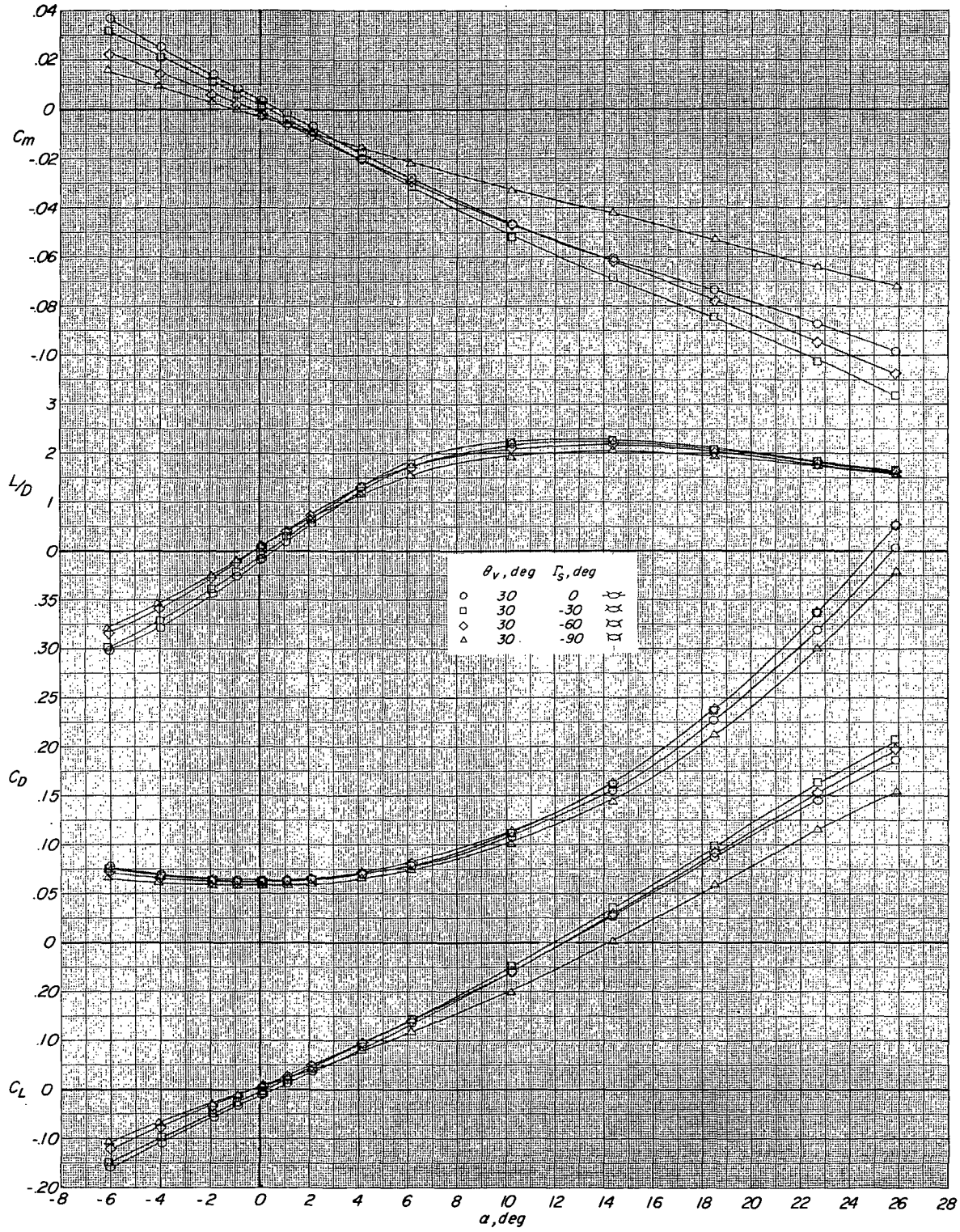

(a) M = 150.

Figure 9.- Effect of outboard-stabilizer dihedral on the longitudinal aerodynamic characteristics of the configuration with vee-tail on. $\Gamma_S = 0^o$ to -90^o.

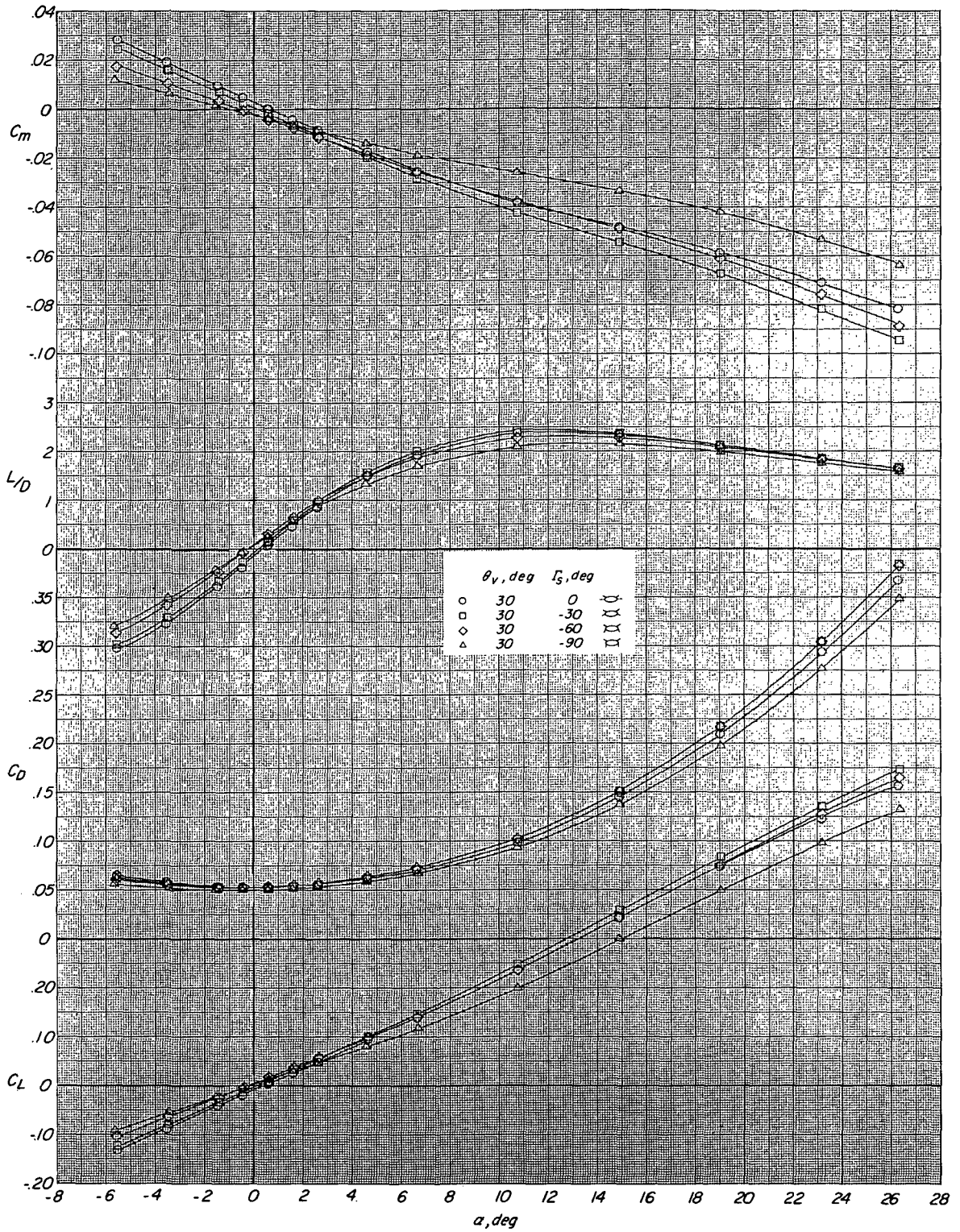

(b) M = 1.90.

Figure 9.- Continued.

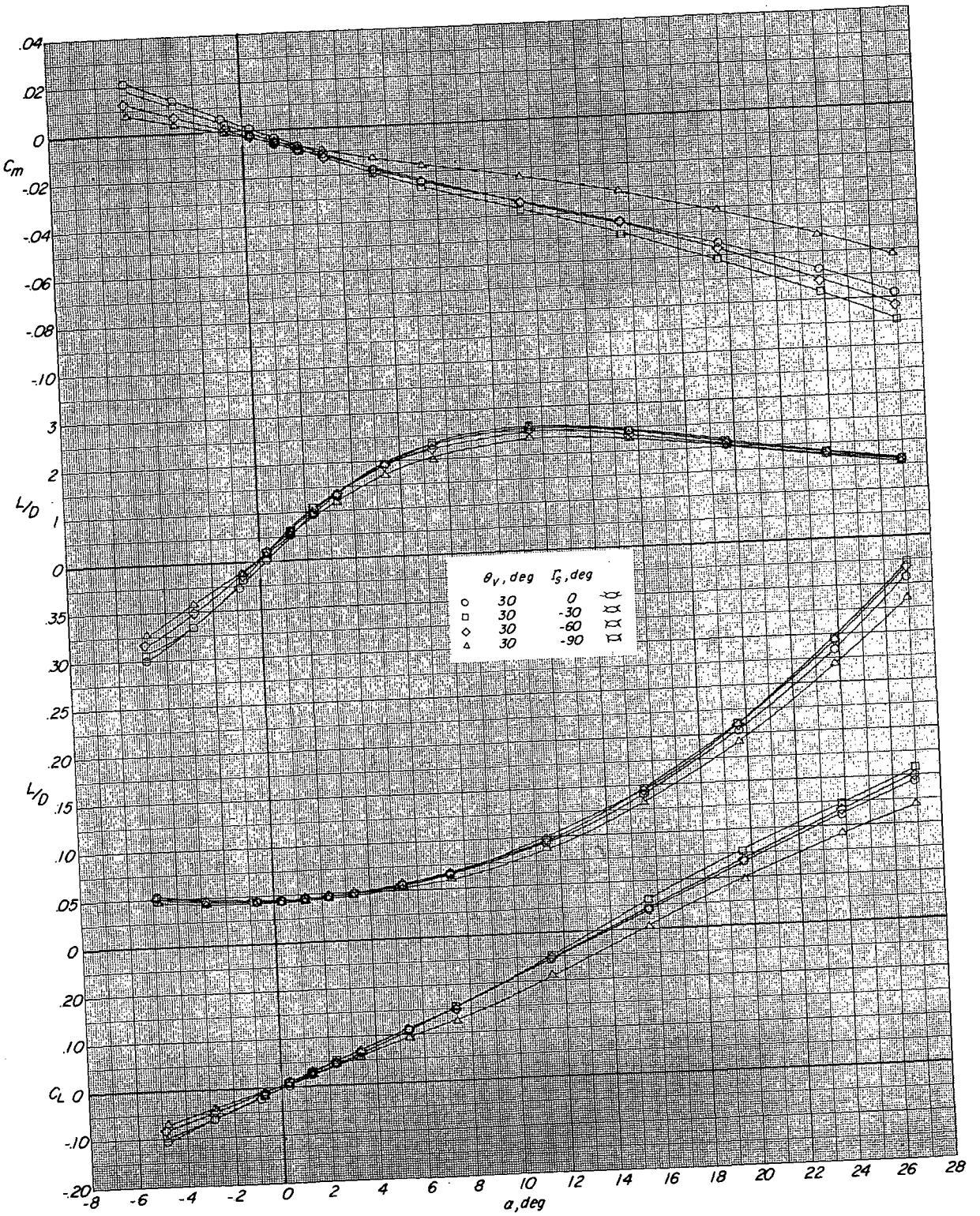

(c) M = 2.36.

Figure 9.- Continued.

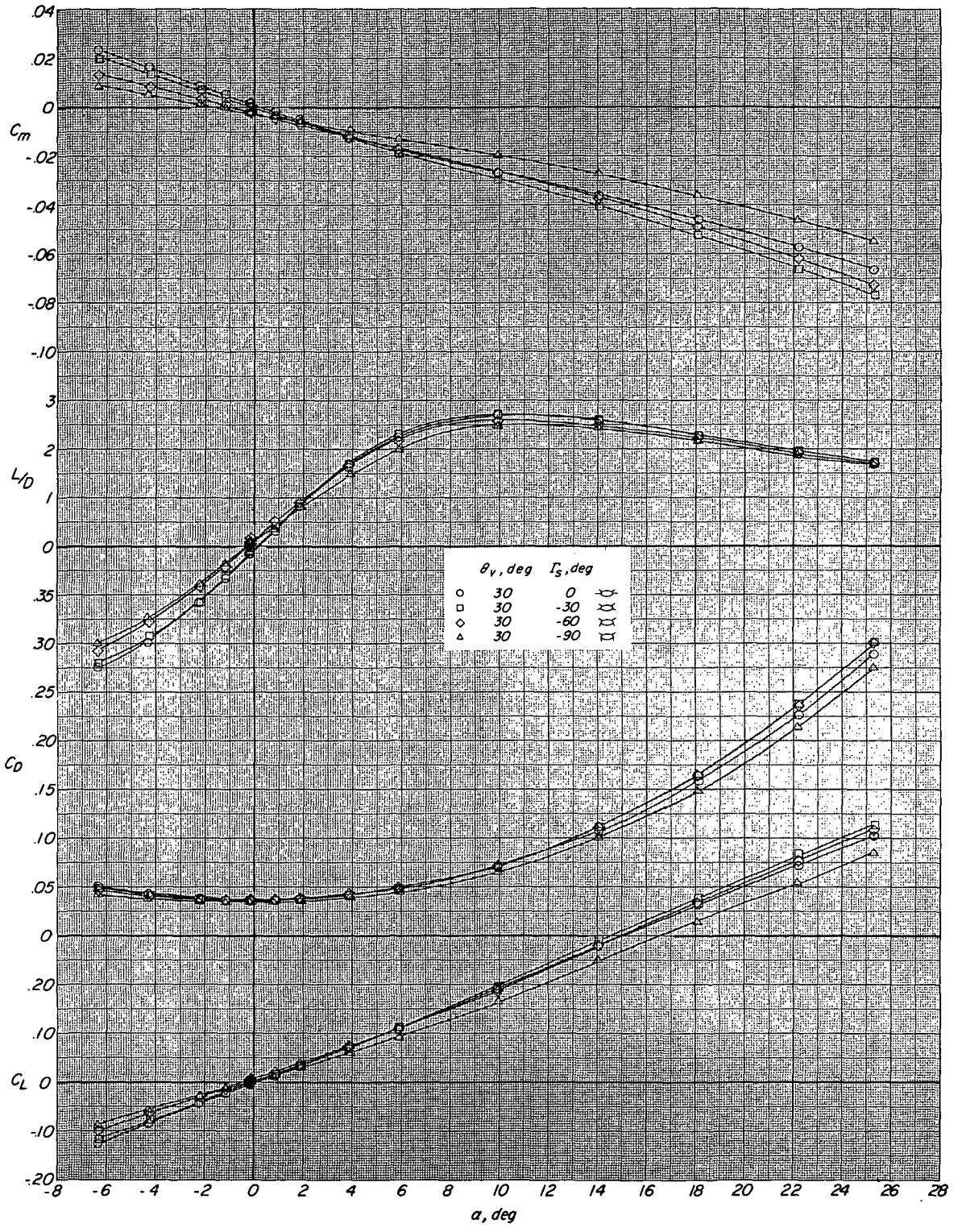

(d) M = 2.86.

Figure 9.- Continued.

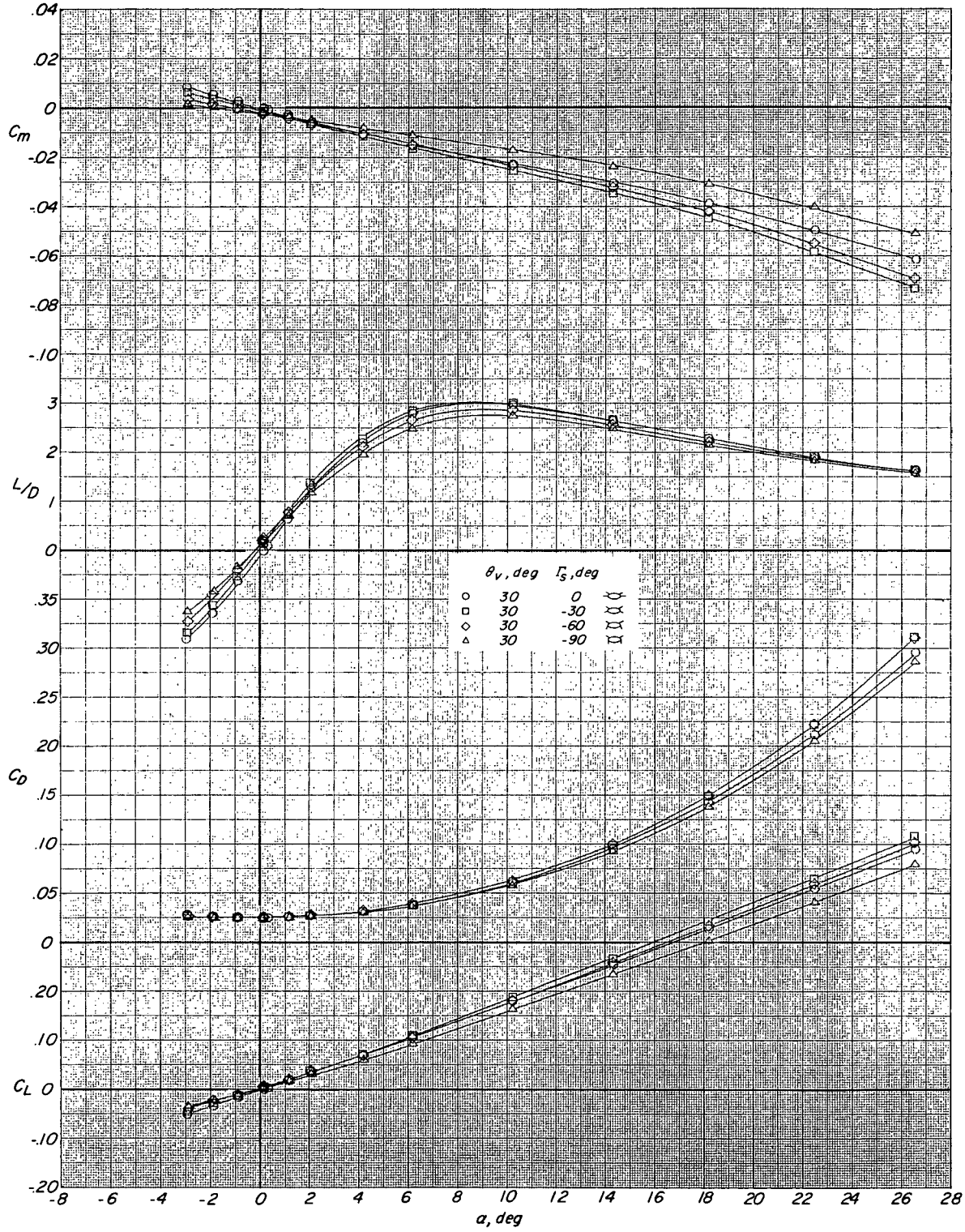

(e) M = 3.96.

Figure 9.- Continued.

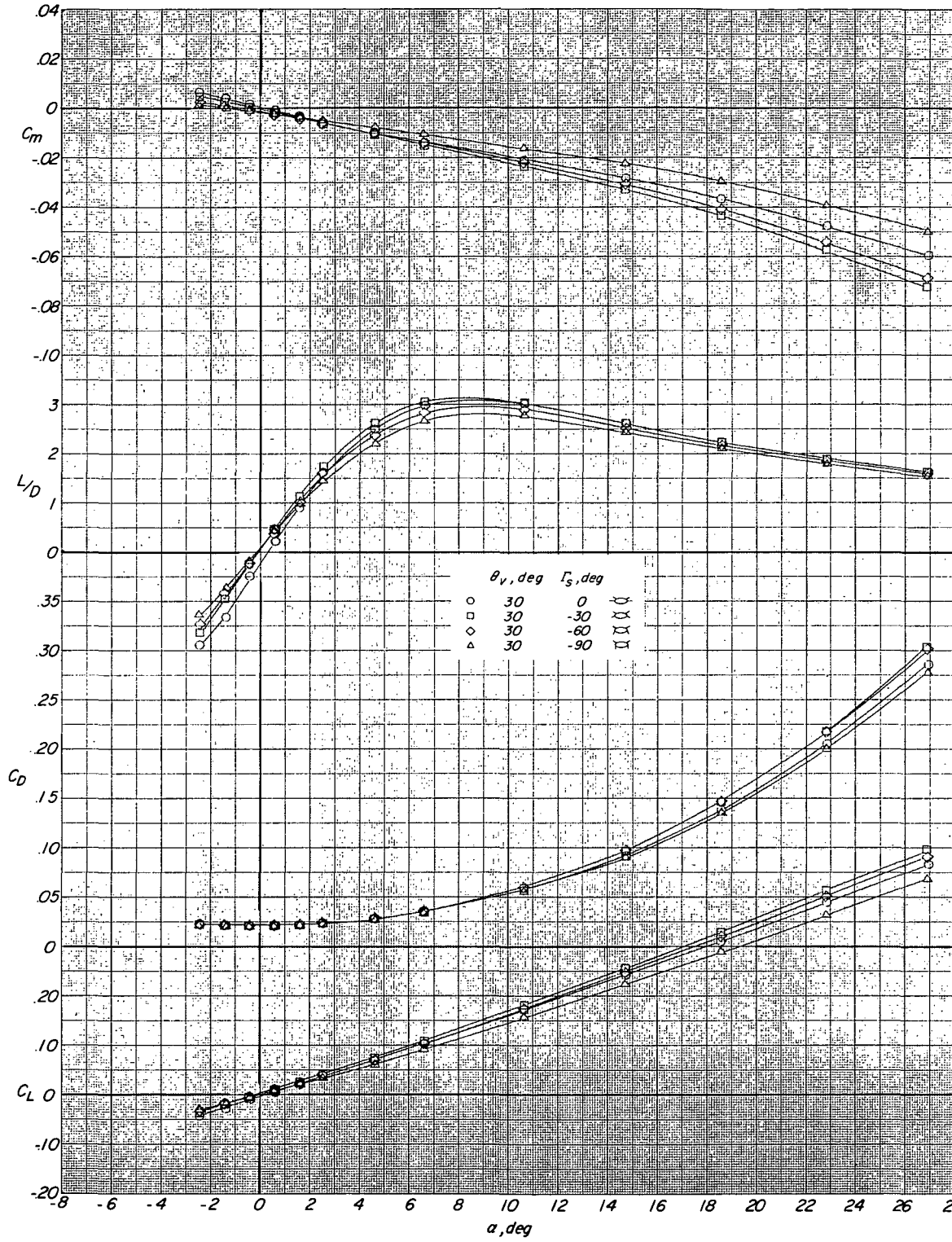

(f) M = 4.63.

Figure 9.- Concluded.

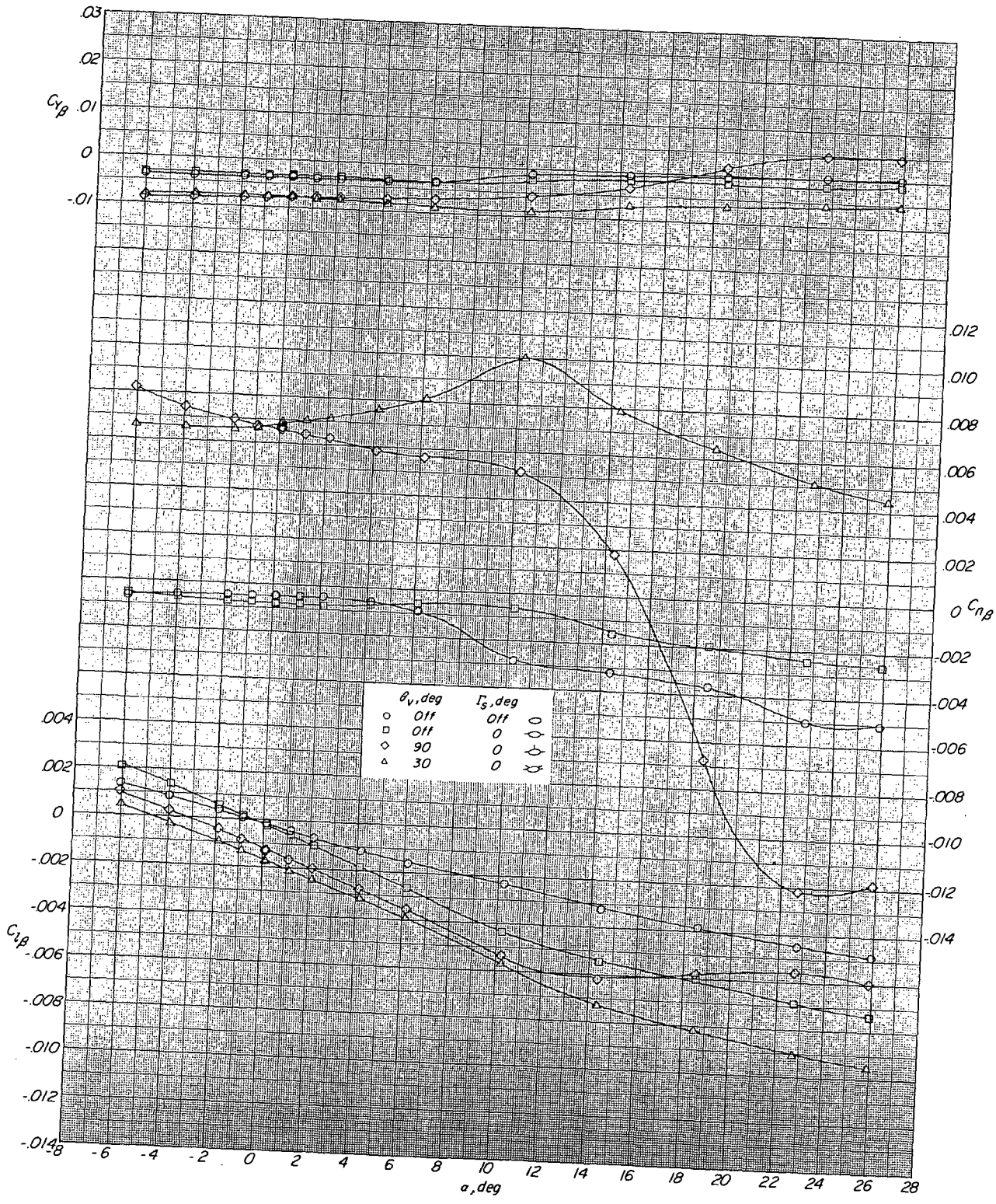

(a) M = 1.50.

Figure 10.- Effect of addition of outboard stabilizers ($\Gamma_S = 0^o$) and vertical tails ($\theta_V = 30^o$ and 90^o) on the lateral-directional stability characteristics of the basic body.

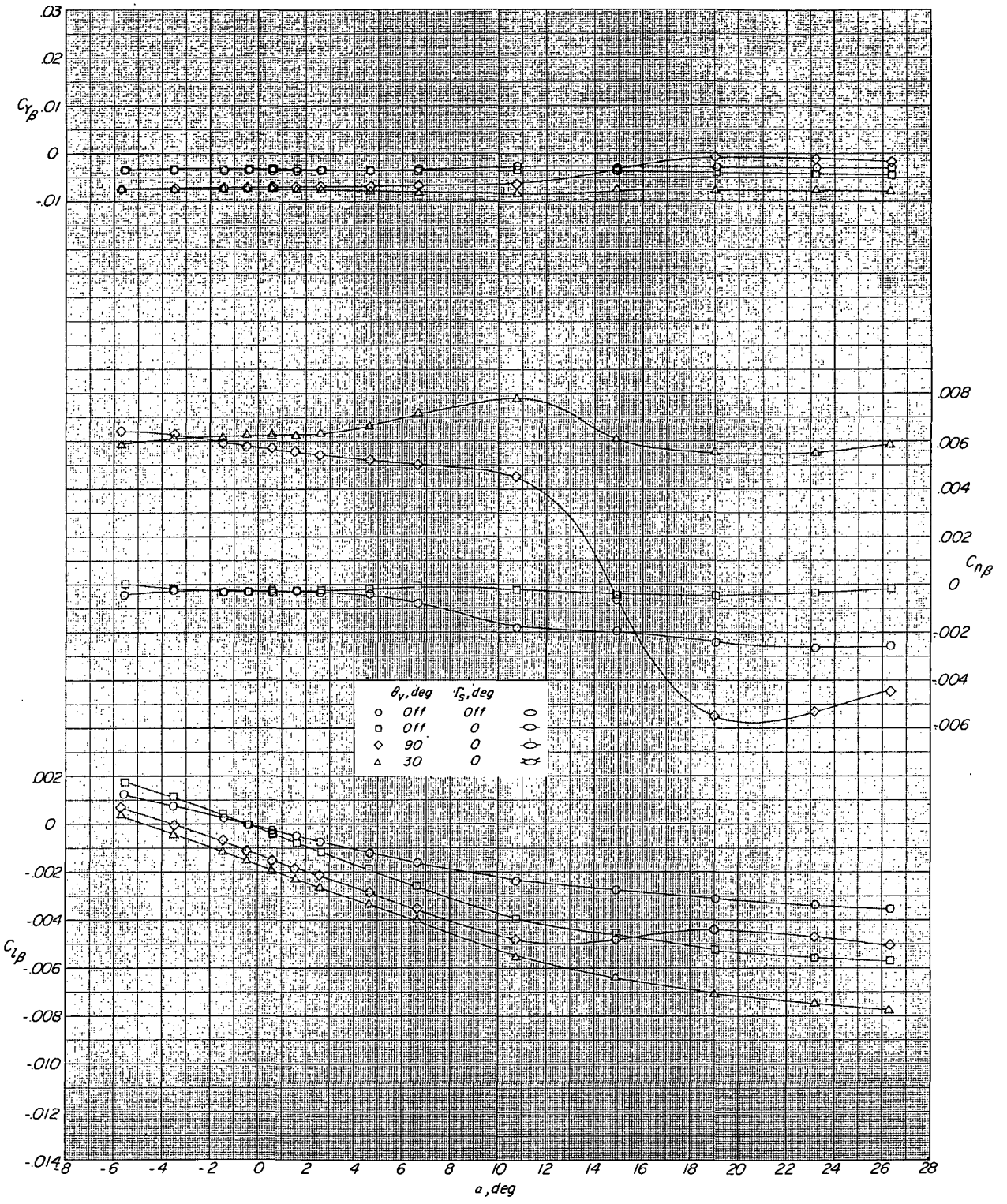

(b) M = 1.90.

Figure 10.- Continued.

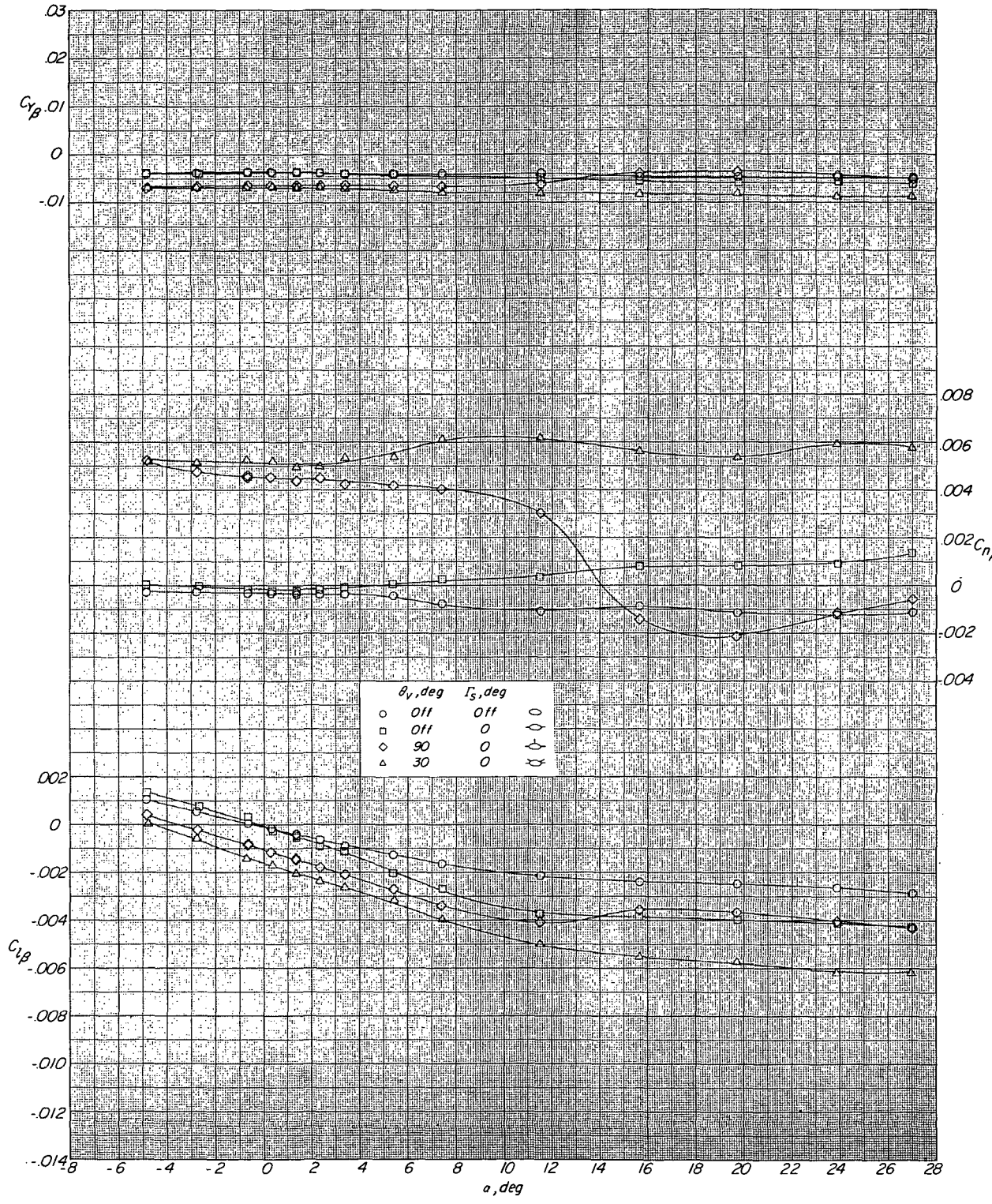

(c) M = 2.36.

Figure 10.- Continued.

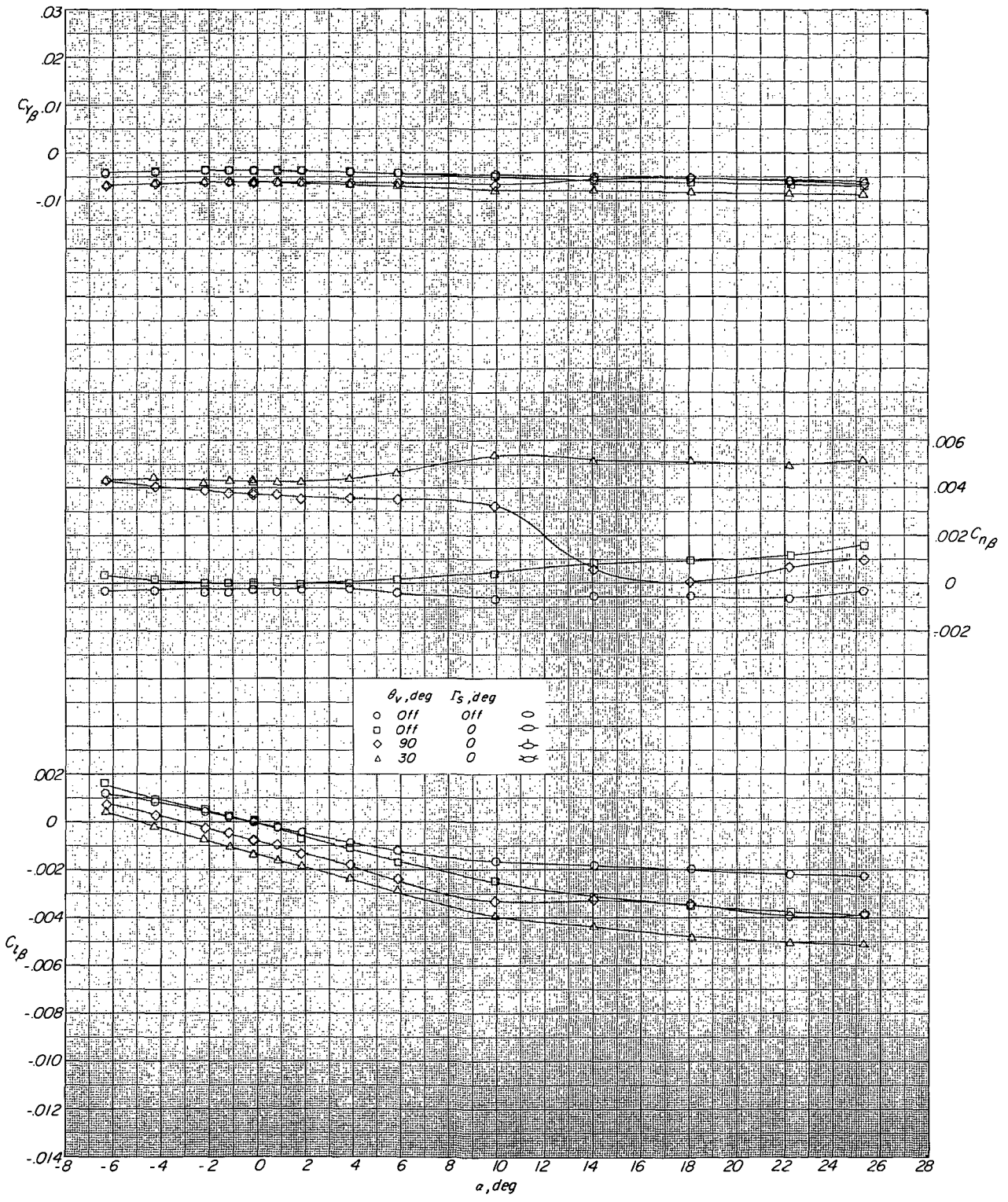

(d) M = 2.86.

Figure 10.- Continued.

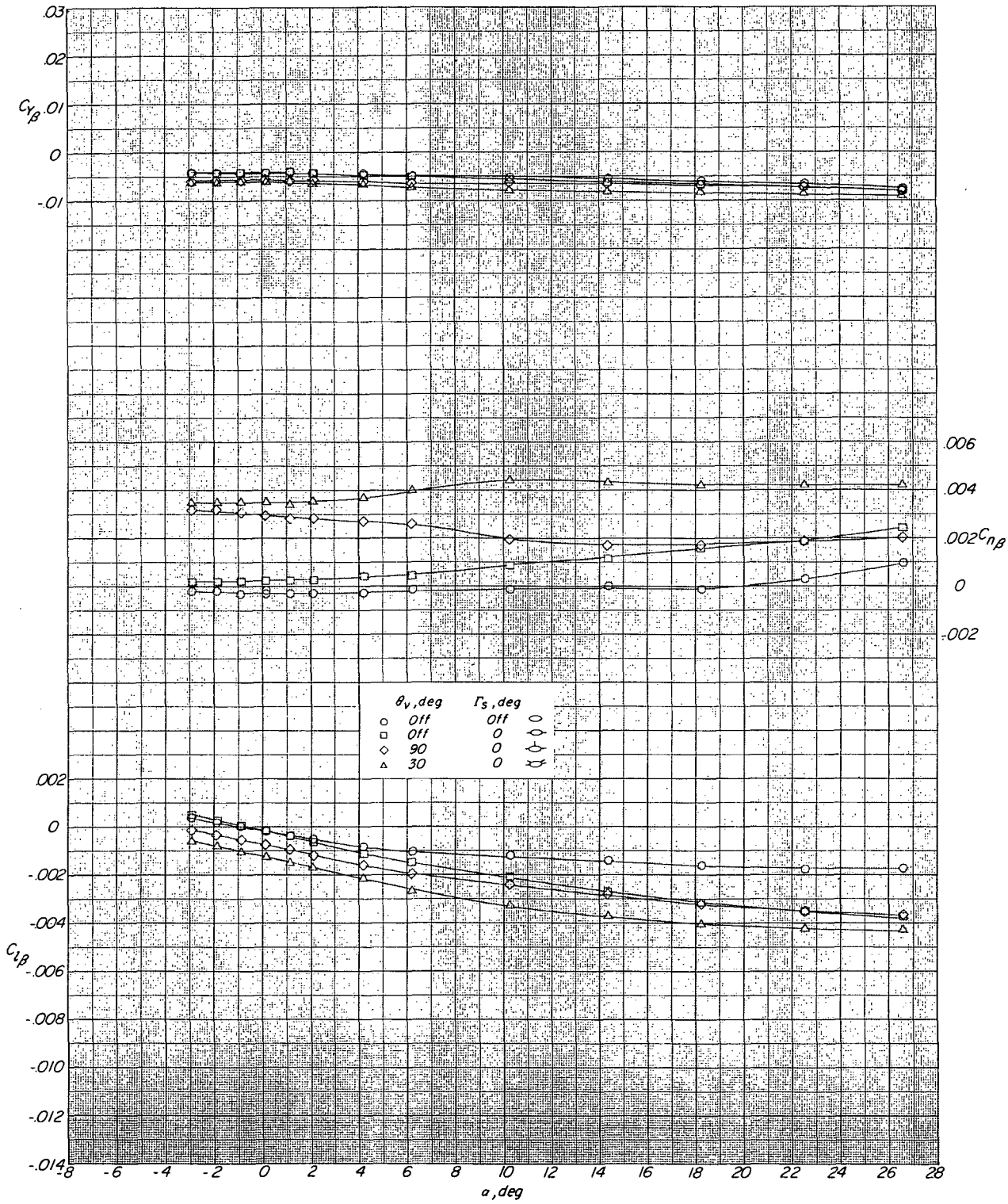

(e) M = 3.96.

Figure 10.- Continued.

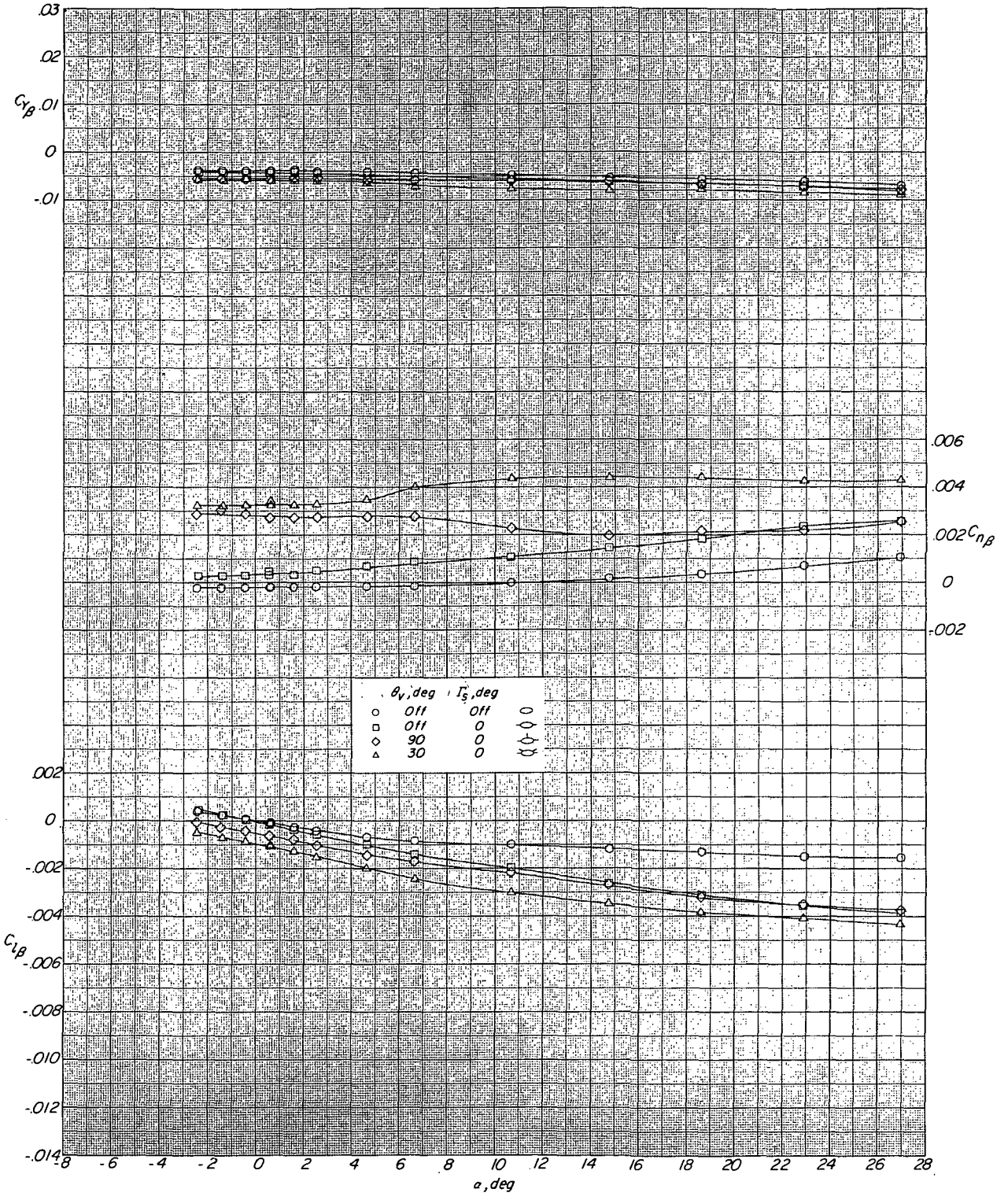

(f) M = 4.63.

Figure 10.- Concluded.

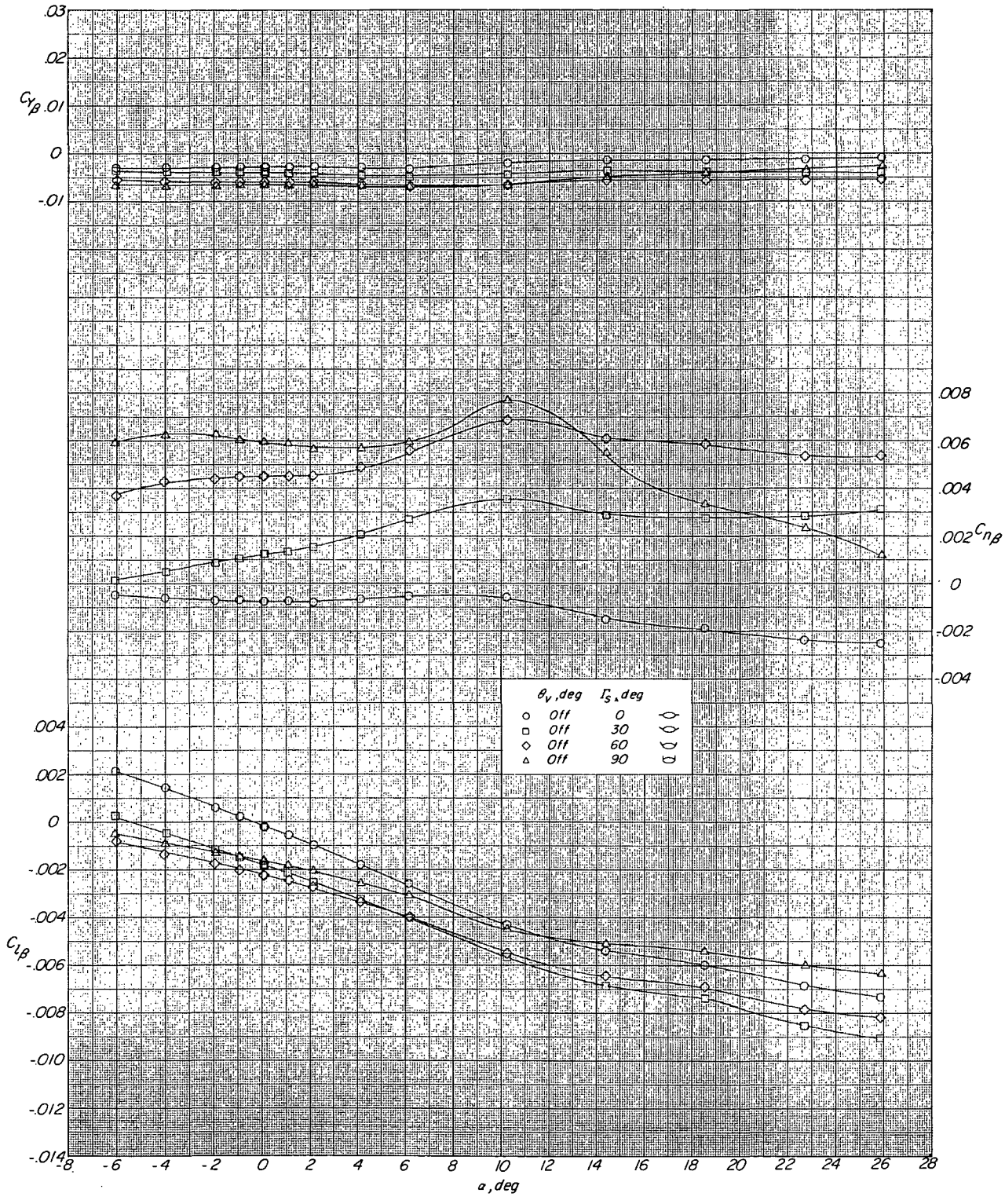

(a) M = 1.50.

Figure 11.- Effect of outboard-stabilizer dihedral on the lateral-directional stability characteristics of the configuration without vertical tail. $\Gamma_S = 0^o$ to 90^o.

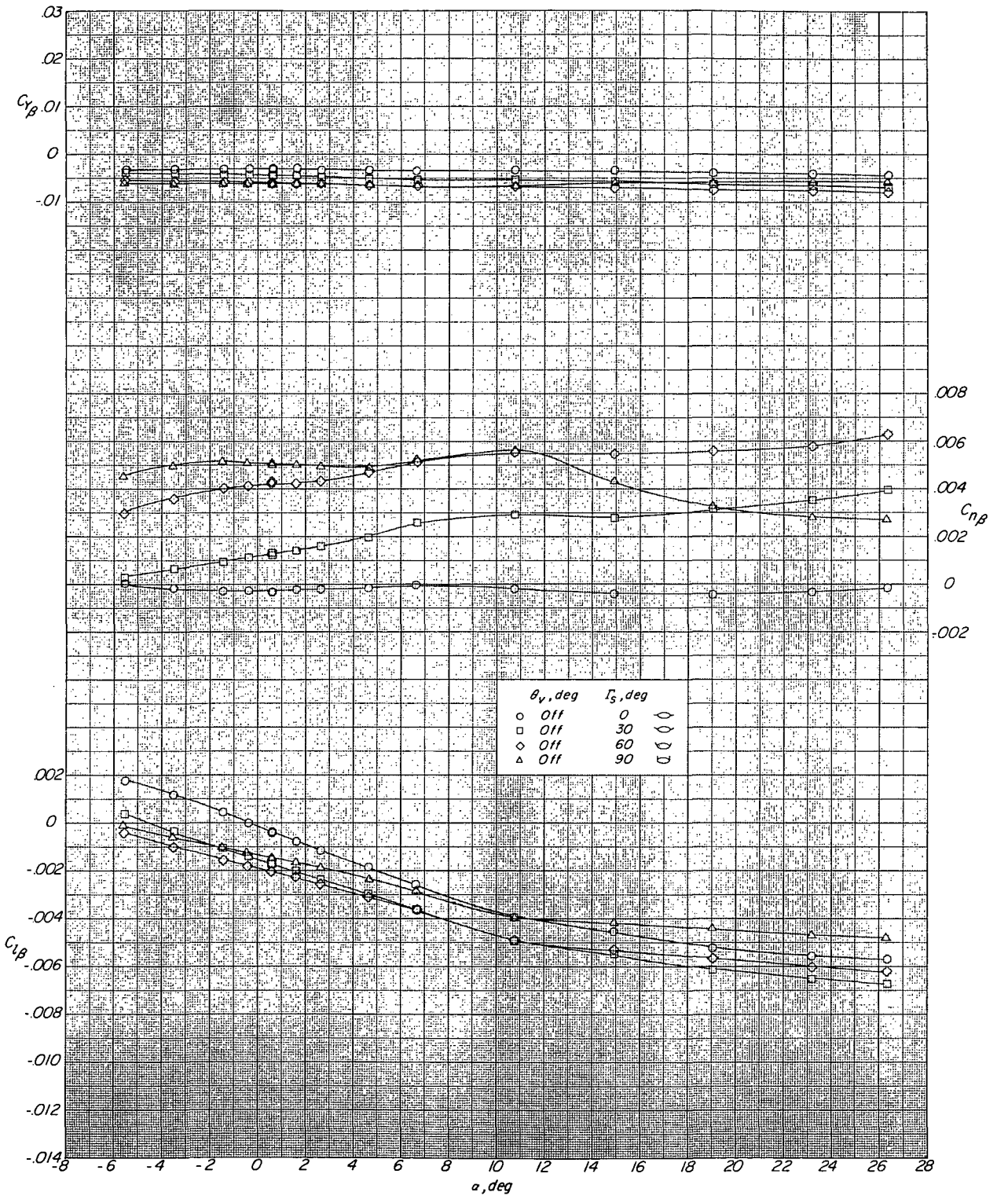

(b) M = 1.90.

Figure 11.- Continued.

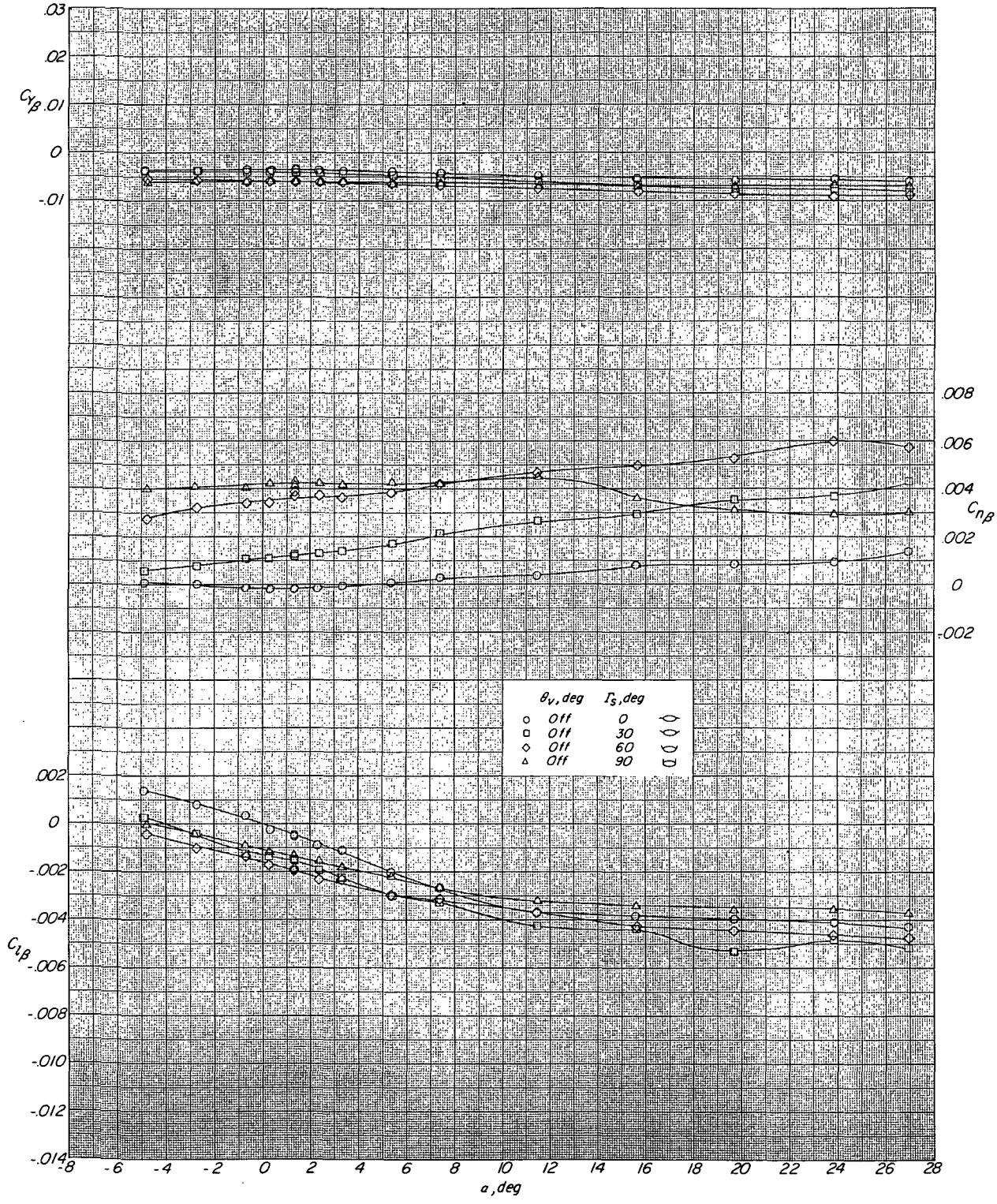

(c) M = 2.36.

Figure 11.- Continued.

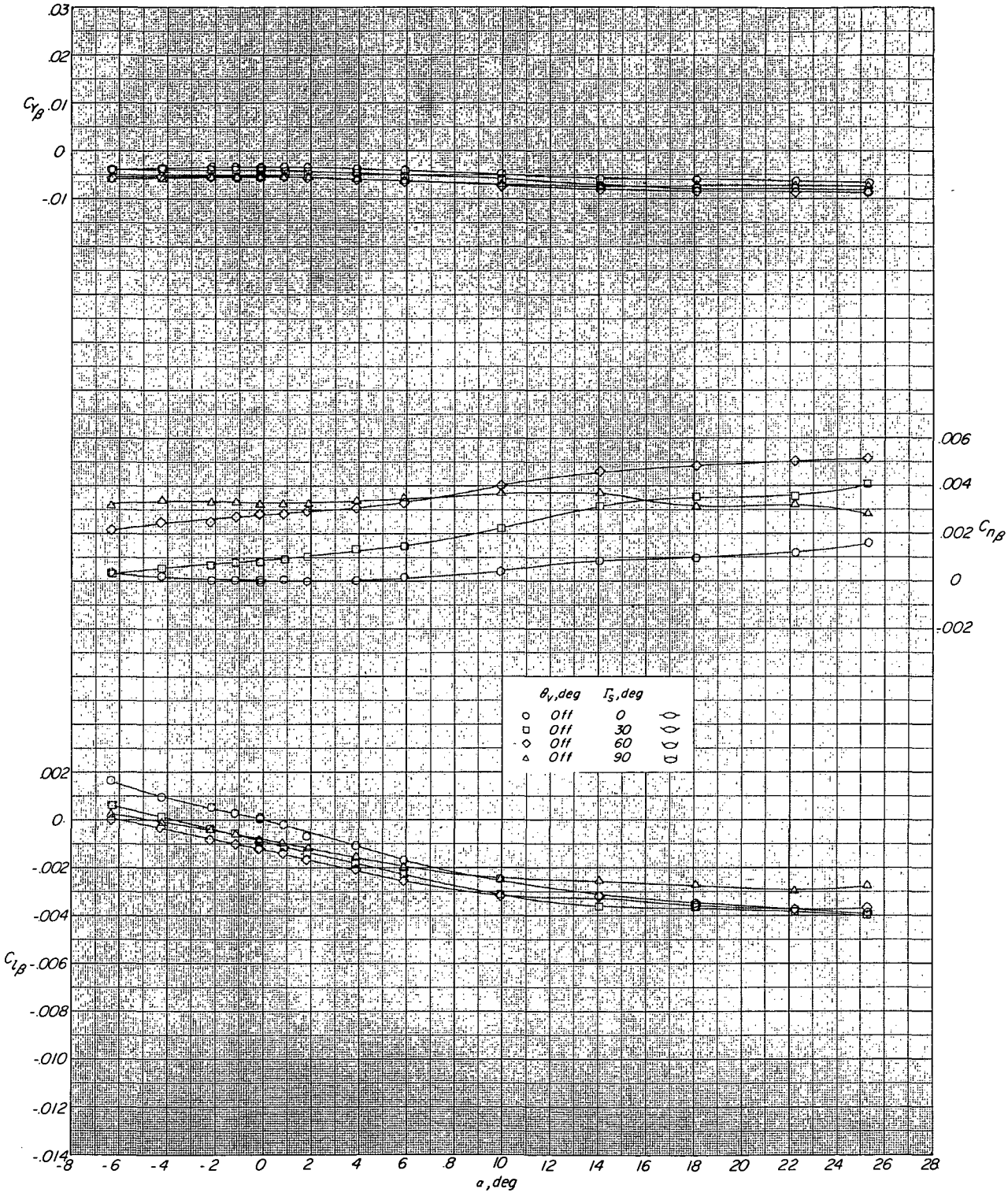

(d) M = 2.86.

Figure 11.- Continued.

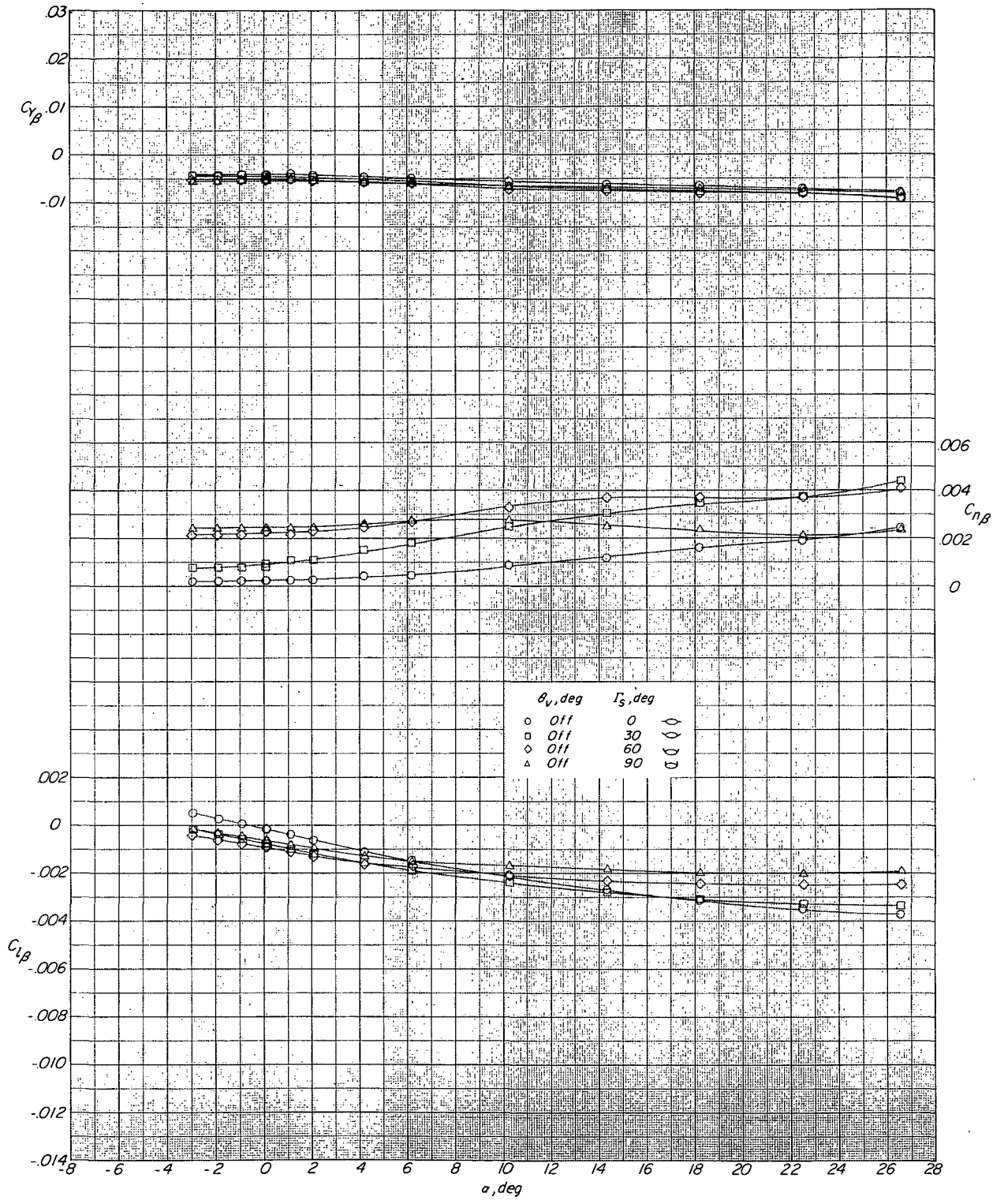

(e) M = 3.96.

Figure 11.- Continued.

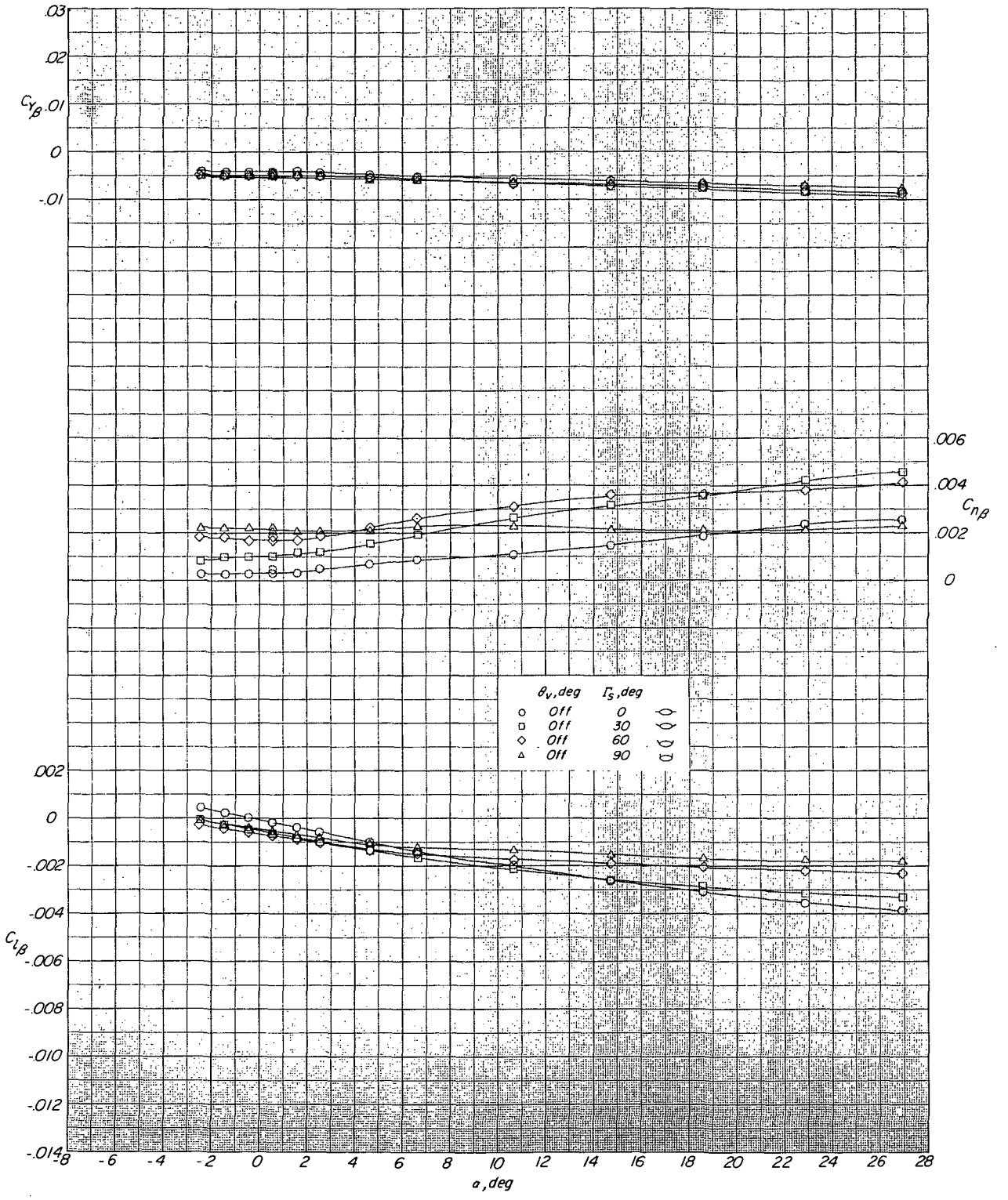

(f) M = 4.63.

Figure 11.- Concluded.

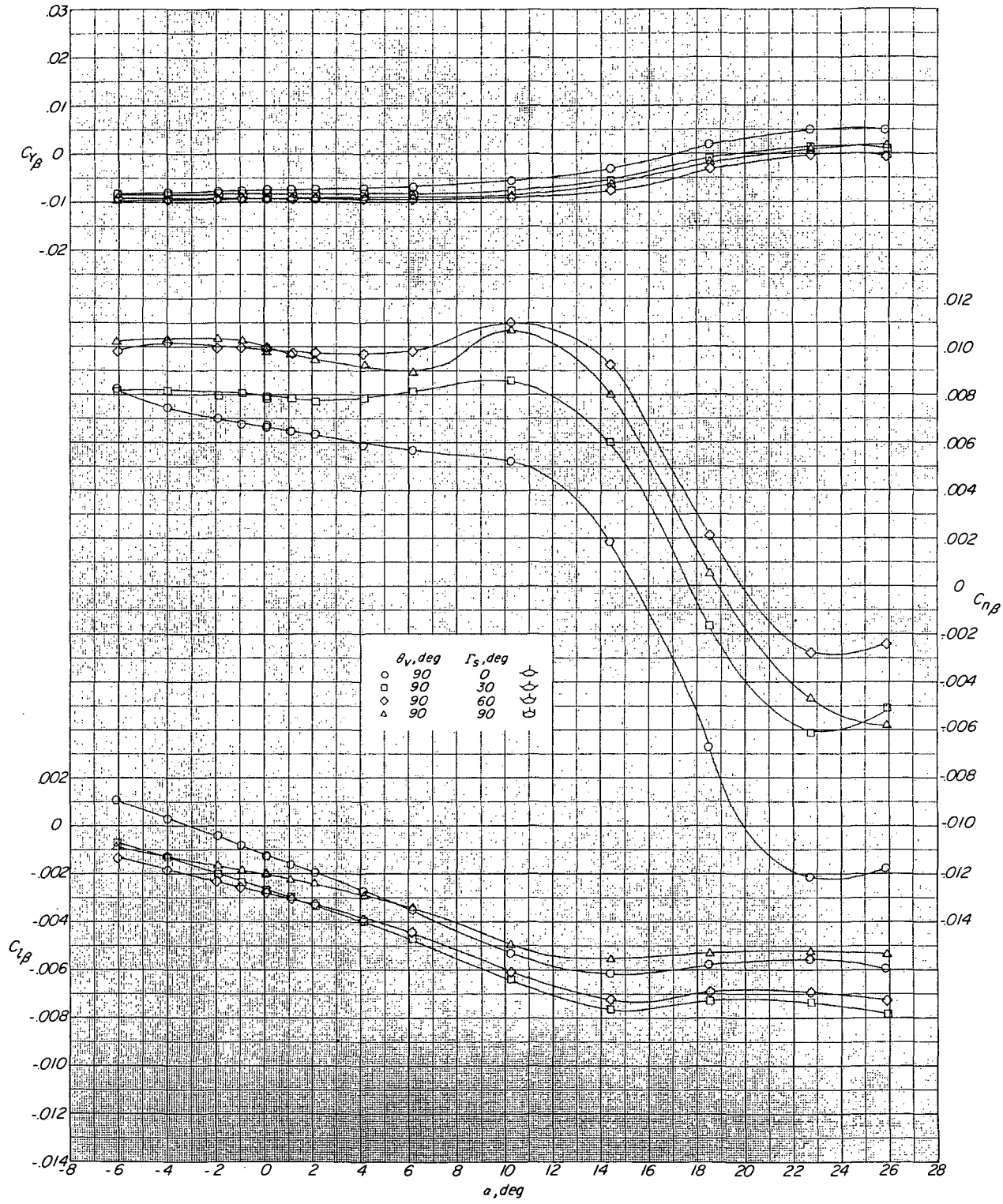

(a) M = 1.50.

Figure 12.- Effect of outboard-stabilizer dihedral on the lateral-directional stability characteristics of the configuration with center vertical tail on. $\Gamma_s = 0^o$ to 90^o.

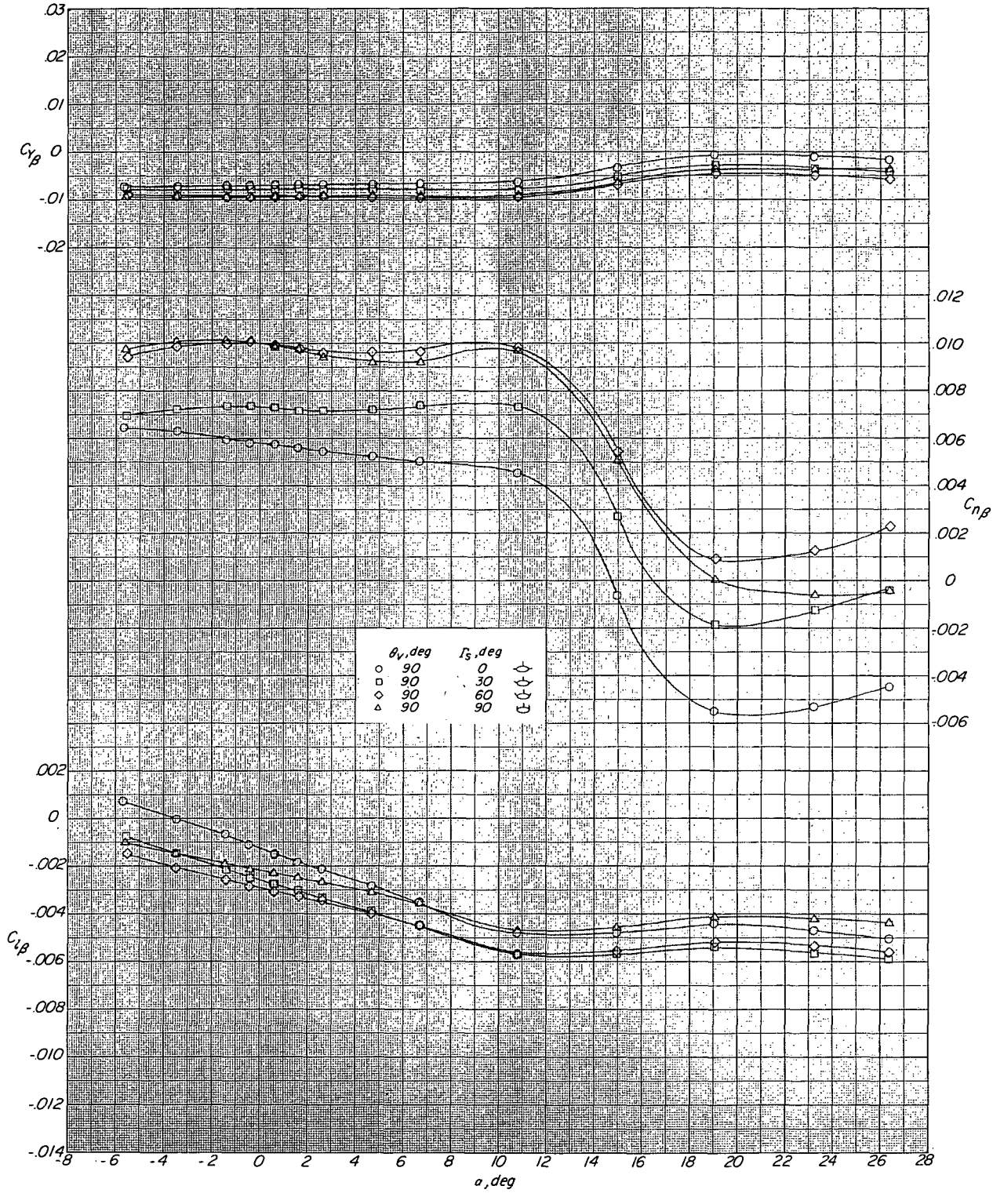

(b) M = 1.90.

Figure 12.- Continued.

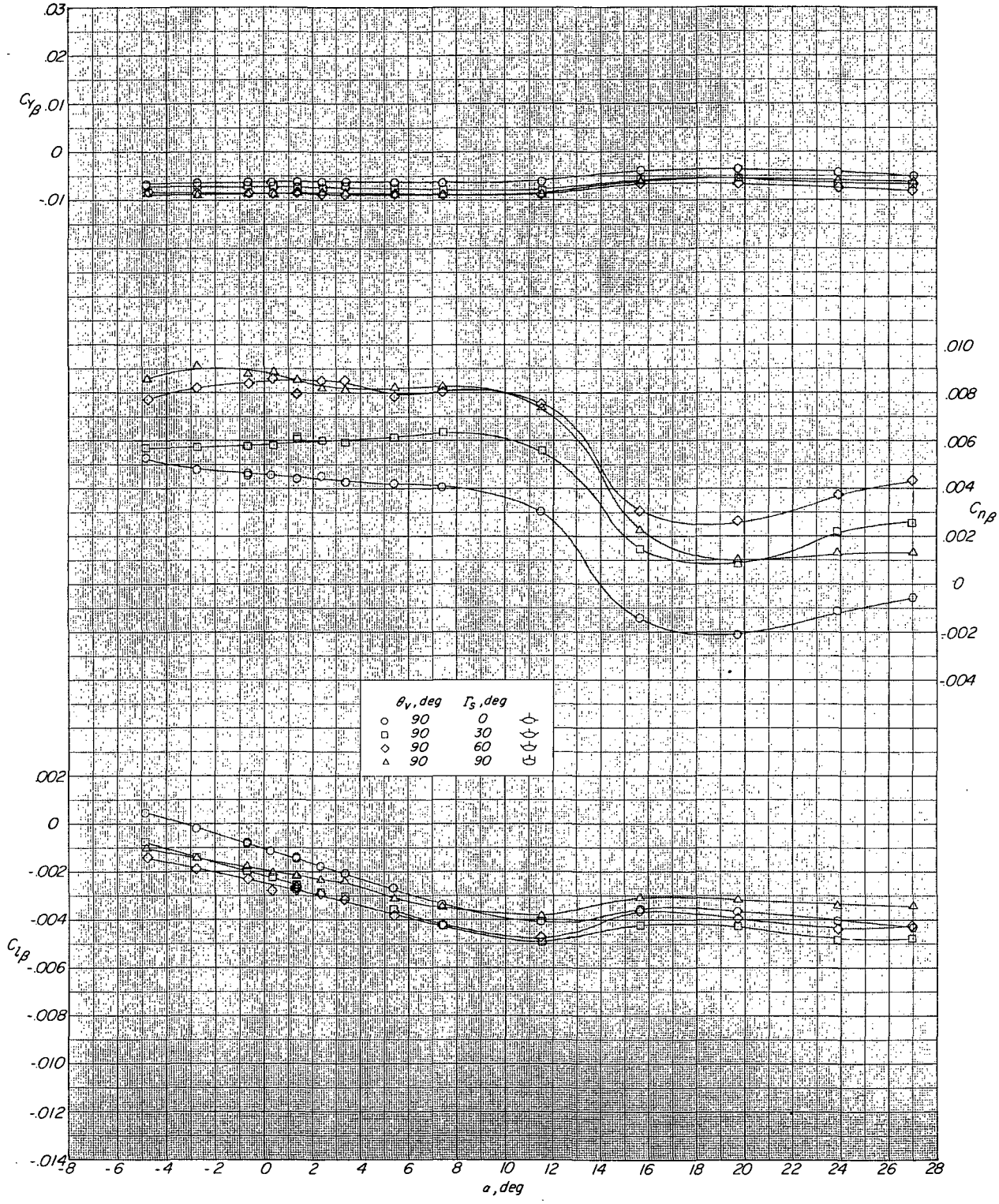

(c) M = 2.36.

Figure 12.- Continued.

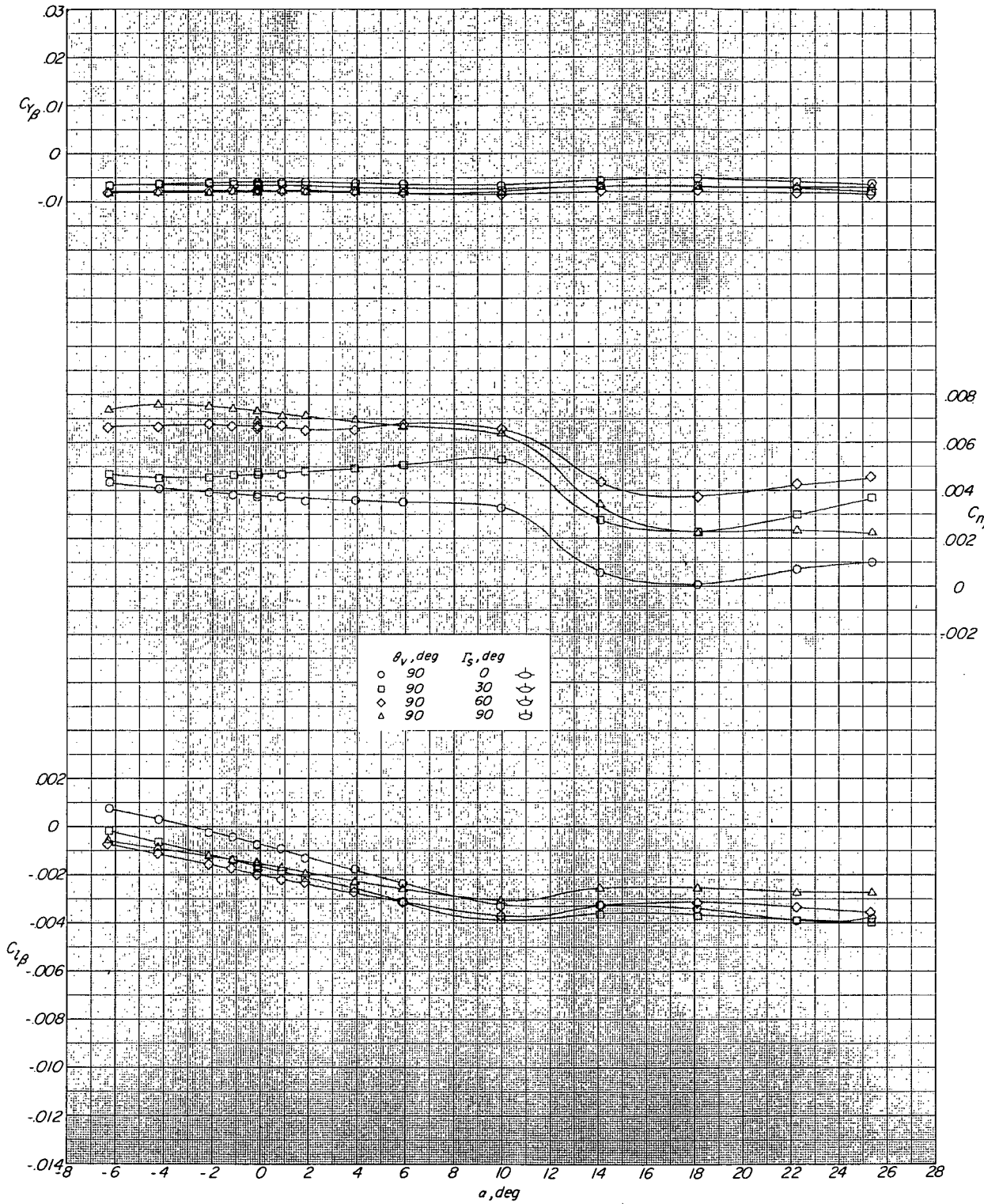

(d) M = 2.86.

Figure 12.- Continued.

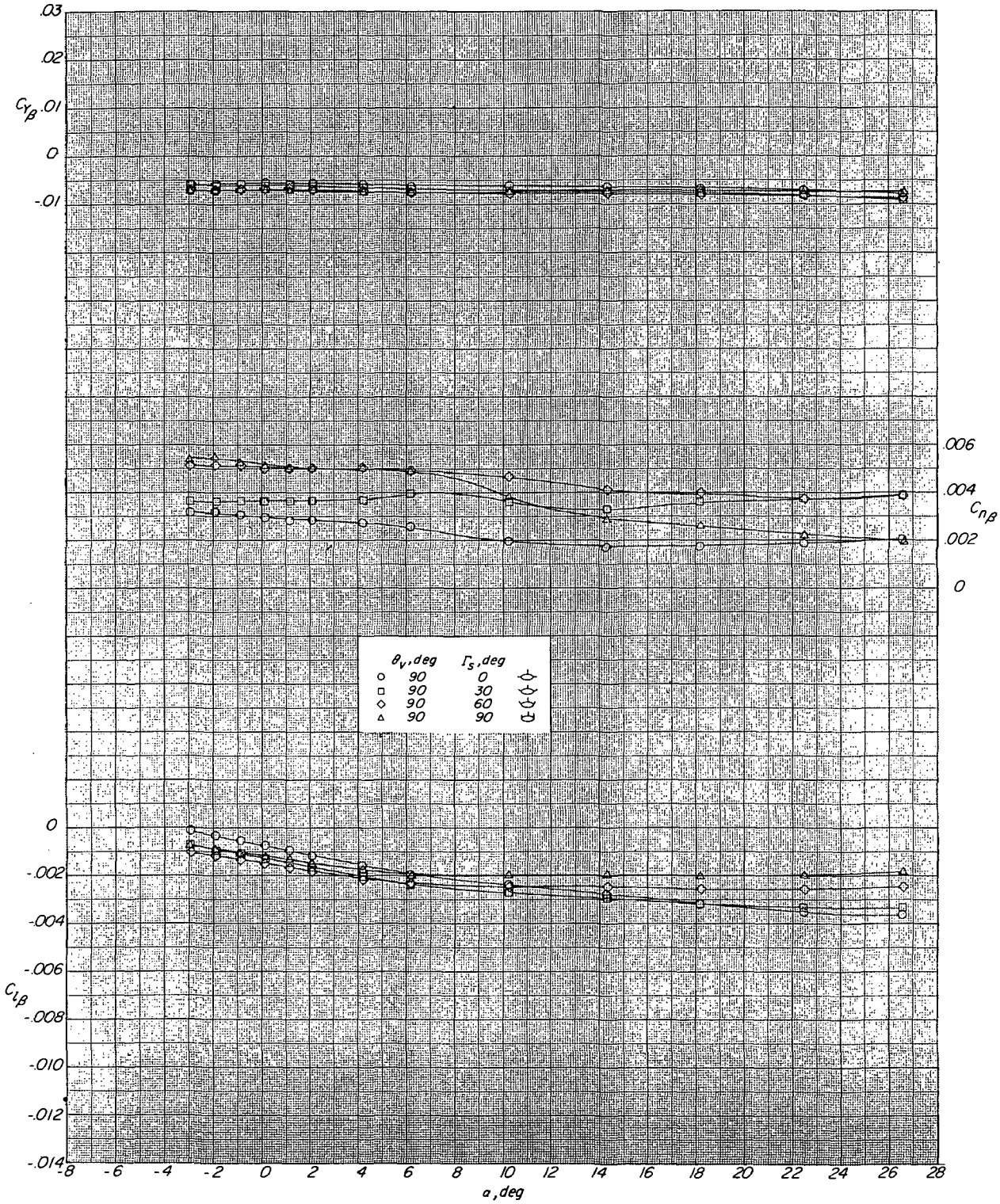

(e) M = 3.96.

Figure 12.- Continued.

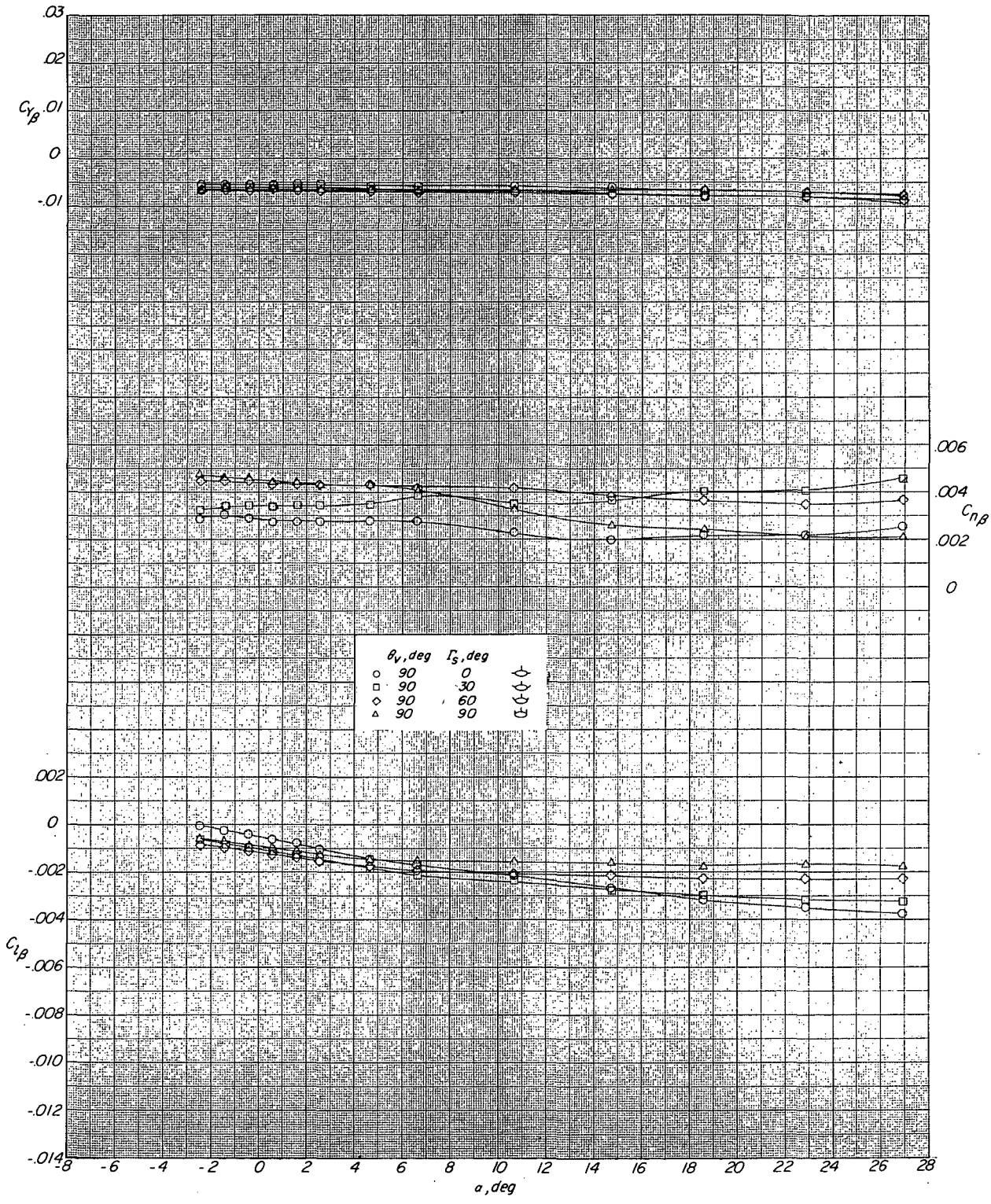

(f) M = 4.63.

Figure 12.- Concluded.

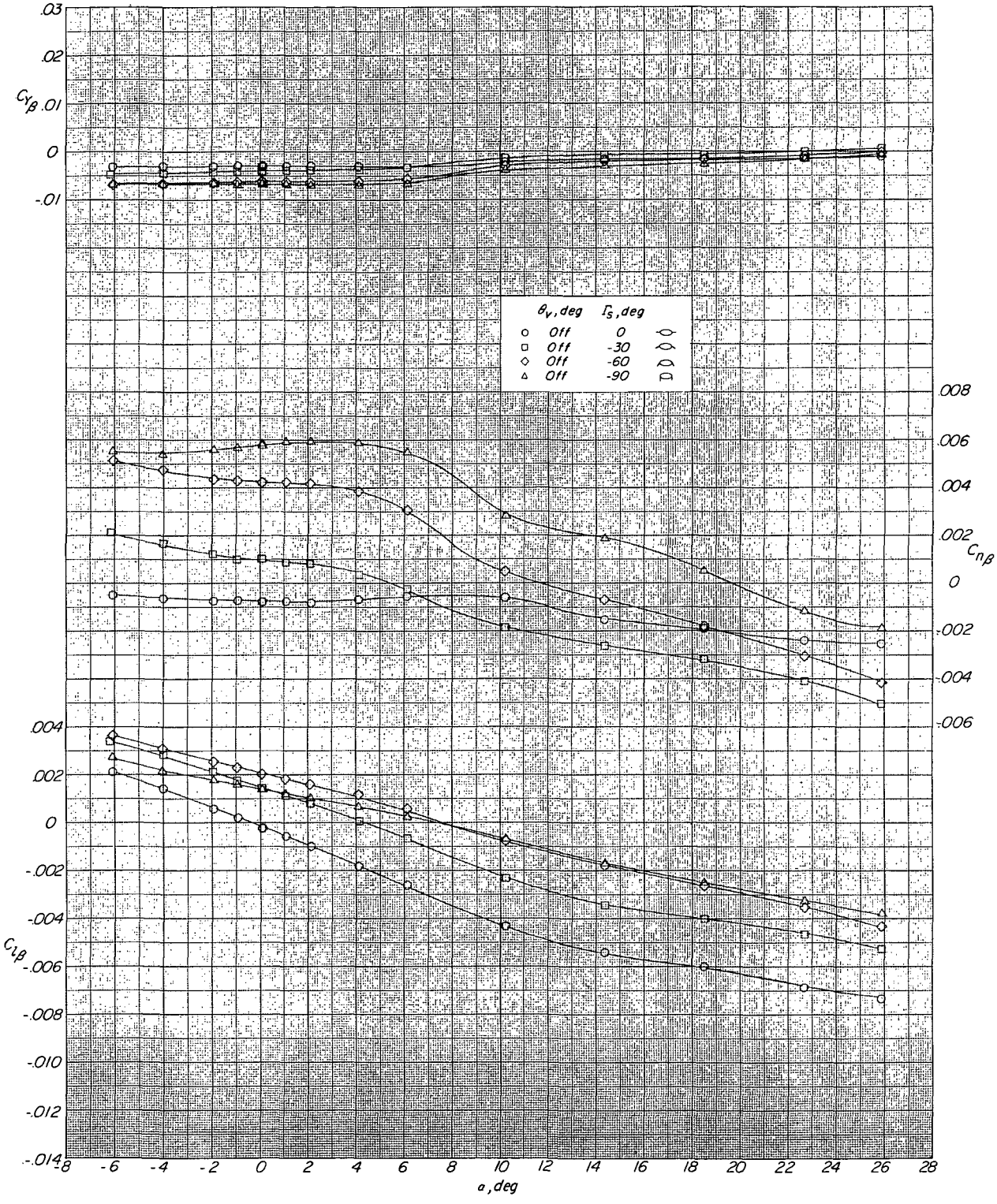

(a) M = 1.50.

Figure 13.- Effect of outboard-stabilizer dihedral on the lateral-directional stability characteristics of the configuration without vertical tail. $\Gamma_s = 0^o$ to -90^o.

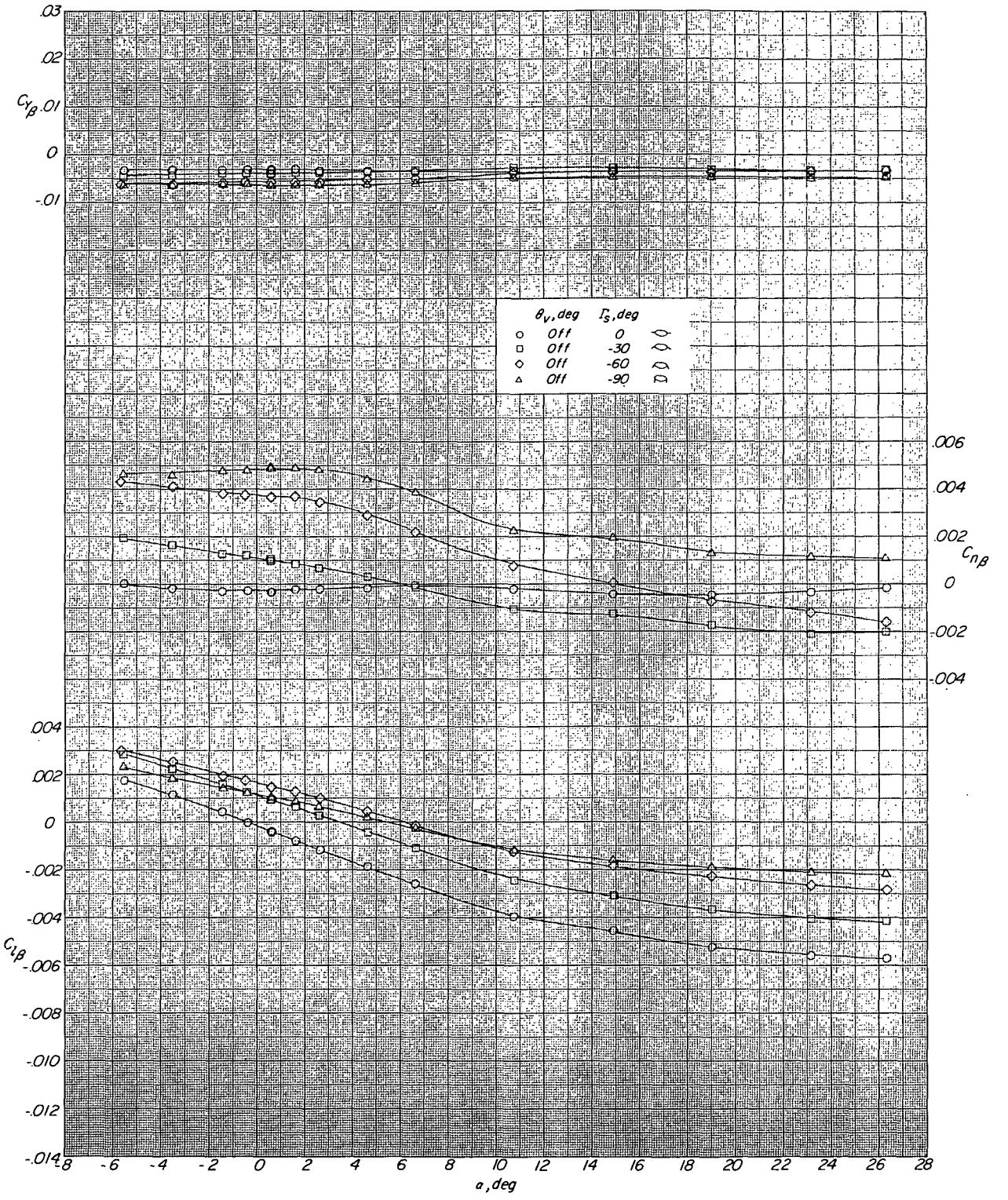

(b) M = 1.90.

Figure 13.- Continued.

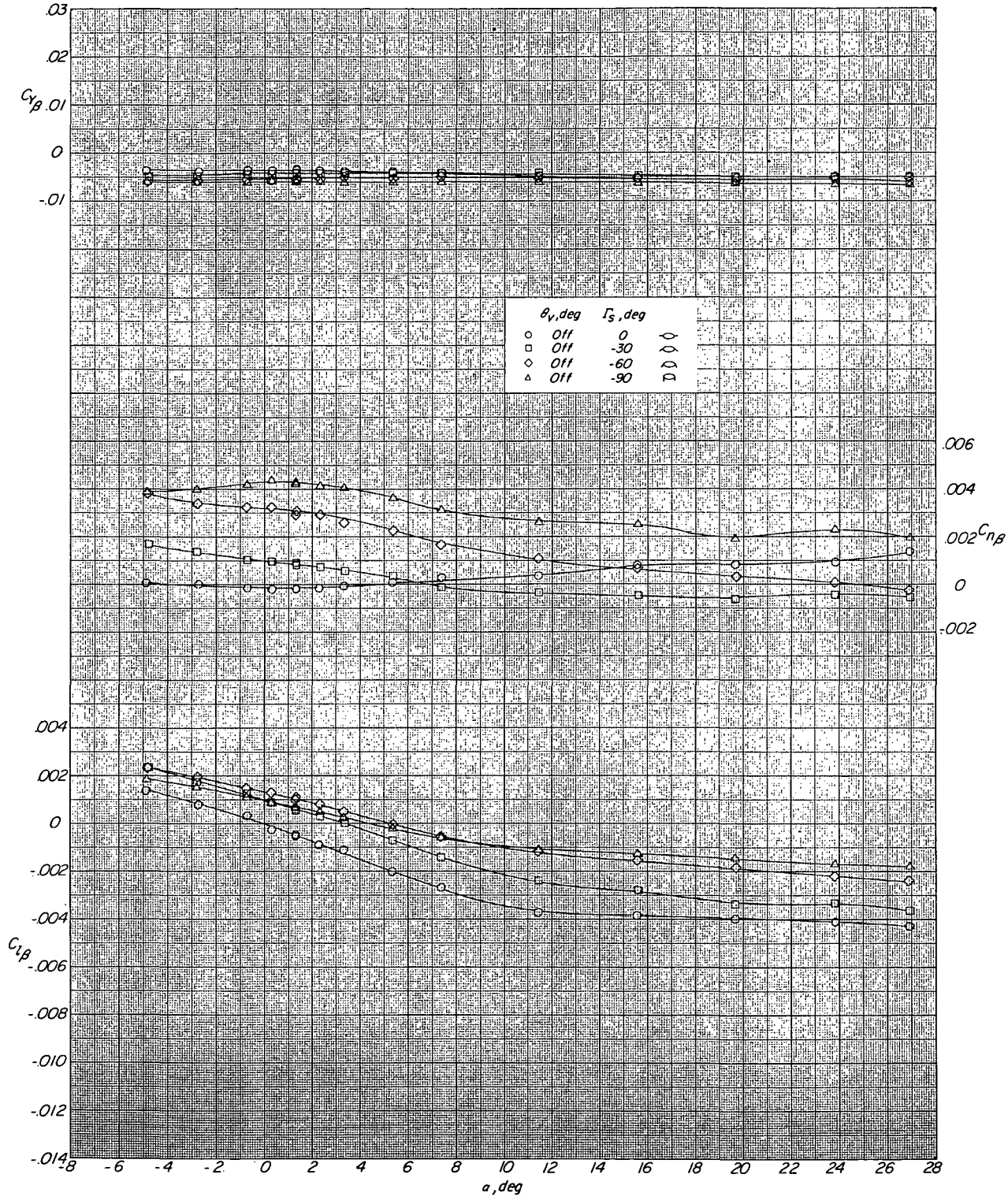

(c) M = 2.36.

Figure 13.- Continued.

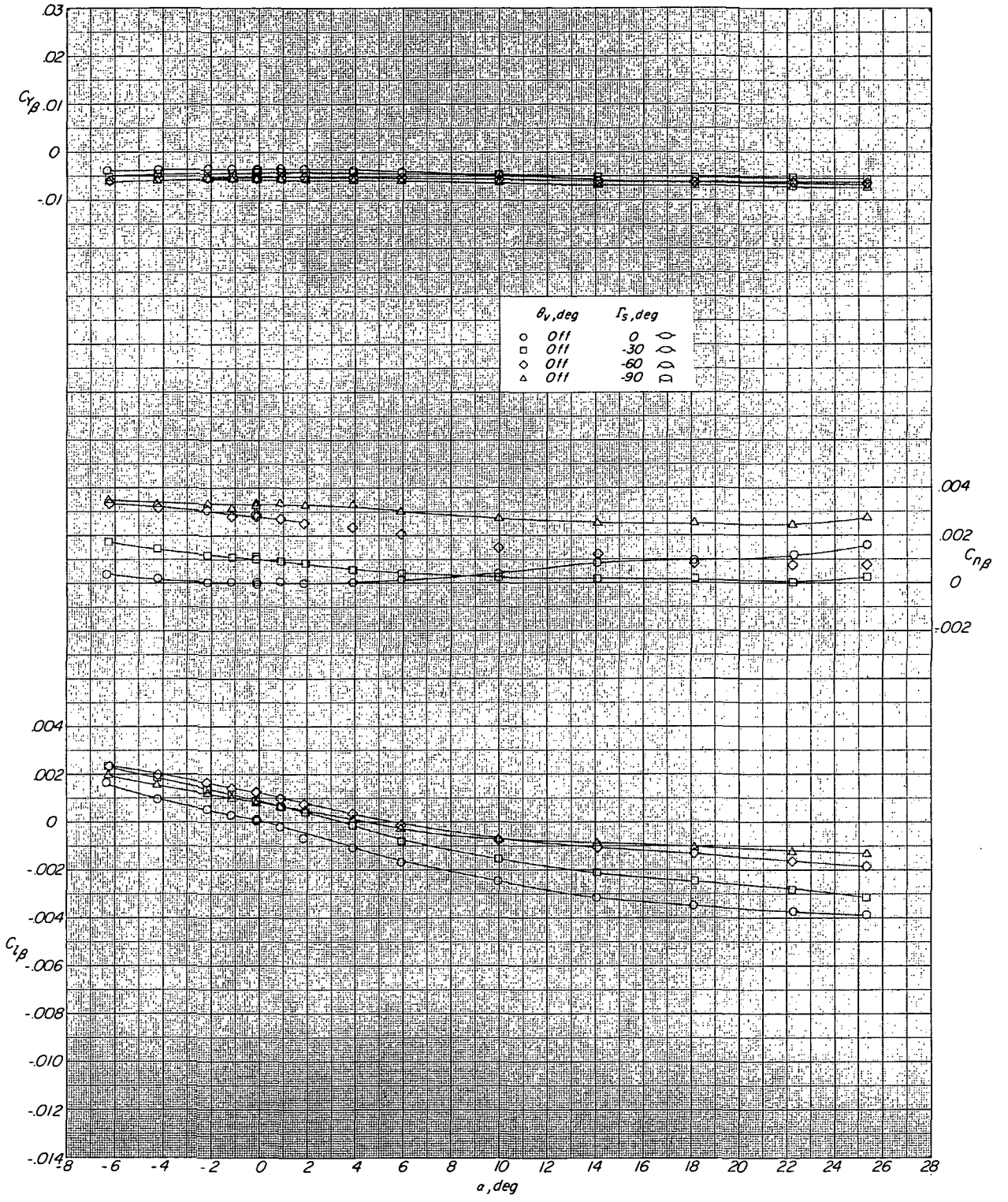

(d) M = 2.86.

Figure 23.- Continued.

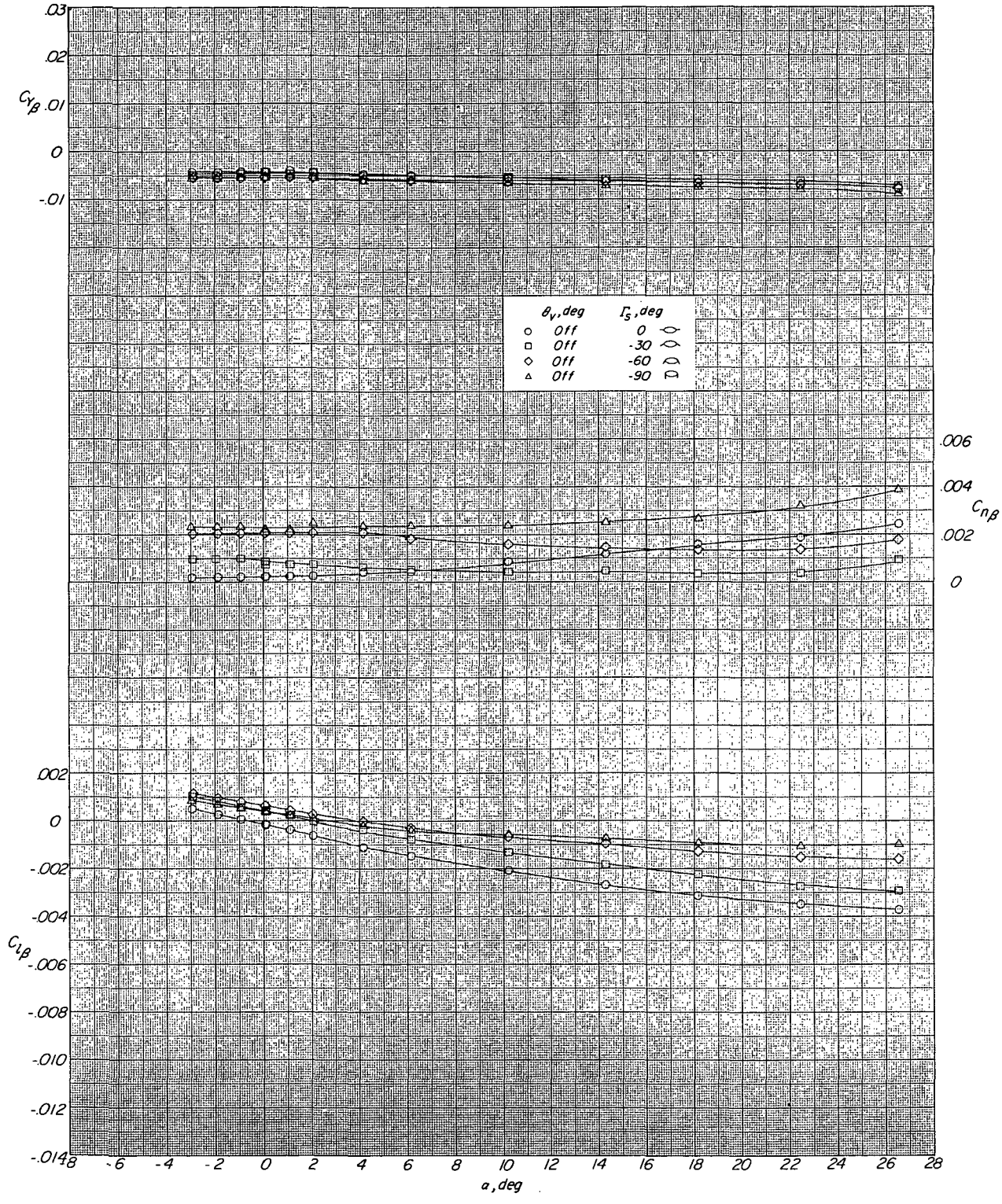

(e) M = 3.96.

Figure 13.- Continued.

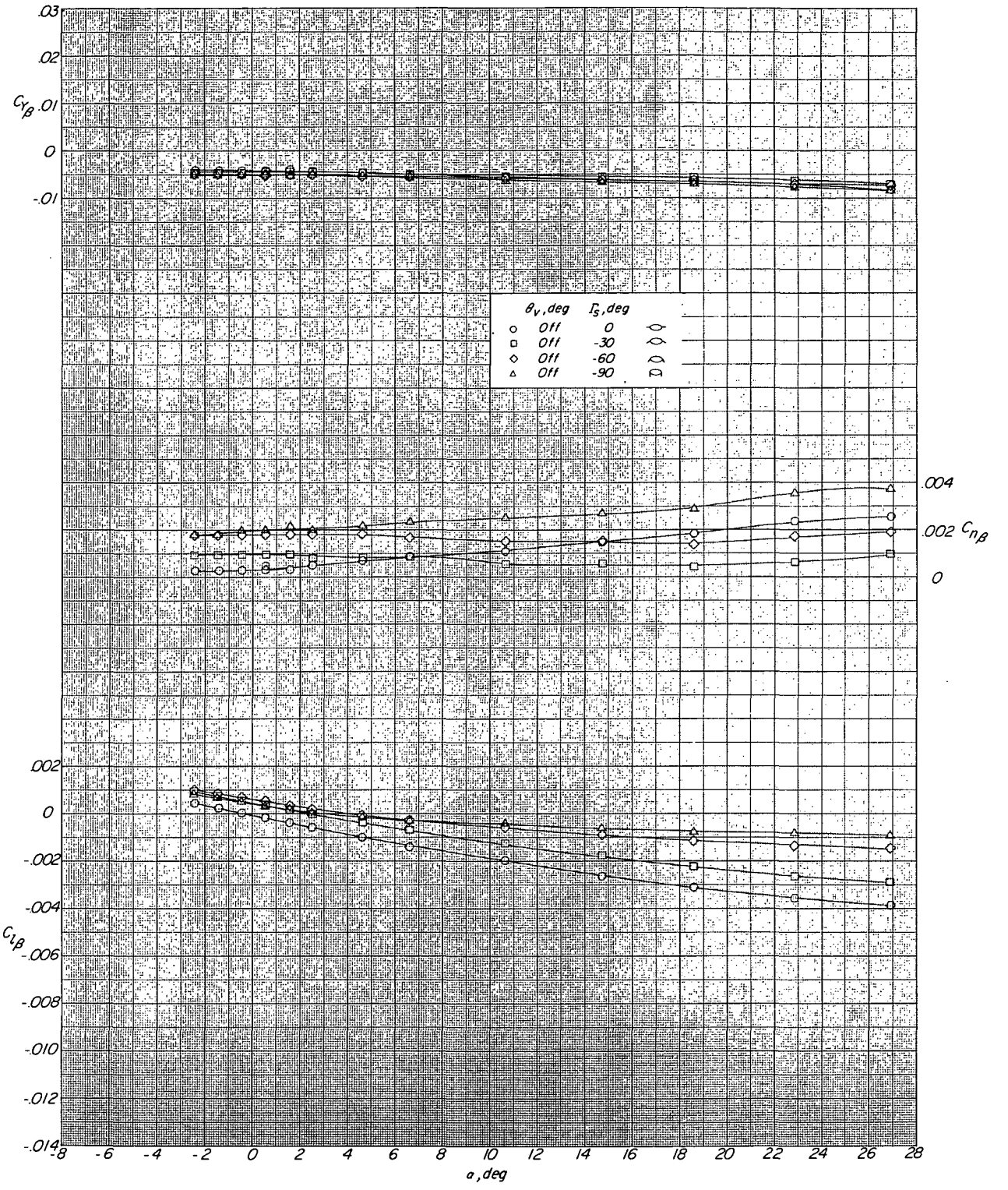

(f) M = 4.63.

Figure 13.- Concluded.

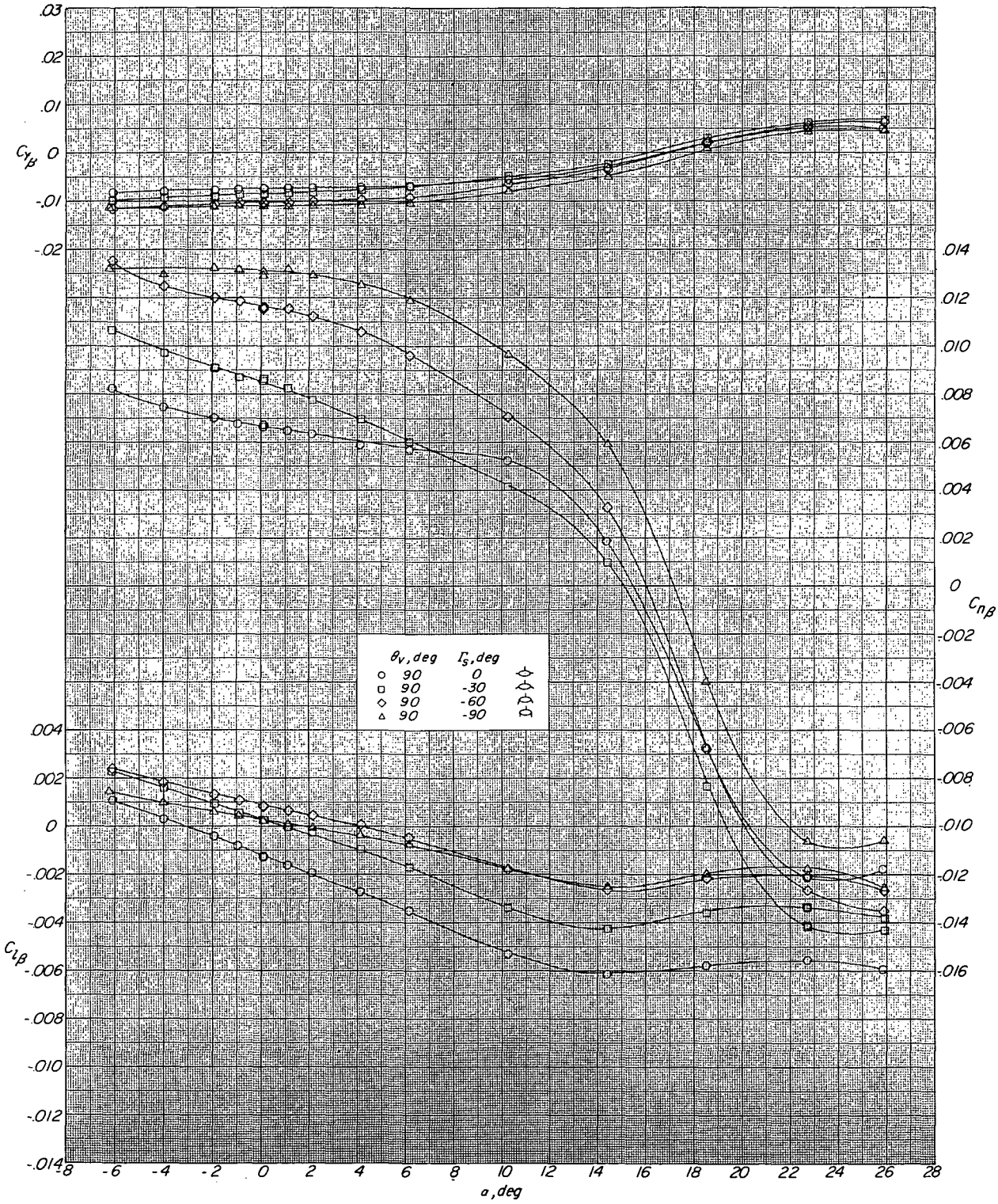

(a) M = 1.50.

Figure 14.- Effect of outboard-stabilizer dihedral on the lateral-directional stability characteristics of the configuration with center vertical tail on. $\Gamma_S = 0^o$ to -90^o.

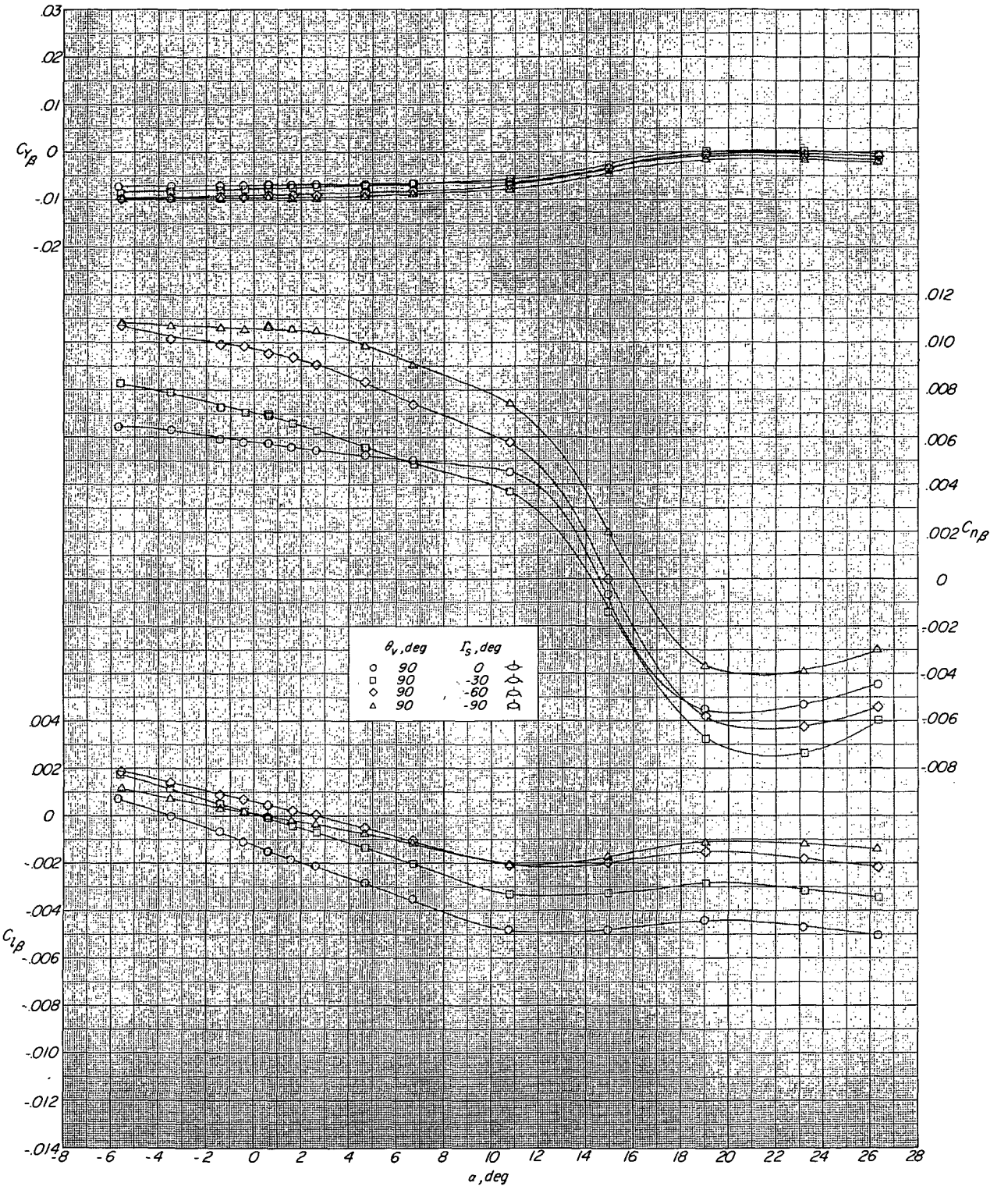

(b) M = 1.90.

Figure 14.- Continued.

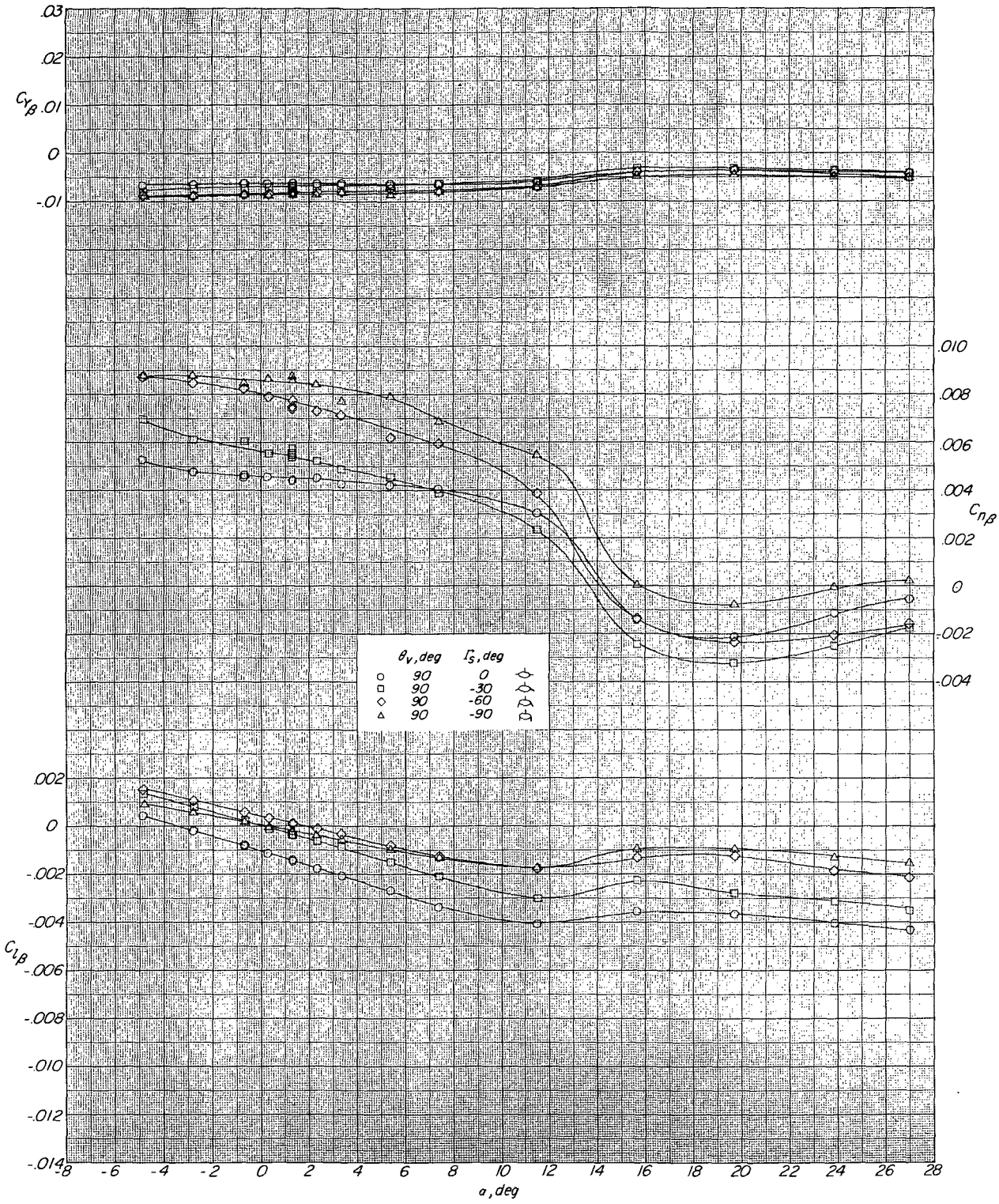

(c) M = 2.36.

Figure 14.- Continued.

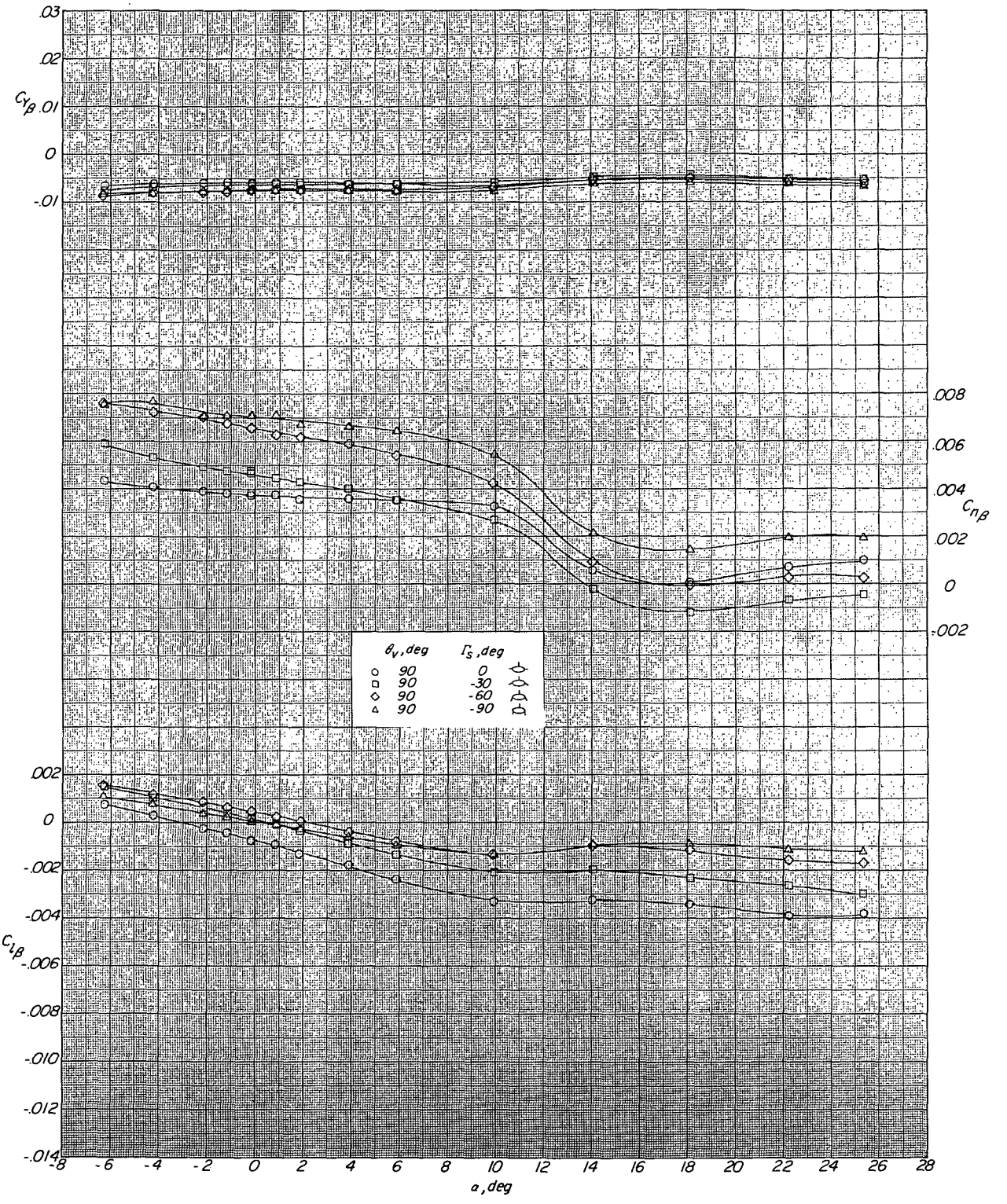

(d) M = 2.86.

Figure 14.- Continued.

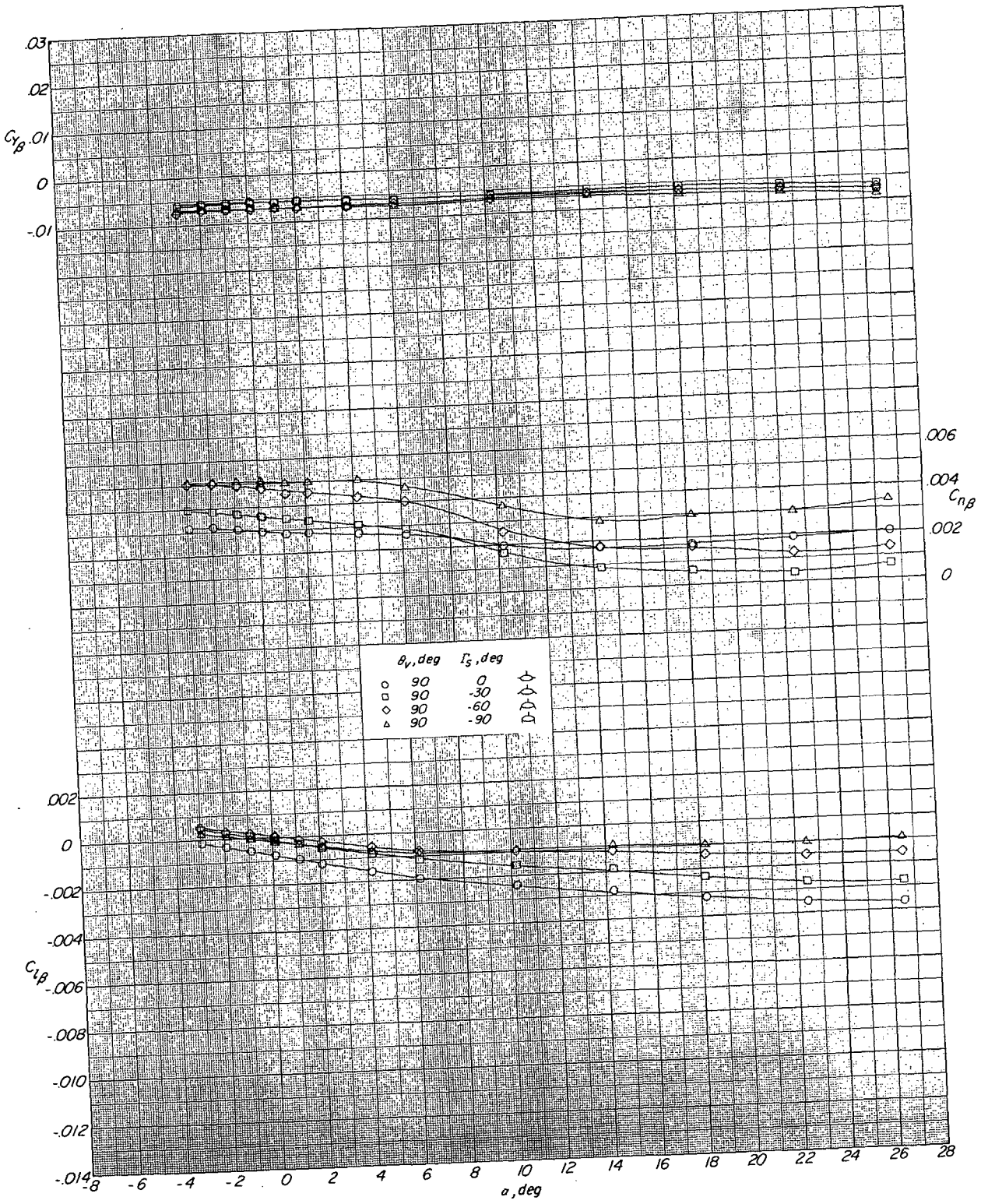

(e) M = 3.96.

Figure 14.- Continued.

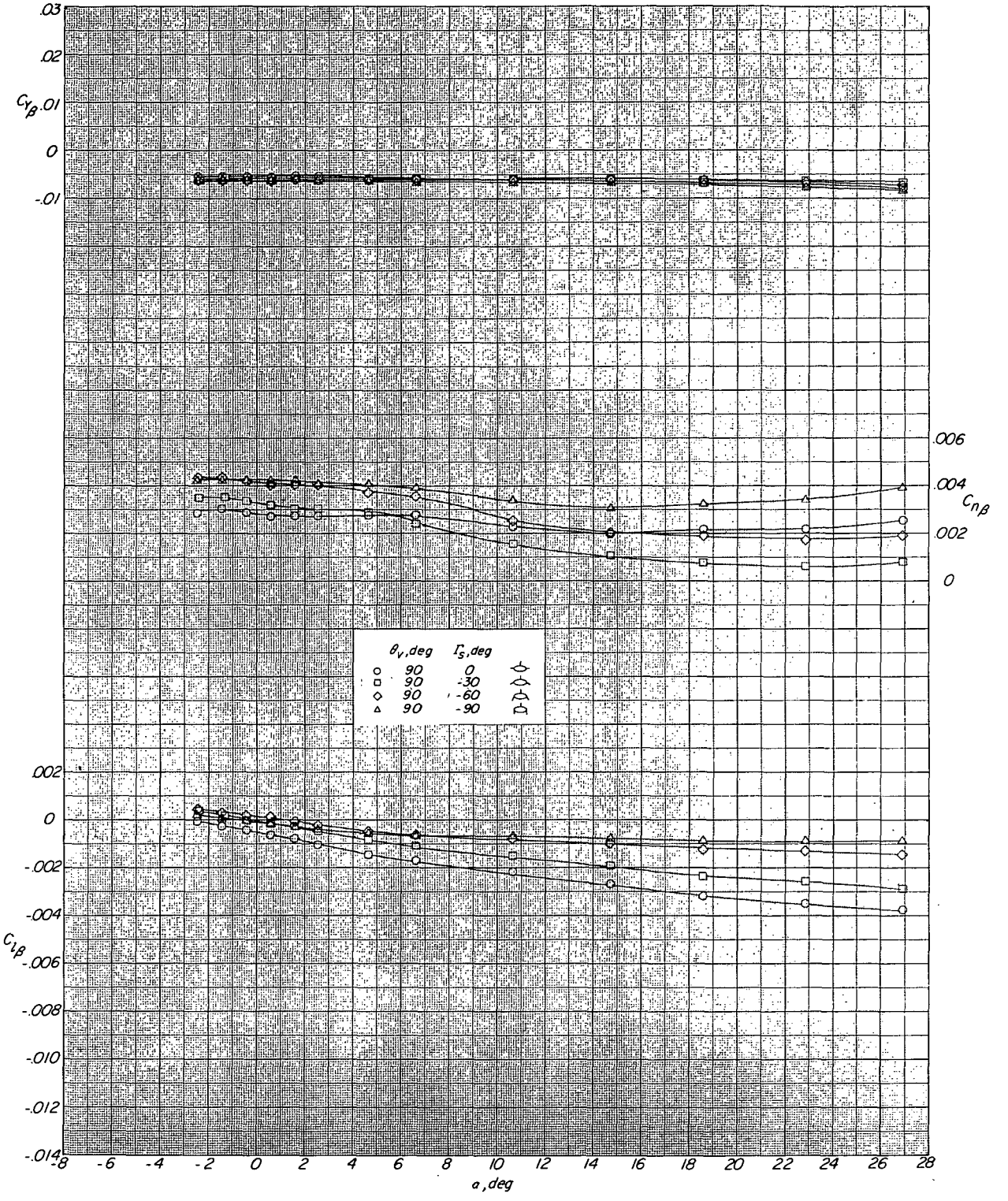

(f) M = 4.63.

Figure 14.- Concluded.

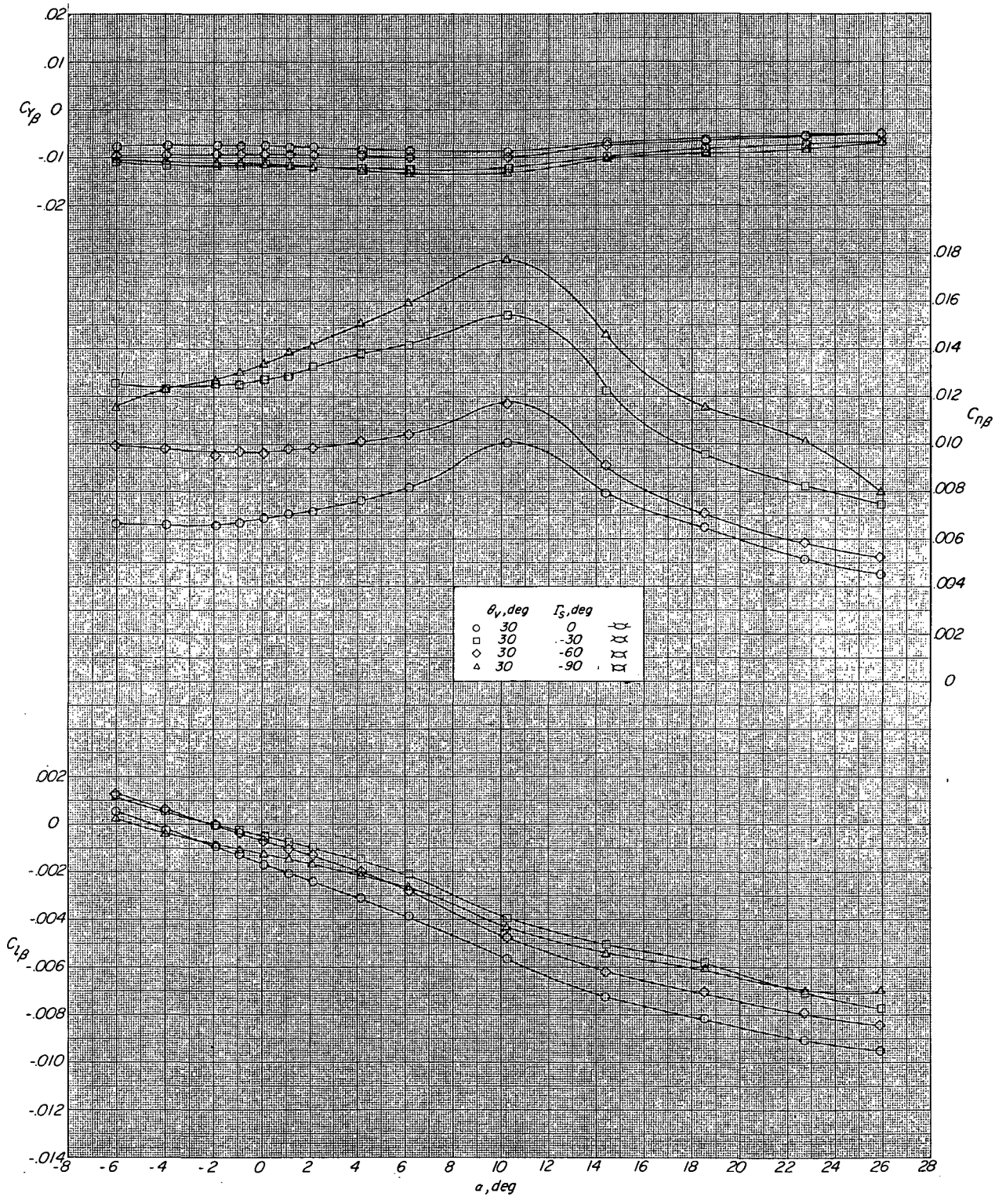

(a) M = 1.50.

Figure 15.- Effect of outboard-stabilizer dihedral on the lateral-directional stability characteristics of the configuration with vee-tail on. $\Gamma_s = 0^o$ to -90^o.

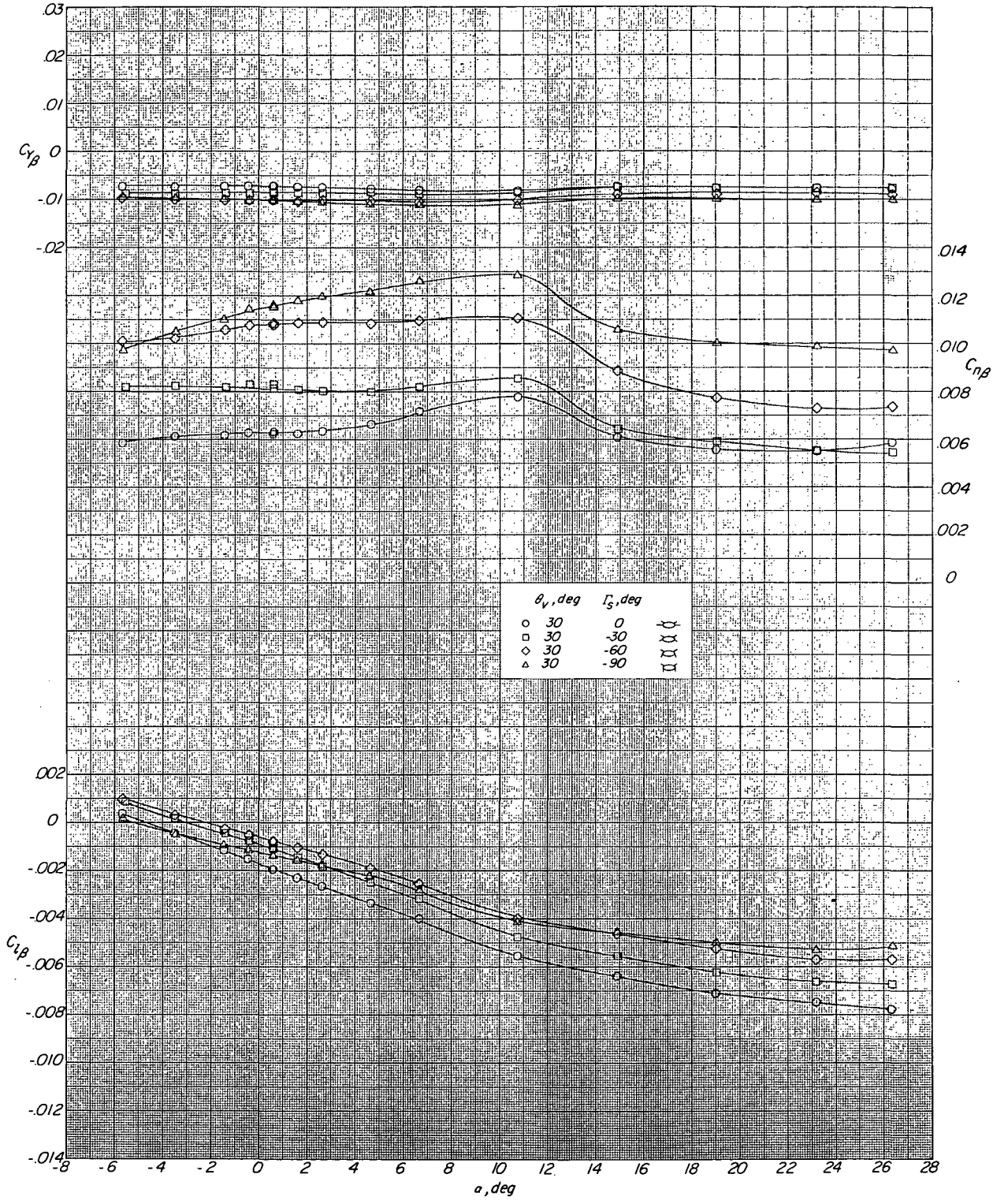

(b) M = 1.90.

Figure 15.- Continued.

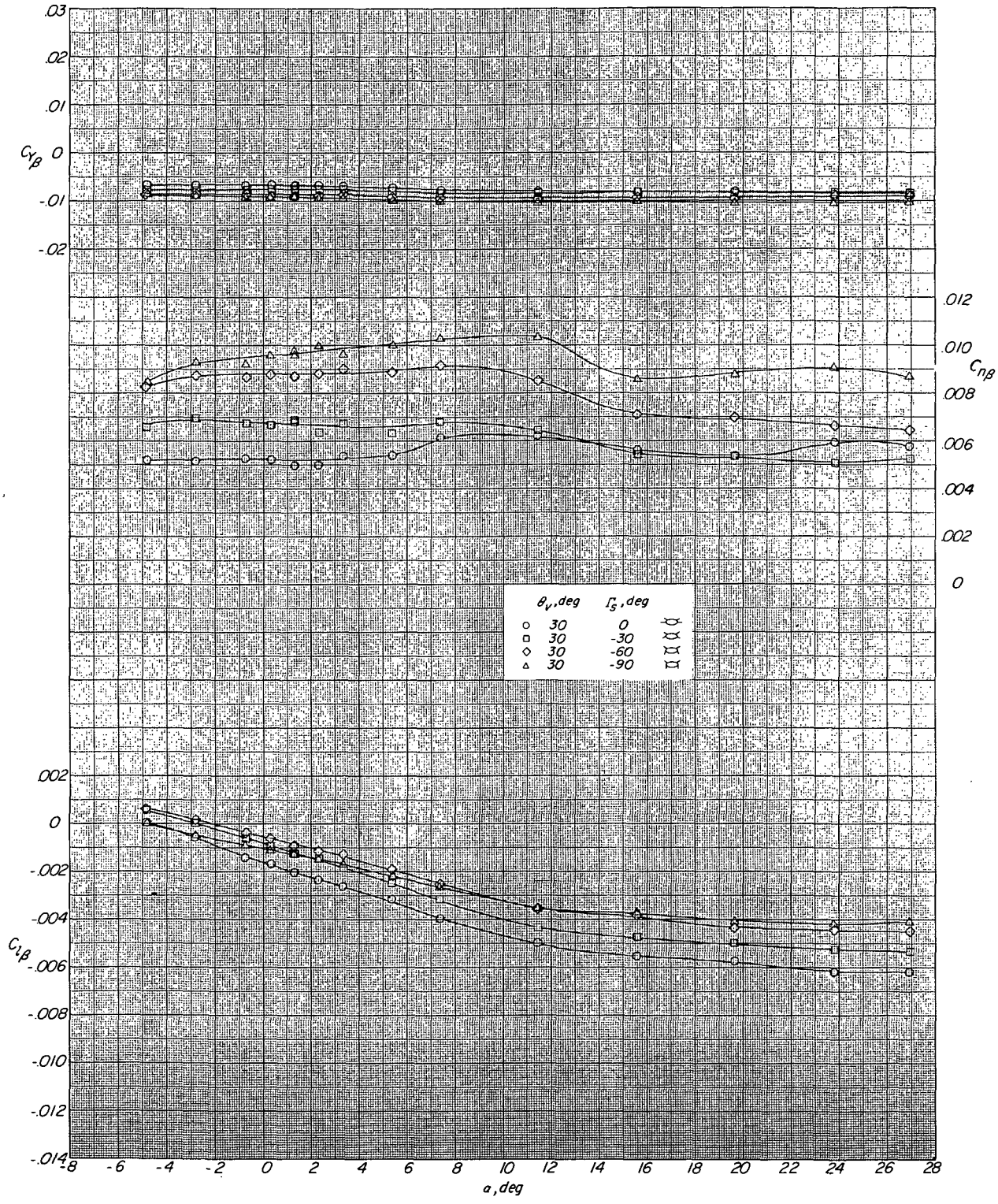

(c) M = 2.36.

Figure 15.- Continued.

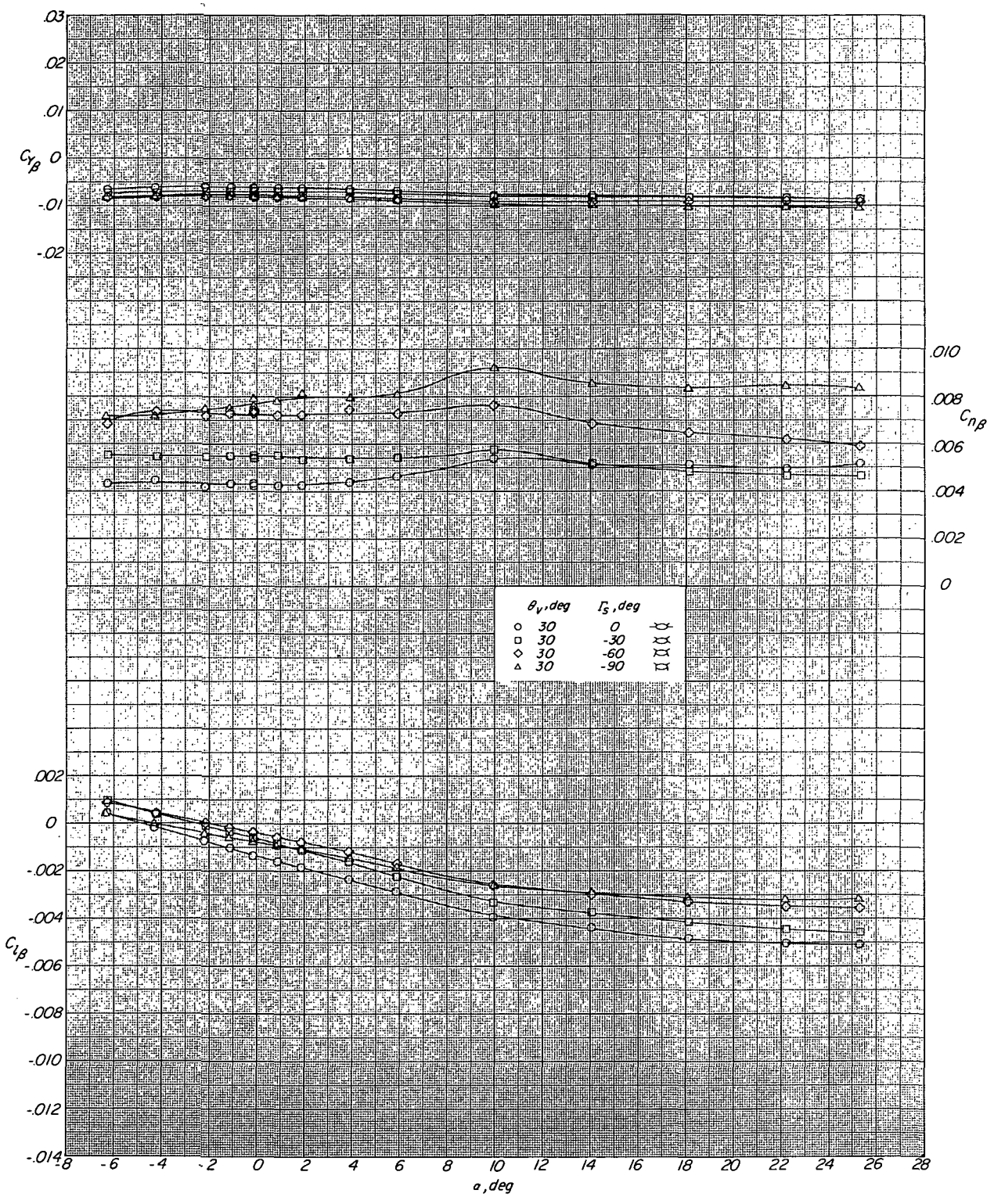

(d) M = 2.86.

Figure 15.- Continued.

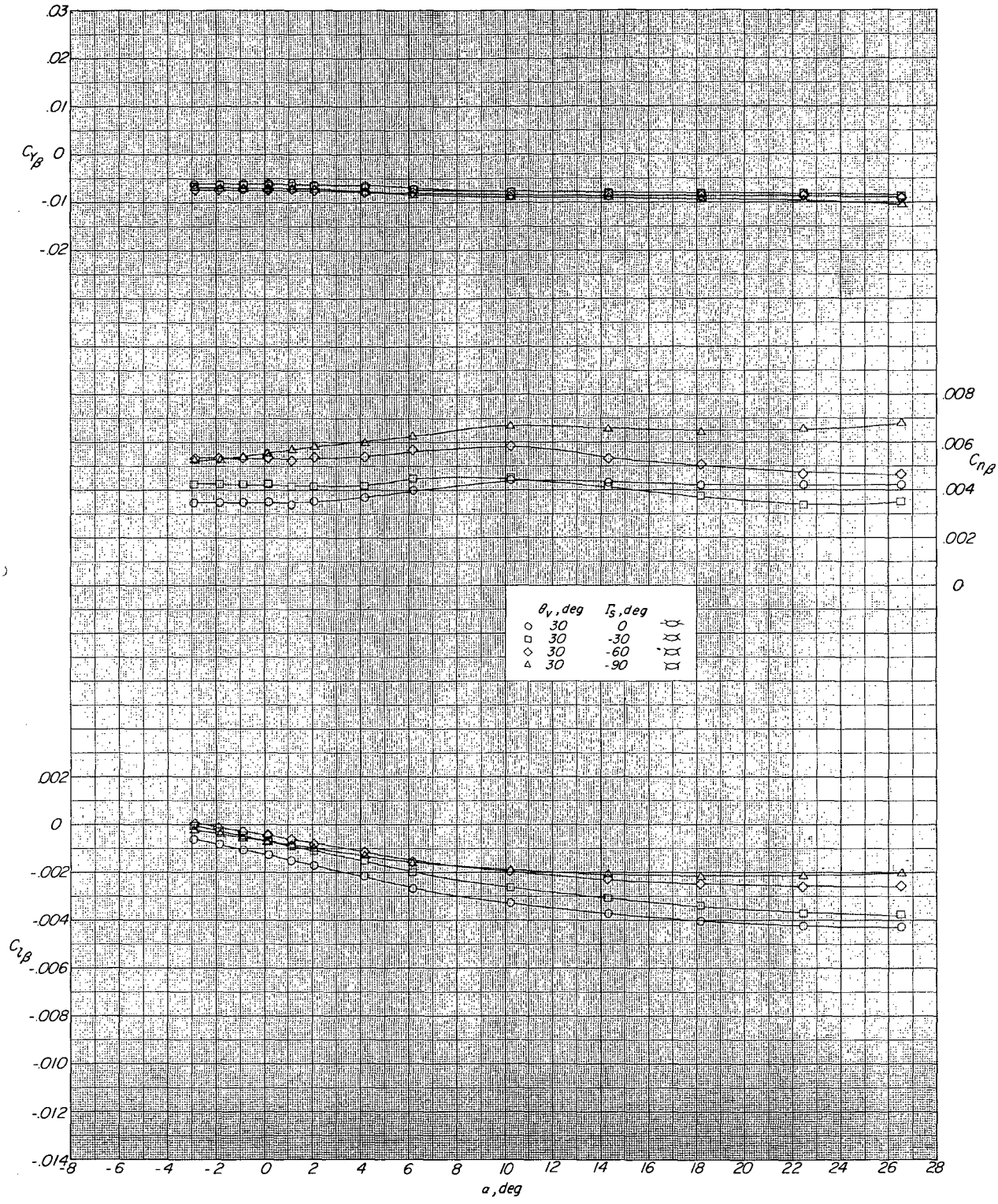

(e) M = 3.96.

Figure 15.- Continued.

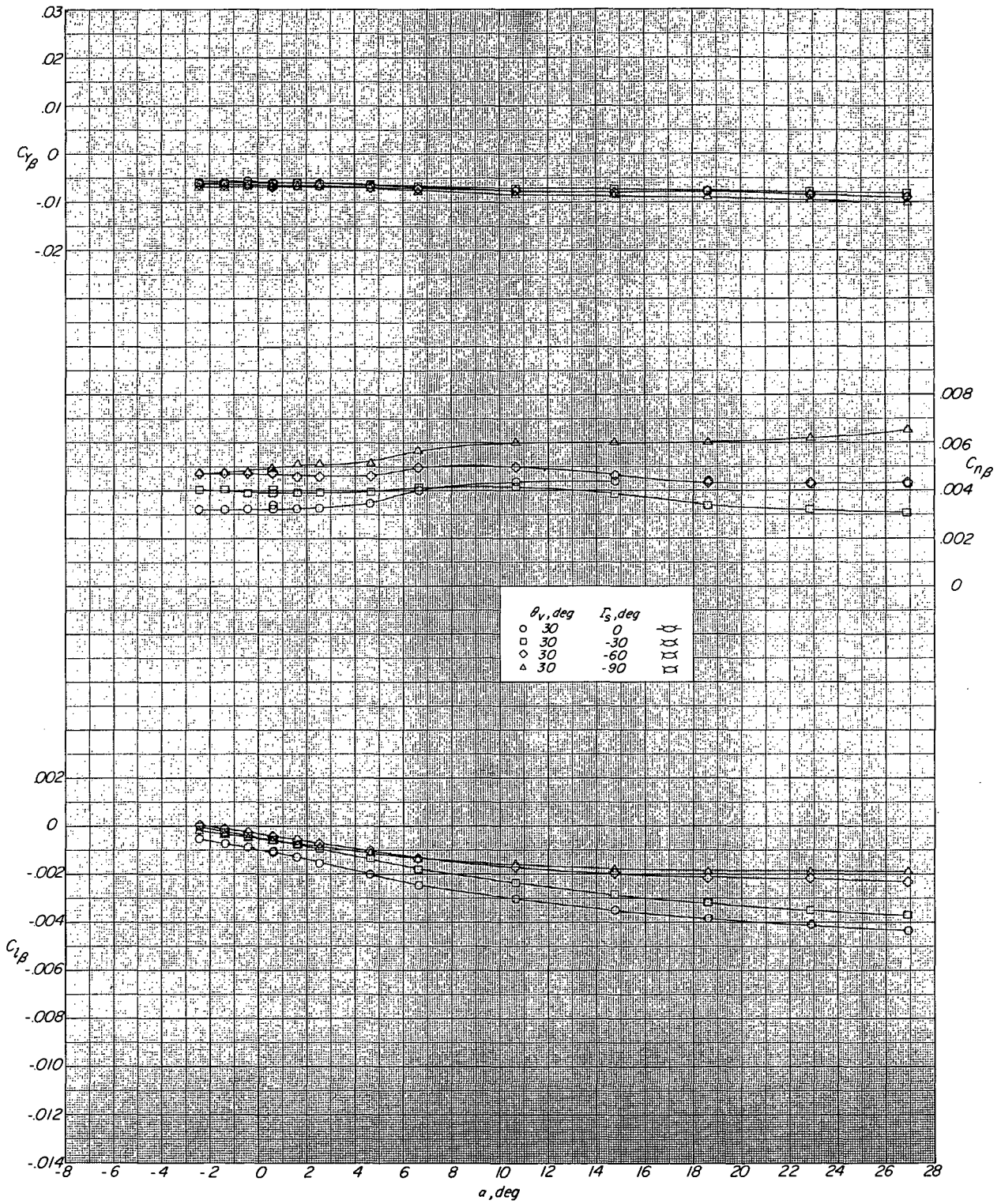

(f) M = 4.63.

Figure 15.- Concluded.

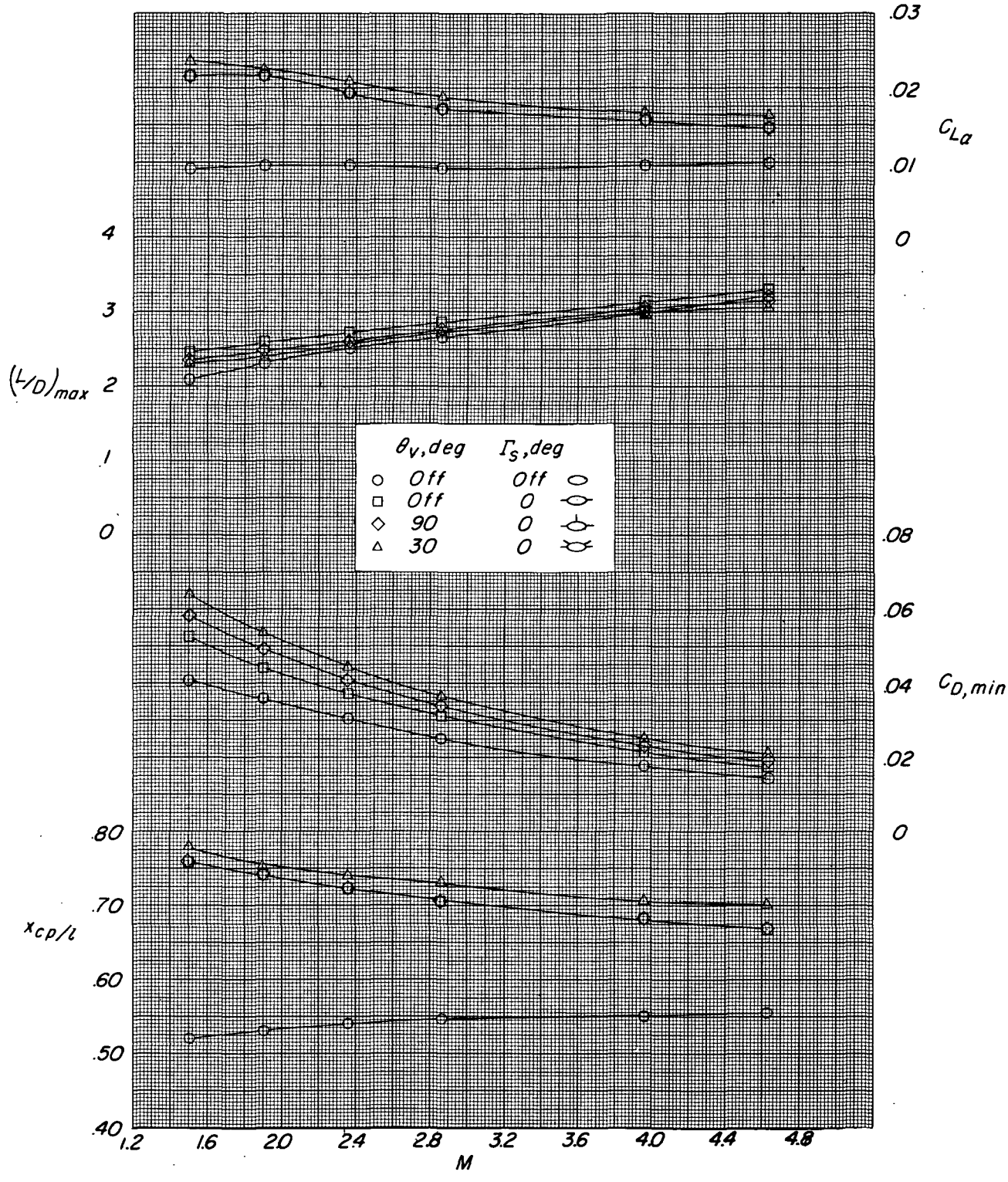

Figure 16.- Effect of addition of outboard stabilizers ($\Gamma_S = 0^o$) and vertical tails ($\theta_V = 30^o$ and 90^o) on various pertinent longitudinal aerodynamic parameters of the basic body as a function of Mach number.

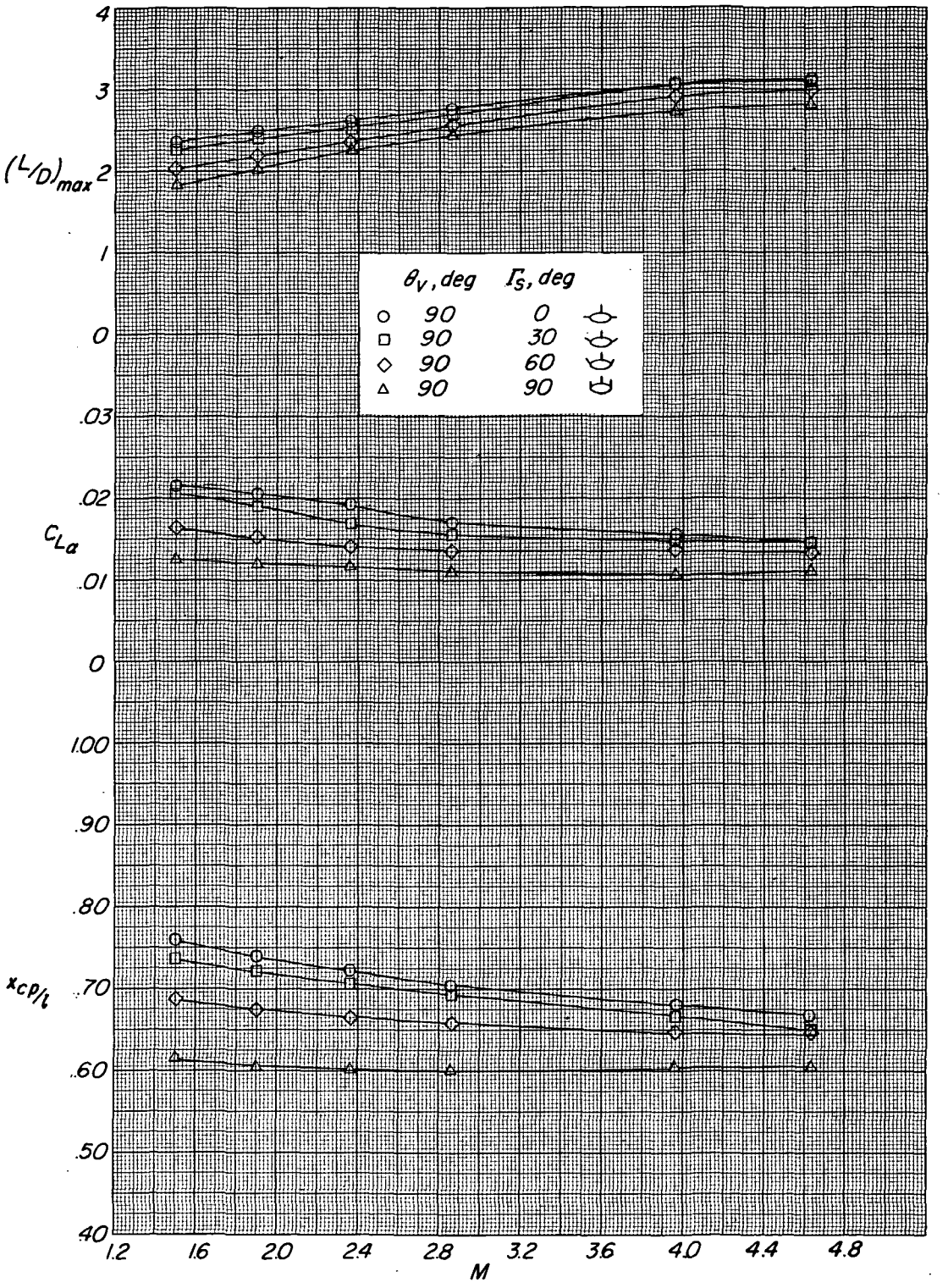

Figure 17.- Effect of outboard-stabilizer dihedral angles on various pertinent longitudinal aerodynamic parameters of the configuration with center vertical tail on as a function of Mach number. $\Gamma_S = 0^o$ to 90^o.

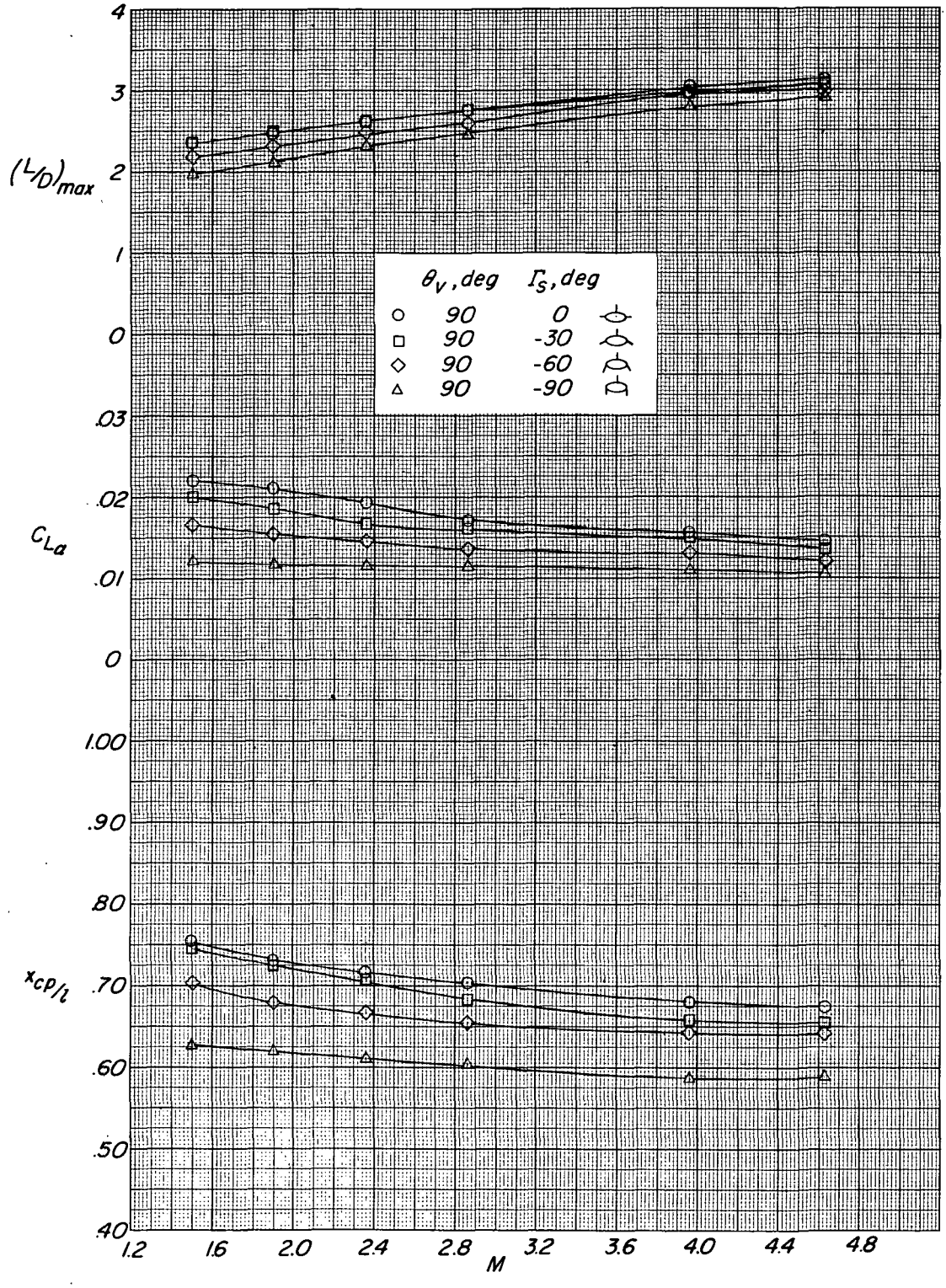

Figure 18.- Effect of outboard-stabilizer dihedral angles on various pertinent longitudinal aerodynamic parameters of the configuration with center vertical tail on as a function of Mach number. $\Gamma_S = 0^o$ to -90^o.

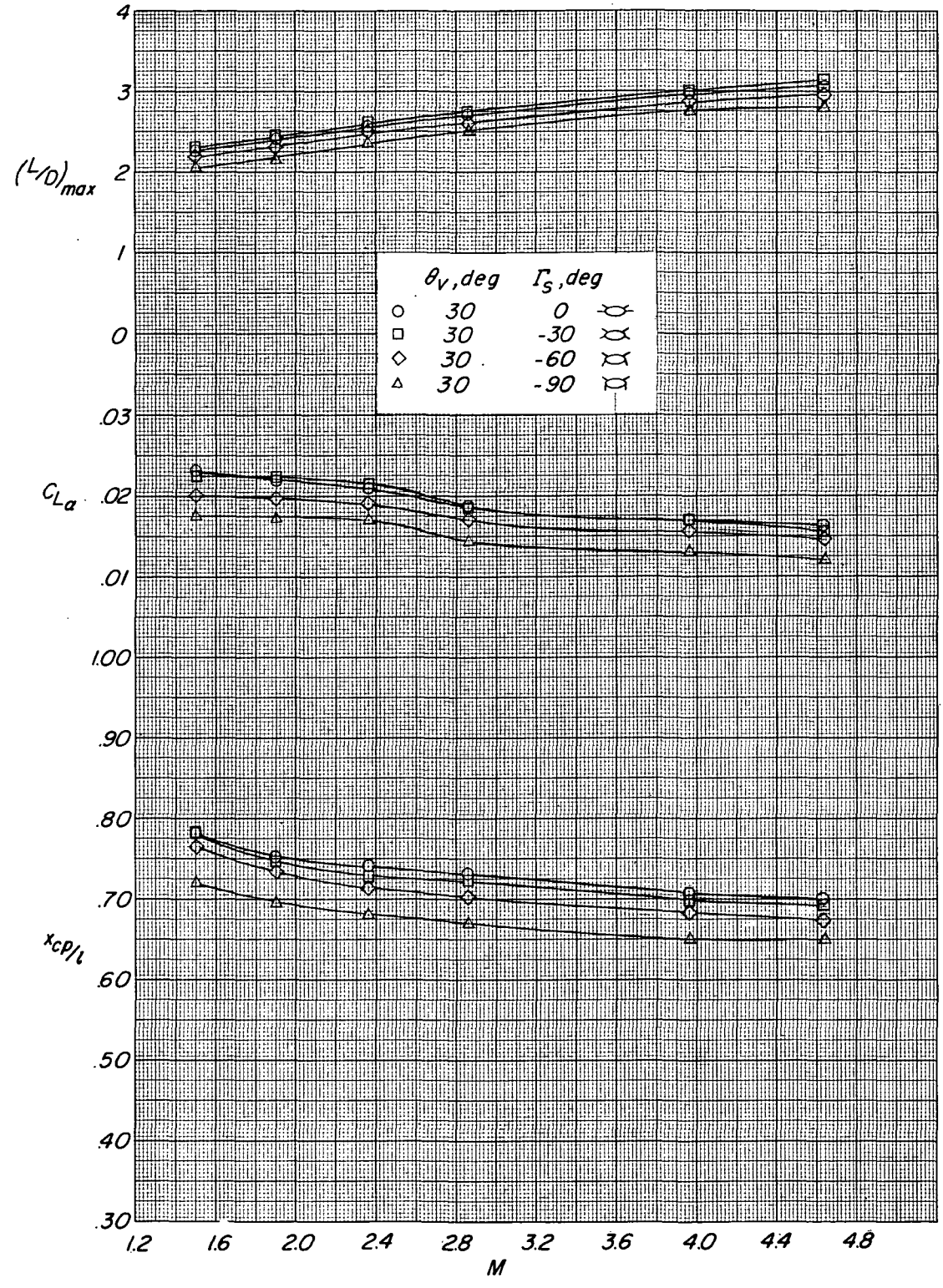

Figure 19.- Effect of outboard-stabilizer dihedral angles on various pertinent longitudinal aerodynamic parameters of the configuration with vee-tail on as a function of Mach number. $\Gamma_S = 0^o$ to -90^o.

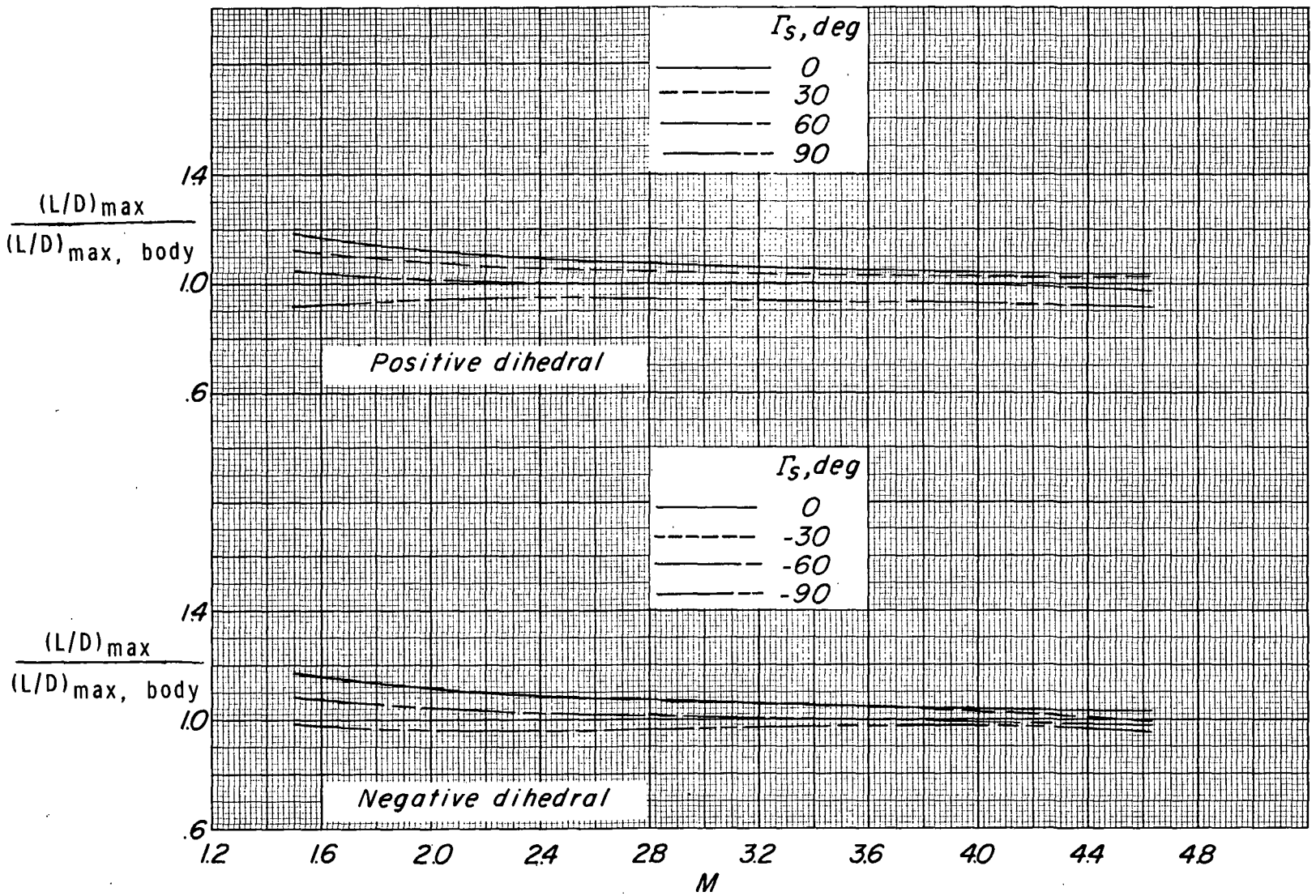

Figure 20.- Effect of addition of outboard stabilizers and variation of dihedral angle on maximum lift-drag ratio as a function of Mach number.

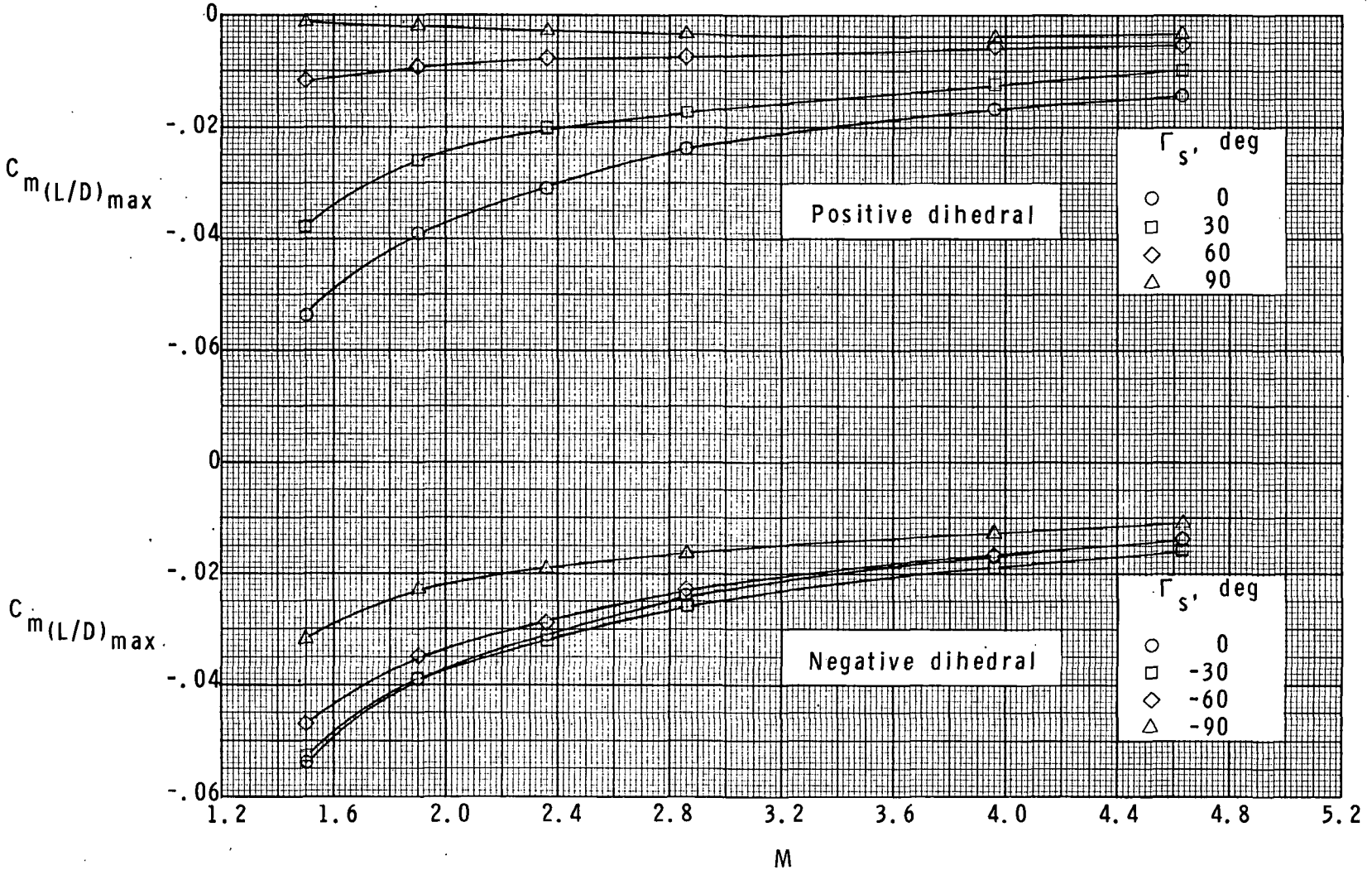

Figure 21.- Effect of outboard-stabilizer dihedral angle on C_m at $(L/D)_{max}$ as a function of Mach number.

NATIONAL AERONAUTICS AND SPACE ADMINISTRATION
WASHINGTON, D.C. 20546

OFFICIAL BUSINESS
PENALTY FOR PRIVATE USE $300

SPECIAL FOURTH-CLASS RATE BOOK

POSTAGE AND FEES PAID
NATIONAL AERONAUTICS AND SPACE ADMINISTRATION
451

U.S.MAIL

POSTMASTER: If Undeliverable (Section 158 Postal Manual) Do Not Return

"The aeronautical and space activities of the United States shall be conducted so as to contribute . . . to the expansion of human knowledge of phenomena in the atmosphere and space. The Administration shall provide for the widest practicable and appropriate dissemination of information concerning its activities and the results thereof."

—NATIONAL AERONAUTICS AND SPACE ACT OF 1958

NASA SCIENTIFIC AND TECHNICAL PUBLICATIONS

TECHNICAL REPORTS: Scientific and technical information considered important, complete, and a lasting contribution to existing knowledge.

TECHNICAL NOTES: Information less broad in scope but nevertheless of importance as a contribution to existing knowledge.

TECHNICAL MEMORANDUMS: Information receiving limited distribution because of preliminary data, security classification, or other reasons. Also includes conference proceedings with either limited or unlimited distribution.

CONTRACTOR REPORTS: Scientific and technical information generated under a NASA contract or grant and considered an important contribution to existing knowledge.

TECHNICAL TRANSLATIONS: Information published in a foreign language considered to merit NASA distribution in English.

SPECIAL PUBLICATIONS: Information derived from or of value to NASA activities. Publications include final reports of major projects, monographs, data compilations, handbooks, sourcebooks, and special bibliographies.

TECHNOLOGY UTILIZATION PUBLICATIONS: Information on technology used by NASA that may be of particular interest in commercial and other non-aerospace applications. Publications include Tech Briefs, Technology Utilization Reports and Technology Surveys.

Details on the availability of these publications may be obtained from:

SCIENTIFIC AND TECHNICAL INFORMATION OFFICE

NATIONAL AERONAUTICS AND SPACE ADMINISTRATION

Washington, D.C. 20546